# Herpes Simplex Virus-2 Reactivation from Viral Latency in Autonomic Ganglia

by

Julianna Pieknik

Dissertation submitted to the Faculty of the Emerging Infectious Diseases Graduate Program Uniformed Services University of the Health Sciences in partial fulfillment of the requirements for the degree of Doctor of Philosophy 2018

## FINAL EXAMINATION/PRIVATE DEFENSE FOR THE DEGREE OF DOCTOR OF PHILOSOPHY IN THE EMERGING INFECTIOUS DISEASES GRADUATE PROGRAM

Name of Student: Julianna Pieknik

Date of Examination: Monday, March 26, 2018
Time:   1:00 PM
Place:   Room A2052

DECISION OF EXAMINATION COMMITTEE MEMBERS:

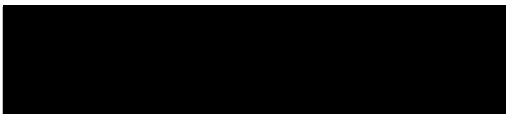|  | PASS | FAIL |
|---|---|---|
| Joseph J. Mattapallil, BVSc, MS, PhD<br>DEPARTMENT OF MICROBIOLOGY & IMMUNOLOGY<br>Committee Chairperson | ✓ | — |
| Phil Krause, MD, CAPT, USPHS<br>DEPARTMENT OF EMERGING INFECTIOUS DISEASE<br>Dissertation Advisor | ✓ | — |
| Chou-Zen Giam, PhD<br>DEPARTMENT OF MICROBIOLOGY & IMMUNOLOGY<br>Committee Member | ✓ | — |
| Andrew L. Snow, PhD<br>DEPARTMENT OF PHARMACOLOGY<br>Committee Member | ✓ | — |
| Jason Lees, PhD<br>DEPARTMENT OF MEDICINE<br>Committee Member | X | — |

## APPROVAL OF THE DOCTORAL DISSERTATION IN THE EMERGING INFECTIOUS DISEASES GRADUATE PROGRAM

Title of Dissertation: "Herpes Simplex Virus-2 Reactivation from Viral Latency in Autonomic Ganglia"

Name of Candidate:     Julianna Pieknik
                       Doctor of Philosophy
                       March 26, 2018
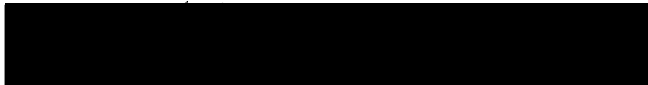
**DISSERTATION AND ABSTRACT APPROVED:**

DATE:

4/4/18

Joseph J. Mattapallil, BVSc, MS, PhD
DEPARTMENT OF MICROBIOLOGY & IMMUNOLOGY
Committee Chairperson

3/26/18

Phil Krause, MD, CAPT, USPHS, Ret
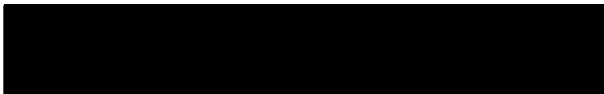DEPARTMENT OF EMERGING INFECTIOUS DISEASE
Dissertation Advisor

3/26/18

Chou-Zen Giam, PhD
DEPARTMENT OF MICROBIOLOGY & IMMUNOLOGY
Committee Member

3/26/18

Andrew L. Snow, PhD
DEPARTMENT OF PHARMACOLOGY
Committee Member

3/26/18

Jason Lees, PhD
DEPARTMENT OF MEDICINE
Committee Member

# ACKNOWLEDGMENTS

# DEDICATION

For my mother and father, I am truly blessed to be your daughter.

# COPYRIGHT STATEMENT

The author hereby certifies that the use of any copyrighted material in the dissertation manuscript entitled: "Herpes Simplex Virus-2 Reactivation from Viral Latency in Autonomic Ganglia" is appropriately acknowledged and, beyond brief excerpts, is with the permission of the copyright owner.

[signature]_____

Julianna Pieknik

# ABSTRACT

Title of Dissertation:

Herpes Simplex Virus-2 Reactivation from Viral Latency in Autonomic Ganglia

Julianna R. Pieknik, Doctor of Philosophy, 2018

Thesis directed by:

Philip R Krause, M.D., Deputy Director, Food and Drug Administration Office of Medical Products and Tobacco Center for Biologics Evaluation and Research Office of Vaccines Research and Review and Professor, Department of Microbiology and Immunology, USUHS

Herpes Simplex Virus-2 is a worldwide, major human pathogen that causes recurrent disease over the lifetime of its host. According to current dogma, HSV-2 reactivation occurs from the sensory, sacral dorsal root ganglia. However, a growing body of evidence reports the virus latent in another branch of the peripheral nervous system, the autonomic ganglia. It is unclear whether spontaneous reactivation is occurring in these additional sites, potentially contributing to recurrent genital skin lesions and observed clinical symptoms like urinary retention or responsible for subclinical reactivations in the dermis.

Due to the small size of virions and the rare spontaneous event of reactivation, a fluorescent herpes simplex virus is an invaluable tool for localizing virus in cells. Unfortunately, available fluorescent mutants lack the required sufficient genetic stability

or normal kinetics of replication and reactivation. We hypothesized that by using a brighter, non-dimerizing fluorescent protein, we could engineer a functional mutant virus to begin to address some of the key questions related to reactivation of HSV-2. We constructed a fluorescent HSV-2 strain by fusing the fluorescent mNeonGreen protein to the VP26 minor capsid protein. This mutant virus displayed normal replication and *in vivo* recurrence phenotypes, providing an improved tool for investigating reactivation from latency.

In order to explore the full extent of the tropism of reactivation we used the guinea pig vaginal infection model that develops spontaneous recurrent genital skin lesions and signs of autonomic dysfunction in the form of urinary retention and constipation. Examining three anatomical locations: the sensory dorsal root ganglia (DRG), the mixed population of parasympathetic and sympathetic neurons of the major pelvic ganglia (MPG) and the sacral sympathetic ganglia (SSG) by *ex vivo* explantation, we discovered that HSV-2 is not only latent, but its reactivation can be induced from the DRG and the SSG. Upon fluorescently labelling cryosections, we observed signs of *in vivo* reactivation within the DRG and SSG. We further validated our observations by using Droplet Digital Reverse Transcriptase Polymerase Chain Reaction (ddRT-PCR) to quantify gene expression. Our findings elevate the significance of autonomic neurons in HSV pathogenesis and suggest the sacral sympathetic ganglia could be important sites of viral reactivation in the presence and absence of lesions.

# TABLE OF CONTENTS

# LIST OF TABLES

# LIST OF FIGURES

# CHAPTER 1: Introduction

## Introduction to Herpes Simplex Virus 2

### Taxonomy, Genome and Structure

Herpes Simplex Virus 2 (HSV-2), also known as Human Herpesvirus 2 (HHV-2), is one of two species of simplex viruses that belong to the eight-member *Herpesviridae* family that typically infect humans. HSV-2 is grouped into a three member *alphaherpesvirinae* subfamily with HSV-1 and Varicella Zoster Virus based on their shared neurotropism (30). Its large 154.7 kb genome is organized into a linear double-strand of DNA which is made up of two unique long regions ($U_L$) and the short unique region ($U_S$). Both of the long and short regions are bounded by inverted repeats ($R_L$, $R_L$', $R_S$ and $R_S$' respectively), as well as with termini containing direct repeats called the "a" sequences (39; 118). There are at least74 protein-coding genes and 1 non-coding Latency Associated Transcript (LAT) (39).

The viral DNA is tightly wrapped around a spermine and spermidine polyamine-rich proteinaceous spindle creating a torus-shaped core (49). This core is encased in an icosahedral protein capsid, 100-125nm in diameter, made when Viral Protein (VP) 5, VP19C, VP23, and VP26 self-assemble (15; 153). Nine hundred copies of VP26 (6 on each hexon) are located externally on 150 hexons of VP5 (15; 148; 153). HSV-2's small 12 kDa capsid protein, VP26, is comprised of 112 amino acid residues and encoded by gene *UL35* (31). For many herpesviruses, the small capsid protein is essential for proper replication kinetics (17; 152). Although inessential in HSV-2, small capsid protein null mutants have reduced production of virus in cells from the baby hamster kidney cell line

and the murine corneal scarification model (2; 35). Between the capsid and envelope lies the proteinaceous tegument which functions to transport the capsid to the nucleus, regulates transcription, translation and apoptosis, and is involved in DNA replication, immune modulation, cytoskeletal assembly, viral assembly and final egress (71). The envelope is a lipid bilayer with twelve different types of glycoproteins(g): gL, gM, gH, gB, gC, gN, gK, gG, gJ, gD, gI and gE, some of which are essential, others disposable (58). The glycoproteins have complex and overlapping roles involved in membrane fusion, entry and immune evasion mechanisms.

## Immune Evasion

The success of HSV-2 as a human pathogen is in part due to its ability to evade the immune system by escaping and hiding latent in the sacral dorsal root ganglia. However over the centuries of co-evolution with *Homo sapiens*, it has evolved multiple strategies. HSV-2's Viral Host Shutoff Protein (VHS) causes degradation of cellular mRNA, allowing takeover of the cellular machinery for its own purposes (126). Infected Cell Protein (ICP) 27 also interferes with cellular processes by inhibiting splicesosome assembly and host splicing. Glycoprotein D blocks lysosomal fusion with endosome, and together with gJ blocks apoptosis. ICP47 inhibits MHC class I pathway by preventing binding of viral antigen to transporter associated with antigen presentation (TAP) (48). Glycoprotein B's identical amino acid sequence causes disruption of the associated invariant chain (Ii) and therefore MHCII inhibition(47). Glycoprotein G binds chemokine, effectively removing the cellular signal for help from migrating immune cells, while gC binds complement, inhibiting both the classical and alternate complement

pathways and thus preserving the cellular environment it requires to enter and replicate unfettered ( 47). Studies have showing gE and gI can bind IgG thereby preventing antibody dependent cytotoxicity and antibody neutralization (92; 104). Collectively, these immune evasion tools have allowed HSV-2 to spread all over the world, creating a significant global disease burden.

## Prevalence and Incidence

Herpes Simplex Virus-2 (HSV-2) has co-evolved with us before our ancestors became *Homo sapiens* making it a ubiquitous global pathogen and the leading cause of recurrent genital herpes cases worldwide (91; 145). In 2015, the World Health Organization estimated that 417 million people aged 15-49 years are infected with HSV-2. The global prevalence is variable, from 12.3% in males and 29% in females in eastern Europe and Asia increasing to 20%–30% range for most western European countries and the United States (Fig I.1) (42; 93; 125; 140). HSV-2 infection is more common in females, with a seropositive rate of 18% in North America, while the seropositive rate of HSV-2 infection in males is 12% (91). The highest prevalence of HSV-2 is found in sub-Saharan Africa, exhibiting a 70% seropositive rate among women and around 55% among men (91). The incidence or number of new HSV-2 infections in 2012 was estimated to be 19.2 million, highest in the younger age groups and declined with age (91). The infection rate can also be attributed to the rate of sexual activity. Heavily exposed populations, such as commercial sex workers, are almost uniformly infected (143).
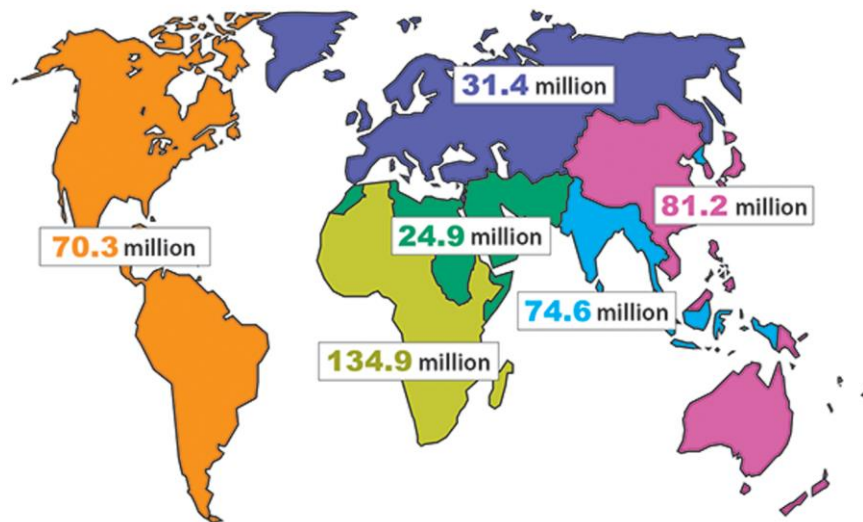
Figure 1. Adapted from Global Estimates of Prevalent and Incident Herpes Simplex Virus Type 2 Infections in 2012. PLoS ONE 10(1): e114989. https://doi.org/10.1371 journal.pone.0114989, copyright (2015) Permission not required as per Creative Commons Attribution (CC BY) license https://creativecommons.org/licenses/by/4.0/.

## Clinical Disease and Transmission

Characterized by painful blisters that ulcerate and form sores on the genitalia, fever, itching, and inflammation routinely accompany HSV-2 infection. Occasionally, infected patients also present with lower extremity pain, urinary retention and constipation (6). These episodes, called outbreaks, reappear throughout the lifetime of infected hosts, last approximately two weeks in the absence of treatment, then resolve. However, most infected individuals (80-90%) are asymptomatic, regarded as the absence genital skin lesions. They are either asymptomatic with no detectable virus emission or asymptomatic with subclinical infection, where virus is shed in reproductive tract excretions(55). It is thought that subclinical infection is what is most responsible for transmission (59). A sexually transmitted infection, HSV-2 transfers during direct contact

with vaginal or seminal secretions via mucosal membranes or skin to skin via minute abrasions (98).

HSV-2 can also be transmitted vertically, mother to child during childbirth. Neonatal infection can have devastating outcomes including premature birth, low birth weight, and herpes simplex encephalitis. Of newborns infected, seventy percent are born to asymptomatic mothers (10). Infected neonates suffer from lesions, focal or generalized seizures, abnormal liver function and disseminated intravascular coagulation(10). Additionally, their magnetic resonance images also reveal diffuse edema evolving into cerebral atrophy, calcifications, and cystic encephalomalacia (10). Moreover, neonates are not the only victims of HSV-2-attributable neurological complications. Rarely, infected adults exhibit aseptic meningitis (also known as Mollaret's meningitis) and herpes simplex encephalitis though typically only in the immunosuppressed (6). The immunosuppressed, not surprisingly, exhibit far more recurrences and serious neurologic symptoms. They suffer from anogenital or radicular pain, limb numbness or paresis, and recurrent myelitis (51).

## Co-infections

Systematic global analyses have found an epidemiological correlation between HSV-2 and HIV co-infection (46). A recent meta-analysis assessed 14 years of cohort studies, controlled trials, or case-control studies and found that the pooled adjusted risk of HIV acquisition after HSV-2 infection is approximately five times higher than without incident HSV-2 infection and almost twice the risk associated with exposure to prevalent HSV-2 infection (89). This evidence further supports the need for interventions such as

an HSV vaccine to not only aid in reducing new cases of HSV-2 infections but HIV infections as well.

In areas of endemic *Trichomonas vaginalis* infection, positive HSV-2 serology is associated with endometritis and co-infection with HSV-2 was the only genital tract pathogen infection associated with fallopian tube obstruction (24). Other significant co-infections include *Chlamydia trichomatis*, in which HSV-2 attachment and entry into the host cell is sufficient for stimulating chlamydial persistence, and Human Papilloma virus, where co-infection increases the risk of abnormal cervical cytology (32; 139).

## Treatment

Although no vaccine or or method of viral eradication exists, several antivirals are available to manage the infection. Acyclovir, ganciclovir (also its prodrug valganciclovir) and valaciclovir are deoxyguanosine analogues that when tri-phosphorylated prevent viral DNA synthesis by inhibiting the viral DNA polymerase (DNAP) (141). Famciclovir is an acyclic nucleoside analogue that when phosphorylated eventually inhibits viral DNAP, albeit not as effectively as acyclovir (77). Cidofovir is an acyclic phosphonate nucleotide analogue and competitive inhibitor of DNAP (64). Foscarnet is an organic analogue of inorganic pyrophosphate that directly inhibits DNAP and inhibits all known human herpesviruses, including acyclovir-resistant strains(76). Of these treatment options, only acyclovir, famiclovir and valacyclovir are considered relatively non-toxic. While there are plentiful treatment options, resistant mutants do arise do arise and the antivirals only manage but do not cure the infected population. Hence greater understanding of HSV-2 will be required to fully eliminate it from the host.

## HSV-2 Life Cycle

### Entry

HSV first infects the keratinocytes of the mucosal epithelium or skin, although it can infect lymphocytes, epithelial cells, fibroblasts, and neurons. The type of cell it encounters alters its entry pathway. Regardless of cell type, the virus enters in a two-step process, first attaching itself to the host cell's cellular receptors via viral glycoproteins, then triggering hemifusion with the host cell membrane and ensuing pore formation. First, gD binds cell surface receptor herpes virus entry mediator (HVEM) found on lymphocytes, nectin-1 and 2 (expressed on epithelial cells and neurons) or the ubiquitously expressed 3-O-sulfated heparin sulfate (29). Then, gB catalyzes membrane fusion alongside gC while a heterodimer of gH/gL triggers conformational changes that regulate fusion with the host cell membrane (29; 82; 111). Additional evidence suggests a pH-independent endocytosis and and fusion with intracellular endocytic vesicles that allows entry (26). This generates an outer membrane pore that allows tegument and capsid protein release into the host cell cytoplasm. Minor capsid protein VP26 interacts with host proteins: tetraspanin-7, dynein light chains Tctex-1 and RP3 to aid in intracellular locomotion (40). In VP26's absence, tegument proteins can still recruit and use the microtubule motor dynein for transport to the nucleus (114; 150).

## Replication

VP16, capsid protein pUL25 and large inner tegument protein pUL36 direct the capsid to dock with the host's nuclear pore complex. The nuclear localization sequence within pUL36 is recognized by host importin, triggering dislocation of part of its capsid, comprised of 12 copies of the portal protein pUL6 (1; 38). The pressurized viral DNA segment is released into the nucleus, leaving empty capsids docked at the nuclear membrane (117). The host cell immediately tries to chromatinize the viral DNA and directs it to nuclear matrix domains called Nuclear Domain 10 (ND10), where the virus forms pre-replicative sites. PML and ICP8 co-localize and form foci of replication which marginalizes the host chromatin (21). Genome transcription, genome replication and capsid assembly take place in adjacent compartments. The ensuing replicative process occurs in a sequential cascade. VP16 interacts with host cellular transcriptional factors including lysine-specific demethylase 1 (LSD1), circadian locomotor output cycles kaput (CLOCK) histone acetyl transferase, TFIIP, homeodomain octamer binding protein-1 (Oct1) and Host Cell Factor 1 (HCF1) to begin transcription of immediate early (IE) alpha genes: ICP0, ICP4, ICP22, ICP27, and ICP47 using host-supplied RNA polymerase II (66). Then, the alpha proteins begin DNA synthesis alongside transactivating the beta genes for early protein production. Early proteins are involved with DNA replication, which includes, but is not limited to, thymidine kinase and DNA polymerase. UL9 (origin binding protein) binds HSV's origin of replication and circularizes the genome into a theta circle. DNA Polymerase (UL30/UL42), the single stranded binding protein (ICP8), and a helicase-primase complex (UL5/UL8/UL52) bind and allow bidirectional DNA replication (144). Further DNA amplification occurs to generate linear concatamerized

8

copies by rolling-circle replication. Meanwhile, the early beta proteins transactivate the transcription of the late gamma genes, whose proteins are involved in virion structure, capsid assembly and DNA packaging (66).

## Egress

Once the capsid has self-assembled, DNA is spooled around the proteinaceous spindle through the portal and into the toroid core. The viral PORT(portal protein), terminase (TER), portal capping protein (PCP) and a head-full sensing mechanism cleave the newly replicated genome at pac sites. After DNA capsids are formed in the nucleus, they bud into the inner nuclear membrane (INM), considered the primary envelopment, to form an enveloped particle in the perinuclear space (57). Then, the envelope fuses with the outer nuclear membrane to deliver the capsids to the cytoplasm (99). At 15 hours post-infection, gD, gB, and minor capsid protein VP26 have been observed co-localizing at the perinuclear interface (103). Others reported that HSV can reorganize the cytoskeleton and trans-Golgi network which in turn changes exocytosis or sorting machinery, accelerating the capsids re-envelopment (149).

## Latency

Post-primary lytic replication, HSV-2 evades the immune system by entering nearby dendritic ends and traveling retrograde within axons to the sensory neuronal somas bundles in the dorsal root ganglia. It has recently been shown that HSV-2 has found a way to secrete a portion of its gG (SgG) (22). SgG interacts with nerve growth factor (NGF) inducing tyrosine kinase receptor lipid raft relocation on the axonal termini

and increasing innervation of peptidergic axons into the skin's stratum granulosum, thereby allowing efficient viral escape (22). Once the virus arrives at the cell body, it either undergoes replication in the neurons, infecting nearby neurons and glial cells or enters latency. Latency is defined as the persistence of viral genomes without the production of live, infectious virus, but maintains the capacity to reactivate and release viral particles (137). The establishment of latency is hypothesized to be driven by the architecture of the neuron due to the relatively long distance from the nerve terminals to the nucleus of the neuronal cell body. Microtubules and motor molecules of kinesin for anterograde and dynein for retrograde are used to shuttle capsid and associated tegument proteins (43). Presumably, the lack of sufficient co-transport of VP16 to stimulate IE gene transcription has been hypothesized to promote the entrance into latency (56). Upon entry into the neuronal nucleus, the viral DNA forms an episome and instead of the virus modifying the host nucleus chromatin, it is instead modified by the host cell which deposits histones, epigenetically silencing the viral genome (37). During latency, only the noncoding Latency Associated Transcript (LAT), in the form of a stable LAT intron and the unstable primary LAT, and microRNAs (miRNAs) are produced. LAT is thought to aid in viral genome silencing by promoting the association of a heterochromatin marker on lytic gene promoters and protecting neurons from apoptosis (28; 78). There is evidence that LAT-associated miRNAs appear to regulate expression of lytic viral transcripts (ICP0, and ICP34.5) from the opposite strand and influence whether individual HSV-infected neurons will be latently or productively infected (28; 110; 135; 136). Additional evidence suggests that LAT promotes efficient reactivation (9; 80). In the guinea pig model, a mutation in the LAT promoter led to decreased LAT

accumulation and fewer recurrences in the genital skin (80; 94). Using the murine *in vivo*

infection model, the LAT+ virus reactivated at a higher rate than LAT- virus in one study

yet failed to exhibit a different rate between a LAT+ and LAT- virus in another (9; 94).

This suggests that the functions of LAT might be multi-faceted and its mechanisms of

action have yet to be fully elucidated.

## Reactivation

Reactivation involves the virus re-entering the lytic cycle. The initiation of

reactivation from latency is not entirely understood. It is hypothesized that stress signals

change neuronal cell physiology which subsequently cause the epigenetic derepression

involving reversal of repressive histone modifications of the viral genome (78; 105).

These stress signals can arise from immune (fever or steroidal immune suppression),

physical (UV radiation, axotomy, hypothermia) or hormonal changes (glucocorticoid

elevation from psychological stress) (68; 83; 108; 121). Regardless of impetus, initiation

of initial HSV gene expression during reactivation requires c-Jun N-terminal kinase

(JNK), common to many stress responses (27). In a two-stage reactivation program, JNK

activation leads to a histone methyl/phospho switch on HSV lytic promoters allowing

transcription (27). Some believe that in contrast to de novo lytic infection where gene

products are sequentially expressed, during animation or Phase I, all three classes of viral

genes are induced (75). However, recent findings suggest that subsequent RNAs are

spliced after expression, in the context of an *in* vivo infection as opposed to cell culture

models, and that *in vivo* reactivations are likely more directed (Shuang Tang, Krause Lab,

unpublished results). It is hypothesized that if sufficient quantities of key viral proteins

are made in phase I, then phase II, coined the synthesis phase, can begin (75).

Alternatively, once triggered, sporadic gene expression can occur from single neurons in

the absence of infectious virus, also known as abortive reactivations (44; 94). In this

hypothesis of triggered and sporadic gene expression, VP16, chromatin remodeling with

the cellular H3K27 demethylases (UTX/KDM6A and JMJD3/KDM6B) and the H3K9

demethylase (LSD1/KDM1) are likely required for the passage to full reactivation,

which culminates in HSV DNA replication and assembly of new infectious particles (63;

86). Many of these hypotheses are not yet completely supprted or incompatible with one

another. This is in large part due to the diversity and challenges of the models which are

used to explore reactivation.


## Models

### *In vitro, ex vivo*

Although we have some understanding of reactivation from latency, there are still

gaps which need to be covered before our comprehension is complete and eradicating

therapies can be developed. *In vitro* cell culture models attempting to recapitulate latency

and ensuing reactivation have limitations which should be understood before using them

to draw conclusions. The difficulty lies in trying to reduce a multi-faceted process into

three simple steps of establishment, maintenance and reactivation and reflecting the

architecture of an interconnected neuronal web and innervated tissue (112).  Non-

neuronal, non-human neuronal; and human neuronal cell lines are three categories of

latency and reactivation cell culture models. Normal diploid human fibroblasts are readily

available, but not neuronal and therefore not the natural cell type for latency (60). Rat

pheochromocytoma (PC12) cells are not technically neurons, but can be differentiated to be neuron-like with the limitation that key human host cell proteins might not be conserved in these rat cells and their absence might make a difference(54). Rat prenatal sympathetic neurons and neonatal or adult murine sensory neurons are suitable for latency yet could still be misleading if there are unknown important differences between human and rodent neurons. Adult *rodentia* (either murine, rat or guinea pig) primary cell culture offers more benefits than it does drawbacks including the establishment of latency, easily induced reactivation and a differentiated neuronal phenotype (12; 147). Importantly, axotomy (the removal of the bundle of somas from their axons via dissection) alone has been shown to be able to induce viral reactivation from these ganglia and therefore a reliable and well established model of reactivation (13; 45; 95). To address this potential pitfall, one could use the human cell lines SY5Y or differentiated Teratocarcinoma (NT2) cell lines (137). They are readily available, the right host species, but they are not of neuronal origin. If they were differentiated, they could prove useful, although they have not been used for latency and reactivation studies yet (25). Induced pluripotent stem cells are human and readily available, yet latency is not established in them(137). Immortalized ganglion cell lines are human and suitable for latency but reactivation is not efficient yet and it could be beneficial to develop this model further(137). While imperfect, there is still much to be learned in each context.

### *In vivo*

Humans are the only natural host for HSV-2. HSV-2 DNA has been found in human sacral dorsal root ganglia and HSV-1 in both the sensory and autonomic ganglia

of the head and neck (8; 142). Cadavers are not always readily available, and ganglia can only be tested soon after death (to avoid post-mortem reactivation) at time of autopsy, due to the location of ganglia within the spine and other ethical concerns preventing experimental and invasive human study. Animal models provide an excellent tool for studying latency and reactivation. HSV-2 can infect mice, rabbits, non-human primates and guinea pigs. Each animal model provides benefits as well as unique challenges.

**Mouse Model**

Mice have been used to study HSV acute infection and latency by skin, ocular, foot pad and genital routes of infection (20; 52). Unfortunately, severity of acute infection can cause significant mortality without the addition of acyclovir or anti-HSV immunoglobulin administration which potentially obfuscates the findings. As long as the mice are protected from death, they can go on to establish latent infection if exogenously pretreated with progesterone or antibodies to gD(109). Regrettably, mice do not spontaneously reactivate as seen in humans in that they don't exhibit recurrent lesions. This is often remedied by using means of induction such as UV radiation, steroidal immune suppression or hypo/hyperthermic stress (50).

In a murine intravaginal challenge with HSV-2, during the acute infection (5-7 days post-infection), immunolabelled HSV-2 antigen was observed not only in the expected sensory dorsal root ganglia, but in the parasympathetic neurons of the major pelvic ganglia and the sacral sympathetic chain(109). Conversely, another lab using HSV-1 in the murine genital model revealed autonomic parasympathetic enteric neuron-related pathogenesis, but no evidence of virus in the sympathetic chain(73). Between

14

these two observations, it was unclear if this was a difference attributable to HSV-1 versus HSV-2 or an unidentified variable. Also, it is unclear if latent virus could reactivate from the major pelvic ganglia and sacral sympathetic chain in the murine vaginal infection model.

**Rabbit Model**

Although an excellent model for ocular HSV-1 pathogenesis, HSV-2 does not reactivate efficiently in the rabbit eye model. Similar to the murine model, mortality is a significant hindrance to its use. They are also costly in comparison to the murine model. However they can spontaneously reactivate and shed virus in their tears (61).

**Nonhuman Primate Model**

The genetic similarity of nonhuman primates to humans makes them an obvious ideal choice for HSV-2 research. They are permissive to infection with hormonal treatment, establish latency and reactivate spontaneously recapitulating human disease(5). The only challenge is the high cost per animal, housing and care.

**Guinea Pig Model**

Arguably the gold standard for HSV-2 infection, the guinea pig vaginal infection model is permissive to infection without hormonal treatment, develops genital skin lesions, develops urinary retention and constipation, establishes latent infection and reactivates spontaneously(128). A scoring system has been developed to judge the severity of disease (Table 1.) A footpad model has also been used to reveal a greater

quantity of virus spreading to the DRG and spinal cord after vaginal infection which is innervated by sensory, sympathetic and parasympathetic innervation than footpad infection which is only innervated by sympathetic and sensory nerves suggesting an important role of the autonomics(107). There is also an ocular infection model that has served to provide evidence of latent and reactivating virus in the autonomic ganglia and sensory dorsal root ganglia as well as an observation of a lack of LAT in the parasympathetic ganglion suggesting either a low-level chronic infection as opposed to a latent and reactivating infection(85).

## The Nervous System

The nervous system contains two branches: the central and the peripheral nervous systems. HSV-2 rarely infects the central nervous system, comprised of the spinal cord and the brain. However when it does, it is often fatal. HSV-2's primary site of latency and reactivation is understood to be the peripheral nervous system which is further delineated into three types of neurons: sensory, motor, and autonomic. HSV-2 is known to establish productive and latent infection in the cell bodies of sensory neurons which are clustered together into discrete pockets within the spine, called ganglia (Fig.2). More specifically, HSV-2 is known to be found and reactivates from within the sacral dorsal root ganglia, located adjacent to the sacral spinal column designated S1-S5. These neurons are highly heterogeneous in size, with somas ranging from 10-100 um in diameter(134). They are also surrounded by satellite glial cells (SGCs), and full of rough endoplasmic reticulum, or Nissl bodies, making a Nissl stain appropriate for detection (138).
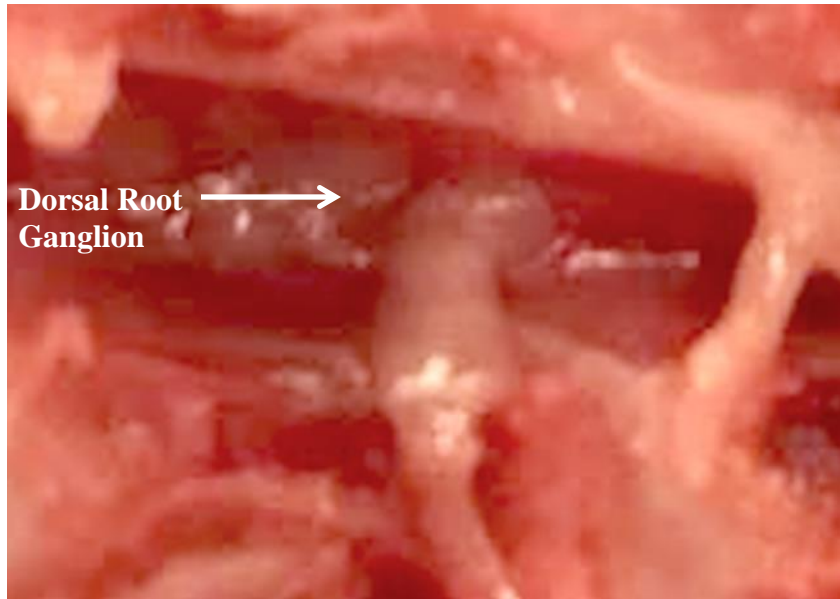
Figure 2. Guinea Pig Dorsal Root Ganglion nestled in an orifice in the spine that has been cut in half across the sagittal plane with the spinal cord removed.

Sensory neurons are responsible for sending signals of touch, pain, pressure, temperature from the skin, limbs and body wall to the central nervous system. Due to route of infection, HSV-2 enters the termini of neurons whose somas congregate in the coccygeal and sacral plexus. These neurons innervate a specific dermatome of the genital skin and buttocks associated with sites of viral reactivation-induced lesions and have been extensively studied in association with HSV infection.

The other branch of the peripheral nervous system, the autonomic neurons, is further segregated into two categories: parasympathetic and sympathetic. Parasympathetic neurons control "rest and digest" involuntary functions (SSLUDD): salivation, sexual arousal, lacrimation, urination, digestion and defecation (97). Because of the clinical symptoms of erectile dysfunction, urinary retention and constipation arising with HSV-2 infection, it has long been hypothesized that parasympathetic neurons were infected alongside the sensory neurons. Their preganglionic neurons arise from the

sacral region, the same vicinity of HSV-2 primary site of latency in the DRG and their

terminal ganglia lie within the tissues they innervate, including but not limited to, the

bladder and reproductive organs. The major pelvic ganglia include a mixed population of

parasympathetic and sympathetic innervation (Fig.3 - Fig.5).
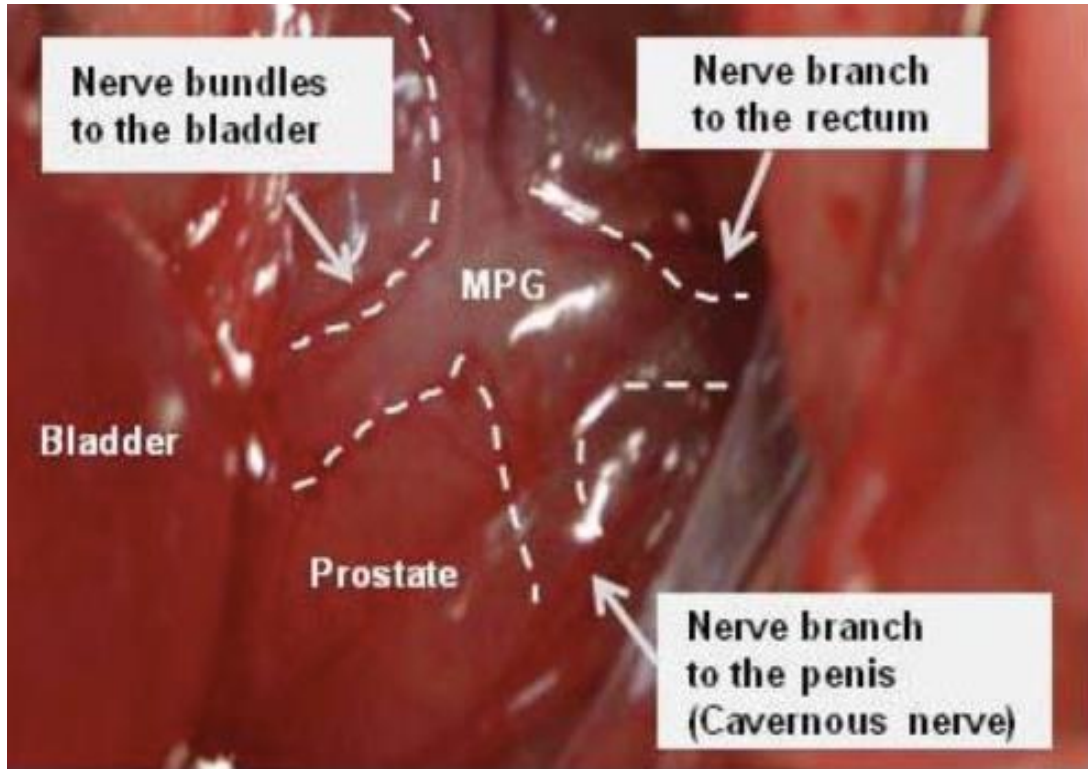


Figure 3. The MPG of a male rat. Adapted from: Functional and molecular changes of the bladder in rats with crushing injury of nerve bundles from major pelvic ganglion to the bladder: role of RhoA/Rho kinase pathway. Kim SJ, Lee DS, Bae WJ, Kim S, Hong SH, Lee JY, Hwang TK, Kim SW - Open Access Int J Mol Sci (2013). © 1996-2018 MDPI (Basel, Switzerland) https://creativecommons.org/licenses/by/4.0/.
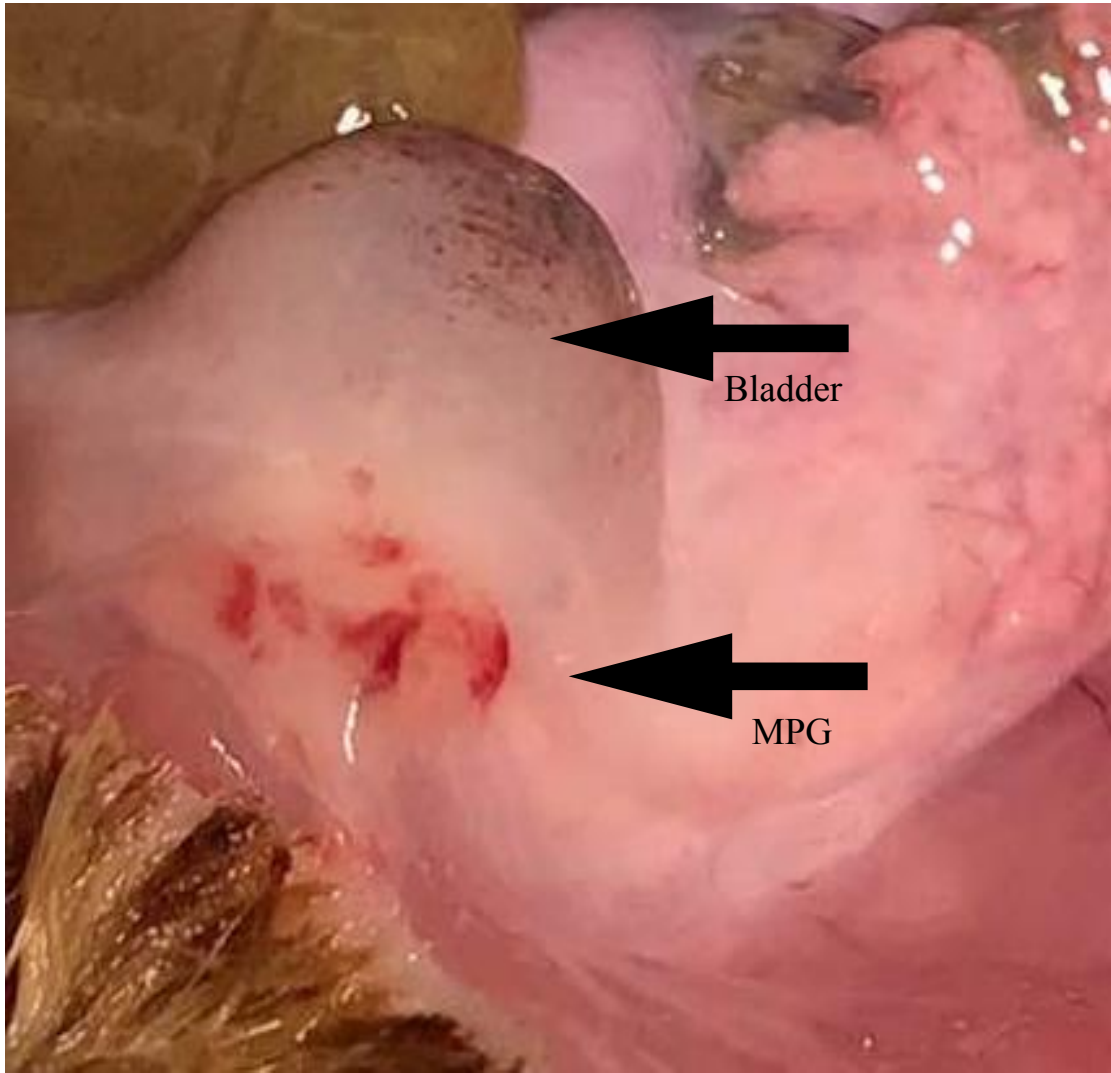
Figure 4. The location of the Bladder and MPG in a female guinea pig.

Paracervical Ganglia

Uterine horns
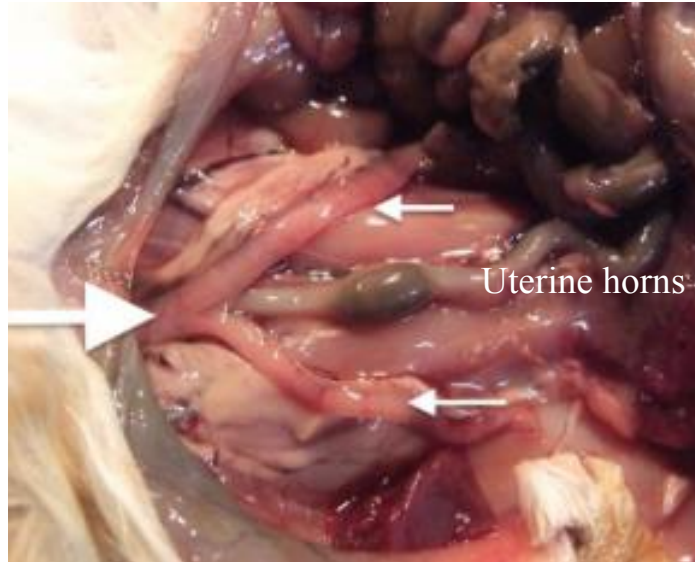
Figure 5. Location of the Paracervical Ganglia in a Female Guinea Pig. Adapted from Source: Drury Reavill, DVM, DABVP (Avian Practice), DACVP https://lafeber.com/vet/guinea-pig-reproduction-basics/.

Sympathetic neurons on the other hand control "fight or flight" responses. Their hormone-controlled activity increases heart rate, respiration and perspiration. Their postganglionic neurons travel within the spinal nerves, distributing sympathetic nerve fibers to the effectors of the skin including blood vessels and sweat glands. This puts sympathetic termini well within reach of HSV's primary site of lytic infection. The sympathetic ganglia that innervate the skin are located next to lumbar regions L4-L6 of humans and L6-S2 of small mammals (79; 87). The sympathetic ganglia that innervate the reproductive tract and bladder lie proximal to the S1-S5 region of the spinal column (119). Their sacral ganglia are chained together and culminate behind a layer of adipose on the anterior surface of the lower lumbar and sacrococcygeal junction. The sacral sympathetic ganglionic (SSG) neurons are morphologically different from those seen in the DRG. There are far more small (< 20um neurons) than large (>40um) and are mostly multipolar as opposed to pseudounipolar, widely interspersed with SGCs, and less

bundled than is seen in the DRG (115). Accumulating evidence over the past 40 years has

finally started to garner the attention that their involvement in HSV infection and the

correlation to autonomic dysregulation deserves (73; 109; 116; 120).
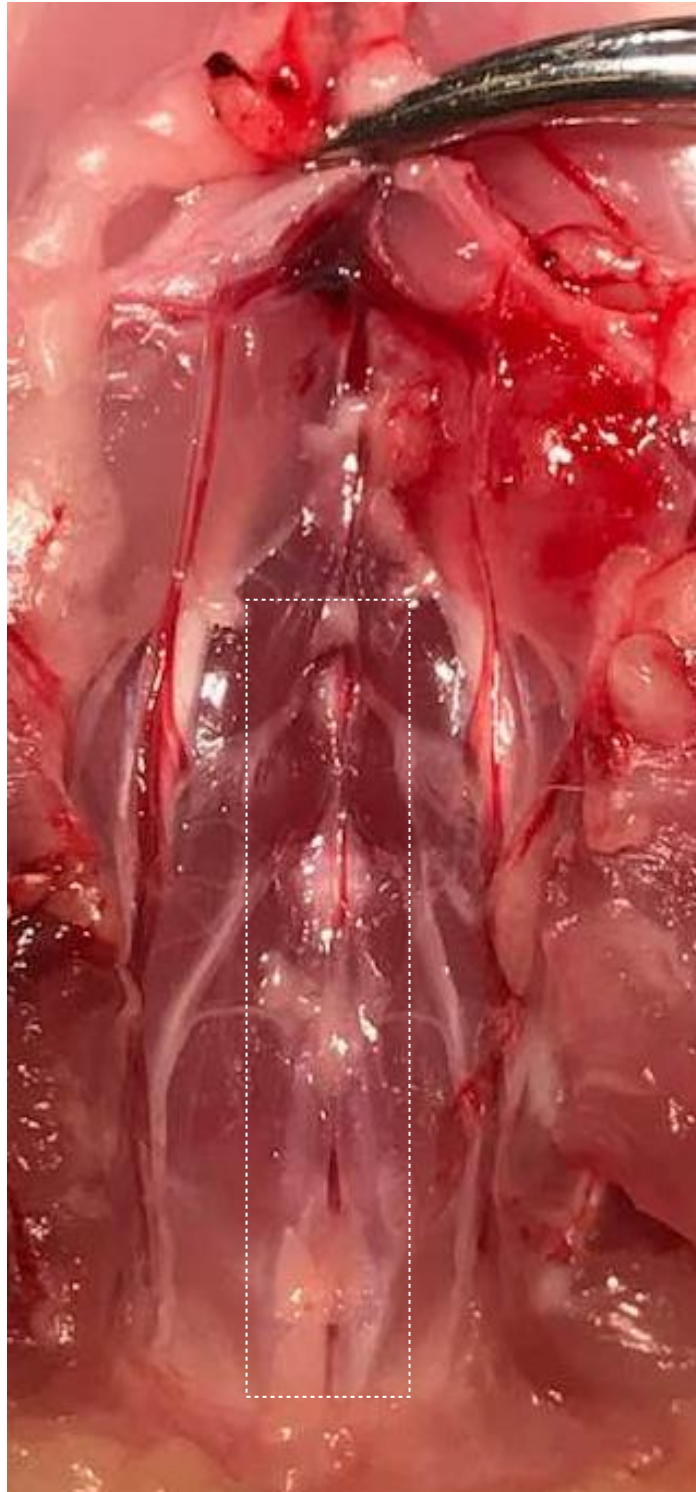
Figure 6. The location of the Sacral Sympathetic Ganglia in a female guinea pig.

**Table 1: Genital Scoring System**



| Score | Number of lesion | Clinical presentation |
|-------|------------------|------------------------|
| 0 | No lesion | |
| 1 | Inflammation or redness | |
| 2 | One or two lesions | |
| 3 | Three to five lesions | |
| 4 | More than five lesions or coalescence of lesions | |

Adapted with Permission from Sungseok Lee's *The Role of Autonomic Neurons in the Pathogenesis of Herpes Simplex Virus Type 1 and 2.* 2015. Dissertation submitted to the faculty of the Virginia Polytechnic Institute. online at https://vtechworks.lib.vt.edu/bitstream/handle/10919/64503/Lee_S_D_2016.pdf

**Fluorescent Protein Selection and Placement**

Fluorescent alphaherpesviruses are important tools allowing neuronal tracing, studies of virus assembly, maturation, transport and importantly reactivation from latency. Fluorescent HSV-1 mutants have been described extensively (65; 101). Mutants were first constructed to produce fluorescent protein (FP) by inserting the corresponding gene into intergenic regions (UL3-UL4, UL26-UL27, UL50-UL51, and US1-US2), or intragenic regions, thus disrupting non-essential genes (7; 100). The first described viral protein-FP fusion was enhanced green fluorescent protein (EGFP) fused to the HSV-1 tegument protein VP22 (41). Major capsid protein VP5 has been used but only maintains infectivity when co-expressed with a wild-type unfused VP5(65). Vertex components UL25 and UL17 tolerate FP fusion however could interfere with capsid binding to the nuclear pore complex or DNA packaging.

Tagging the minor capsid protein, VP26 has been partially successful, partly due to the high copy number (900) per virion (2; 15; 88). When VP26 was fused to dimeric green fluorescent protein (GFP), the dimeric yellow fluorescent protein (YFP), nuclear aggregates, capsid aggregation and diminished plaque size were observed(101). To improve upon existing mutants, viruses fused to monomeric fluorescent proteins (mFPs) were created, which partially alleviated problems associated with aggregates and reduced plaque size(33; 101; 133). Still, these mutants would lose their fluorescence *in vivo,* not replicate efficiently and not cause the pathology witnessed using wild-type strains (7; 81).

To date, no fluorescent HSV-2 has been described or studied *in vivo i*n the guinea pig vaginal infection model and a functional VP26 fusion is most likely the best candidate. A monomeric fluorescent protein, as an N-terminal fusion, with the first 7

amino acids deleted, is regarded as the most efficient HSV-1-mGFP fusion strategy in HSV-1(101). Amongst the monomeric fluorescent proteins, mNeonGreen stands above the rest. Recently Shaner et al. developed and characterized mNeonGreen: comparable excitation/emission peaks as eGFP (506/517 nm), is more acid tolerant than most Fps with a fluorescence pKa of ~5.7, and comes with the additional benefit of being three times as bright and more photo stable than eGFP(124). Although the number of virions produced in a single neuron during *in vivo* reactivation is unknown, the brightest mutant virus possible would be particularly useful when trying to visualize presumably few virions in a reactivating neuron which have been found to host 5-35 genomes (67).

## Goal and Specific Aims

HSV-2, the causative agent of genital herpes, establishes a lifelong infection due to its ability to hide latently, thus evading immune surveillance. Presumably, HSV-2 becomes latent not only in sensory neurons of the sacral ganglia but in both parasympathetic and sympathetic autonomic nerves(107). Early gene expression has been observed from the autonomic ganglia using the guinea pig ocular infection model(85). Yet it remains unknown if HSV-2 spontaneously fully reactivates, forming infectious virions within the autonomic neurons when using presumably the more biologically relevant guinea pig vaginal infection model. This dissertation intends to answer the fundamental question of the extent of HSV-2's tropism of reactivation.

There have been observed differences in HSV 1 and 2, between the murine and guinea pig models, as well as the acute versus latent phases. As we try to reconcile these differences, it is imperative that we are using the optimal tools. To that effect, my aim

was to first construct an optimized fluorescent HSV-2 (described in Chapter 2). The initial important markers of success include intense fluorescence, a fused fluorescent protein and its incorporation into mature virions. Other valuable benchmarks consist of the mutant viruses' ability to generate plaques, cause pathology in the form of genital skin lesions and urinary retention, maintenance of fluorescence well into the latent phase, and the ability to cause recurrent lesions. This aim introduces a new tool and provides evidence of its useful robustness in both the explantation model and immunolabelled cryosections.

My second aim was to define the types of neurons involved in reactivation (Chapter 3). This was achieved by observing the recently constructed, optimized, and characterized reactivating virus within parasympathetic and sympathetic neurons. I proposed to use the newly defined, green-fluorescing HSV-2 for vaginal inoculation of guinea pigs to identify the neurons from which HSV-2 is reactivating. Elucidating the neurons from which HSV-2 reactivates from provides valuable insights into its tropism or possible innate neuronal differences.

# CHAPTER 2: *A VP26-mNeonGreen capsid fusion HSV-2 mutant reactivates from viral latency in the guinea pig genital model with normal kinetics*

**Abstract**

Fluorescent herpes simplex viruses (HSV) are invaluable tools for localizing virus in cells, permitting visualization of capsid trafficking and enhancing neuroanatomical research. Fluorescent viruses could also be used to study virus kinetics and reactivation *in vivo*. However, current fluorescent herpes simplex viruses do not have sufficient genetic stability or normal kinetics of replication and reactivation, both of which would be required for such studies. We engineered an HSV-2 strain expressing the fluorescent mNeonGreen protein as a fusion with the VP26 capsid protein. This virus has normal replication and *in vivo* recurrence phenotypes, providing an essential improved tool for further study of HSV-2 infection.

**Introduction**

Fluorescent alphaherpesviruses are important tools in neuroanatomical research, because fluorescent virus can cross synapses, aiding in mapping of neuronal pathways. They also allow for studies of virus assembly, maturation, and transport. Herpes simplex virus 1 (HSV-1) recombinants bearing fluorescent protein-tagged capsid protein (VP26) have proved particularly useful, due to the large number of fluorescent molecules per virion (3; 16; 34; 36; 88; 102; 127; 132). Previously described fluorescent HSV-1 mutants have used the dimeric green fluorescent protein (GFP), the dimeric yellow fluorescent protein (YFP), or the enhanced GFP, as well as monomeric versions of GFP, red fluorescent protein (RFP) and other fluorescent proteins (FPs) (65; 101).

Efforts to optimize fluorescent viruses have focused on HSV-1 in which fluorescent proteins have been inserted into the N-terminal region of VP26. These viruses are infectious, but nonetheless have shown important differences from wild-type

virus (4; 34; 36; 81; 101; 102; 127; 132). Dimerization of GFP and YFP, leading to nuclear aggregates, has been a persistent challenge (36; 101; 102; 127). Previous work examined the utility of replacing dimeric fluorescent proteins with monomeric ones, which reduced but did not completely eliminate aggregates, and were still associated with replication defects that manifested as diminished plaque size (4; 34; 101; 132). Some of these previous constructs also reverted to a non-fluorescent virus, likely due to competition from non-fluorescent mutants that arise during replication in culture (7; 81; 101).

Fluorescent viruses have the potential for aiding in study of HSV latency and reactivation, potentially making it easier to identify loci of viral reactivation or of incipient recurrent lesions. Studies of viral reactivation from neuronal latency are limited because no fluorescent HSV mutant has been shown to reactivate *in vivo* with wild-type kinetics. A previously described HSV-2 that expresses a VP26-eGFP fusion protein is genetically stable and has been useful for *in vitro* studies, but does not reactivate with normal kinetics *in vivo* (11; 12; 14).

Construction of a fluorescent HSV-2 that replicates and reactivates with normal kinetics *in vivo* would enable use of the female guinea pig genital model, in which virus reactivates spontaneously to cause recurrent lesions. We based an HSV-2 small capsid protein (VP26) fusion on the most successful HSV-1 and HSV-2 constructs, which employ N-terminal VP26 fusions with monomeric fluorescent proteins. Small deletions in the N-terminus of HSV-1 VP26 appeared necessary for optimal fusion, so we engineered a corresponding deletion into HSV-2. We also used a recently described monomeric fluorescent protein derived from *Branchiostoma lanceolatum* that is three

times brighter than eGFP, mNeonGreen, which has not been previously used in HSV capsid fusions (124). Using the guinea pig as a well-established spontaneous reactivation model and a novel, monomeric fluorescing virus with an optimized design, we have tested the value of a newly generated tool and novel, bright fluorescent protein, which has potential use in other viruses or protein fusions. Ideally, a capsid-modified strain would have a similar morphology to wild-type strains, replicate with similar kinetics to the parental strain, fluoresce brilliantly enough to visualize with available microscopy, create similar cytopathic effects *in vitro*, cause similar pathology *in vivo*, and reactivate spontaneously from latency.

## Methods

### *In Vitro*

**Virus strains and stock production.** HSV-2 Strain 333 was originally obtained from Gary Hayward (Johns Hopkins University, Baltimore, MD). mNeonGreen was obtained from Allele Biotech (San Diego, CA). Plasmid pUL35NeGr, expressing mNeonGreen as a UL35 (encoding VP26) fusion, was constructed with GeneArt Seamless Cloning per manufacturer's instructions. Briefly, flanking regions of *UL35* sequence (with codons 1-7 deleted from the region downstream of the intended NeonGreen insertion), pUC19L, and NeonGreen were PCR-amplified with the High GC Fidelity Kit (Qiagen, Valencia, CA) and overlapping primers listed below. Equal quantities of the fragments were then recombined into a single plasmid and transformed into DH10B cells. The constructed plasmid was verified by capillary sequencing (Core Facility, CBER, FDA). The mutant

virus Nedel was then created in Vero cells (ATCC® CCL-81™) by homologous

recombination  after co-transfection using Superfect Transfection Reagent (Qiagen,

Valencia, CA), pUL35NeGr, and HSV-2 DNA.  After plaque purification to

homogeneity, the mutant virus was plaque purified 3 additional times.

Overlapping Primer Sequences. pUC19L (Fwd: GAGTCGACGGCATGCAAGCTTGG,

Rse: GAACGCGTGTACCGAGCTCGAATT); HSV-2 upstream flanking region

(Forward: CTCGGTACACGCGTTCGAGGGTC, Reverse:

CTCACCATCGGGACCTTGGGTCG), mNeonGreen (Forward:

AGGTCCCGATGGTGAGCAAGGGC, Reverse:

CTGGGGCGCTTGTACAGCTCGTCC), dUL35 (Forward:

TGTACAAGCGCCCCAGCACCATT, Reverse: TGCATGCCGTCGACTCCGCGCCC)

**Western Blot.** Monolayers of Vero cells were infected with Strain 333 or Nedel at a MOI

of 10. Protein was extracted with Laemmli Buffer and separated using sodium dodecyl

sulfate-polyacrylamide gel electrophoresis(SDS-PAGE) using Nu-Page 4-12% Bis-Tris

gels (Invitrogen) and transferred to nitrocellulose membranes (iBlot™ Transfer Stack,

nitrocellulose, mini).  Membranes were incubated with a rabbit peptide antibody to the C-

terminus of VP26 (95RRTYSPFVVREPSTPGTP112, generous gift from P. Desai) at a

1:500 dilution for 1 hr at RT, horseradish peroxidase-linked secondary anti-rabbit

antibodies (GE Healthcare) were used at a 1:2000 dilution  for 1 hr at RT and detected by

chemilluminescence (ECL) reagent (GE Healthcare). Magic marker protein standard

(Invitrogen) was loaded into the first lane.

**Growth Curve and Plaque size comparison.** Growth of HSV-2 in Vero cells was studied as previously described (80). Briefly, HSV-2 Strain 333 or Nedel infected Vero cells at a multiplicity of infection (MOI) of 0.01, and total virus was collected from cells at 0, 6, 12, and 24 hours post-infection(hpi). Strain 333 or Nedel was quantified by standard plaque assay on Vero cells. The area of plaques was determined by NIS Element software on a Nikon Eclipse Ti-E fluorescent microscope and the 6-point oval tool.

**Transmission Electron Microscopy.** Epoxy-Resin Embedding was performed by Yamei Gao (FDA, CBER) as follows: Samples were fixed with 2.5% glutaraldehyde, post-fixed with 1% osmium tetroxide, stained with 2% uranyl acetate/water, dehydrated in a series of ethanol buffers, infiltrated with 1:1 (Epon12: P.O.), then infiltrated with 100% Epon12, and embedded in block molds. Ultrathin sections were cut by ultra-microtome and were stained with 1% uranyl acetate/water. Samples were examined with the Zeiss L120 transmission electron microscope, and pictures were taken using the Gatan US 1000XP digital camera.

**Primary adult neuron infection.** Dorsal root ganglia were removed from 6 week old Swiss Webster mice, dissociated enzymatically and mechanically, and plated on Matrigel-coated Lab-Tek II chamber slides (ThermoScientific) as previously described (14). Neurons were maintained in Neurobasal A media supplemented with B27, penicillin/streptomycin, Glutamax, neurotrophic factors and mitotic inhibitors (Life Technologies). Three days post-plating, neurons were inoculated with 30 MOI Nedel, fixed with 2% paraformaldehyde 9 h post inoculation, and labeled with isolectin B4 conjugated to rhodamine (Vector Labs, 1:500). Neurons were imaged on inverted fluorescent Olympus IX73 microscope.

*In Vivo*

**Animals.** Female Hartley Guinea Pigs (n=15, 150-200 g, Charles River Breeding Laboratories, Wilmington, MA) were intravaginally inoculated with $1 \times 10^6$ pfu HSV-2 (Strain 333 or mutant virus) as previously described(128). Animals that failed to produce any lesions or developed end-point criteria prior to day 14 post-infection (pi) were removed from analysis, resulting in 7 Strain 333-infected animals and 13 Nedel-infected animals. Their data have been included in the supplemental figures. All animal experiments were performed under protocols approved by the Institutional Animal Care and Use Committee of the Food and Drug Administration (Protocol 1997-08).

**Replication *in vivo*.** Animals were evaluated daily for evidence of genital skin disease, bladder retention, hind limb paresis, paralysis, and death. Primary genital skin disease (Days 1-14 pi) was quantified by a lesion score system on a scale from 0 to 4 as follows: 0 for no disease, 1 for redness/swelling, 2 for one or two lesions, 3 for three to five lesions, and 4 for six or more lesions, coalescence of lesions or 3-5 lesions with neurologic symptoms(128).

**Viral Shedding.** Vaginal swabs were collected 5 times (Day 4, 7, 14, 21, 31 pi, n=7 Delta R, n=13 Nedel). The presence of virus was determined by plaque assay and fluorescence by fluorescence microscopy (Nikon Eclipse Ti-E) using Mouse anti-HSV-2 gH/gL (H2A269-100, Virusys, Taneytown, MD), Mouse anti-HSV gB (HA056-100, Virusys), Mouse anti-HSV gD (HA025-100, Virusys), Goat anti-Mouse IgG (H+L) Highly Cross-Adsorbed Secondary Antibody, Alexa Fluor 546 (Thermo Fisher Scientific, catalog # A-11030, RRID AB_2534089).

**Replication *Ex Vivo*.** Dorsal Root Ganglia were harvested and cultured from 5 guinea pigs intravaginally infected with Strain 333 or Nedel 36 days post-infection, as previously described [14]. Briefly, ganglia were digested in papain, collagenase and dispase (Worthington) before mechanically triturating and plating on Matrigel-coated 8-well Lab-Tek II chamber slides (ThermoScientific), followed by mechanical trituration with a pipette. Cultures were then fixed at 60 or 72 hours post-plating for 5 min in 4% paraformaldehyde, gently rinsed in Phosphate Buffer Saline (PBS) and immunolabelled as described below. Immunolabelled neuronal cultures were evaluated by fluorescence microscopy using a Nikon Eclipse Ti-E or a Zeiss LSM 710 upright confocal laser scanning microscope.

**Cryosectioning.** Animals were cardiac-perfused with PBS followed by cardiac-perfusion with 4% paraformaldehyde. Tissues were dissected, rinsed in PBS and sucrose-protected overnight. Sections were embedded in OCT (TissueTek®) and 10 μm sections were made with a cryostat (Leica). Sections were permeabilized, blocked and immunolabelled

**Immunolabelling of plaques, explanted ganglia, and cryosections.** Antibodies used included: NeuroTrace™ 640/660 Deep-Red Fluorescent Nissl Stain (N21483 Thermofischer Scientific), Mouse anti-HSV-2 gH/gL (H2A269-100, Virusys, Taneytown, MD), Mouse anti-HSV gB (HA056-100, Virusys),  Mouse anti-HSV gD (HA025-100, Virusys) Goat anti-Mouse IgG (H+L) Highly Cross-Adsorbed Secondary Antibody, Alexa Fluor 546 (Thermo Fisher Scientific, catalog # A-11030, RRID AB_2534089). Post-permeabilization and blocking, samples were labelled with the primary antibody for 24 h at 4 °C, secondary antibody for 24 h at 4 °C, labelled with Nissl stain for 2 h at room temperature before DAPI staining. Cryosections also were

treated with TrueBlack™ for 30sec in order to remove autofluorescence from lipofuscin that might otherwise potentially obscure our observations (131; 151).

**Results**

***In vitro* characterization**

Our goal was to develop and characterize a fluorescent HSV-2 variant that could reactivate *in vivo* with wild type HSV-2 kinetics and maintain its fluorescence into the reactivation phase. One of the most successful approaches with HSV-1 and HSV-2 was chosen, but the fluorescent protein was replaced by the three times as bright monomeric mNeonGreen fluorescent protein as an N-terminal fusion to UL35 (VP26) with the first 21 base pairs of UL35 deleted (corresponding to the first 7 codons), under control of the native UL35 promoter. We constructed this HSV-2 mNeonGreen VP26 fusion by homologous recombination, and designated the recombinant as "Nedel". In order to confirm that the fluorescent protein had been fused to the minor capsid protein, we performed a Western blot using an antibody to VP26 (Fig.7). The wild-type capsid protein is 12 kDa; when fused to the 24 kDa mNeonGreen the fusion mutant VP26 migrates at the expected size of 36 kDa.

The fluorescent capsid proteins in Nedel exhibited cellular distribution similar to that of HSV-2 glycoproteins, as assessed by immunolabelling in Vero cells (Fig.8A). Cytoplasmic fluorescent puncta, likely corresponding to assembled virions (Fig. 8B), nuclear fluorescence (Fig. 8C) and proximal-outer membrane fluorescence (Fig. 8D) were observed, co-localizing with the HSV polyclonal antibodies, indicating that the fusion protein was incorporated into intranuclear capsids and mature virions. Occasionally, the fluorescence from the capsid and pAb overlapped in entire rounded

cells without a more distinct fluorescence pattern (Fig.8E). In infected Vero cells (Fig.8F), there was no significant difference in plaque size between HSV-2 Strain 333 (mean plaque area=0.2425 mm2) and Nedel (mean plaque area=0.254 mm2) (Unpaired t test, p=0.8216). To ensure that viral replication was not limited to Vero cells, we assessed its ability to infect primary murine explanted DRG neurons. As is expected for HSV-2, Nedel preferentially infected IB4 positive neurons (Fig.9)(12).

In standard growth curves, Nedel's *in vitro* replicative ability was similar to that of Strain 333 over the course of 24 hours (Fig.10A, Mann-Whitney U test, p=0.8983). In these experiments, monolayers of Vero cells were infected with a multiplicity of 0.01 PFU/cell of Strain 333 or Nedel, and virus was quantified by plaque assay from cultures harvested at indicated times post-infection. By transmission electron microscopy (after either negative staining or epoxy-resin embedding) there was no significant difference between Nedel and Strain 333 in capsid size (~100-125 nm diameter), or virion morphology (Fig. 10B). We did not observe proteinaceous aggregates or capsid aggregation, as has been reported for other fluorescent HSV variants (101).

### *In vivo* guinea pig vaginal infection characterization

The ability of Nedel to infect adult female guinea pigs via the genital tract was also assessed. Among the 14 Strain 333-infected animals, 6 developed bilateral hind-limb paralysis (requiring euthanasia per the animal protocol) and 1 showed no apparent acute infection. Of the remaining 7 showing evidence of acute infection, six developed hind-limb paresis (HLP), urinary retention, or unilateral paralysis. In the Nedel-infected group, two of the 14 animals were euthanized for bilateral hind limb paralysis and 3

additional animals showed one or more of the other neurological symptoms such as limb

paresis or urinary retention. Thus, 12/14 Strain 333-infected animals developed

neurological symptoms, as compared with 5/15 in the Nedel-infected group. While less

neurovirulent *in vivo* than the Strain 333 virus, results in the Nedel group were similar to

the percentage typically observed in animals infected with MS strain (HLP 12-20%)

(129) (19). Despite the difference in neurovirulence, the infection with Nedel resulted in

acute-phase lesions similar to those of Strain 333, although the number of days to peak

mean lesion score lagged by ~2 days (Fig. 11A. Two-way ANOVA, p= 0.868). Vaginal

swabs from 13/13 of Nedel-infected animals yielded 100% green fluorescent plaques on

days 4 and 7 post-inoculation. On day 14, none of the swabs were positive for virus,

signaling the end of the acute infection. The quantity of genital skin lesions appeared

independent of neurological symptoms, as including the euthanized animals' lesion

scores up until their time of death did not significantly impact the overall average of

acute severity scores (Supplemental Fig.14). Recurrence phenotype was determined by

observing genital skin for new lesions each day (Days 15-36 pi) (Fig. 11B). Mean

cumulative recurrences were nearly identical between Nedel and Strain 333-infected

animals, each with 3.6 recurrences over the course of 21 days (Two-way ANOVA, p=

0.932). Vaginal swabs on day 21 and 31 were positive in 15% (2/13) of the Nedel-

infected animals, similar to 14% (1/7) Strain 333-infected animals that also shed

infectious virus on these days. All plaques from positive swabs from the Nedel group

were uniformly fluorescent green. With one exception (on day 21 in the Nedel group),

all of these culture-positive animals had recurrences at the time of swabbing.

### *Ex vivo* explantation model

Viral reactivation was also assessed *ex vivo* from infected animals euthanized on day 36 post-infection. Sacral dorsal root ganglia (DRG) were dissected, enzymatically digested and plated on Matrigel-coated chamber slides. In this model, the axotomy alone stimulates *ex vivo* reactivation (122; 130). Slides were then observed for fluorescence. Fluorescent neurons were first observed in cultures at 60 hours post-plating (Supplemental Fig. 16). At 72 hours post-plating, maximum fluorescence was observed. Cultures were fixed and stained to label neurons and HSV-2 antigen (Fig. 12A -C). The neurons from Nedel-infected animals that exhibited green fluorescence also stained positively for non-capsid HSV-2 antigen, further supporting that Nedel is capable of establishing latency in these neurons and of induced reactivation *ex vivo* after axotomy. Higher fluorescence intensity was observed in neurons with altered morphology, suggestive of cytopathic effect from a recent reactivation. Double instead of triple staining of cultures (Pan-neuronal and DAPI) allowed the analysis of more neurons per field of view (Supplemental Fig. 17), also showing co-localization of green fluorescence and explanted neurons from Nedel-infected animals. Using confocal microscopy, we also observed similar co-localization of green fluorescence (representing the Nedel capsid protein) and red fluorescence (representing HSV glycoproteins) within neurons (Fig. 12D).

### *In vivo* cryosections

To study the ability of the mutant virus Nedel to spontaneously reactivate *in vivo* from neurons, animals were cardiac-perfused and cryosections of the sacral DRG were

examined. Neurons were labelled with Nissl and sections with green fluorescence were confirmed to be HSV-2 positive by immunofluorescent labelling (Fig. 13A-E). Because the control Strain 333 sections were selected at random for staining (while Nedel sections were selected by fluorescence), only one neuron (on a single slide out of twenty stained) was identified that stained positively with the HSV-2 pAb. The Nedel *in vivo*-infected neurons exhibited co-localization of intense fluorescence (green, upper left quadrant) and HSV-2 pAb (red, upper right quadrant) within the nuclei and cytoplasm of neurons (merged, bottom right quadrant). This pattern was seen repeatedly in multiple sections (Fig.13C-E). Thus, fluorescence in Nedel-infected ganglia indicated viral reactivation in these neurons.

Figures
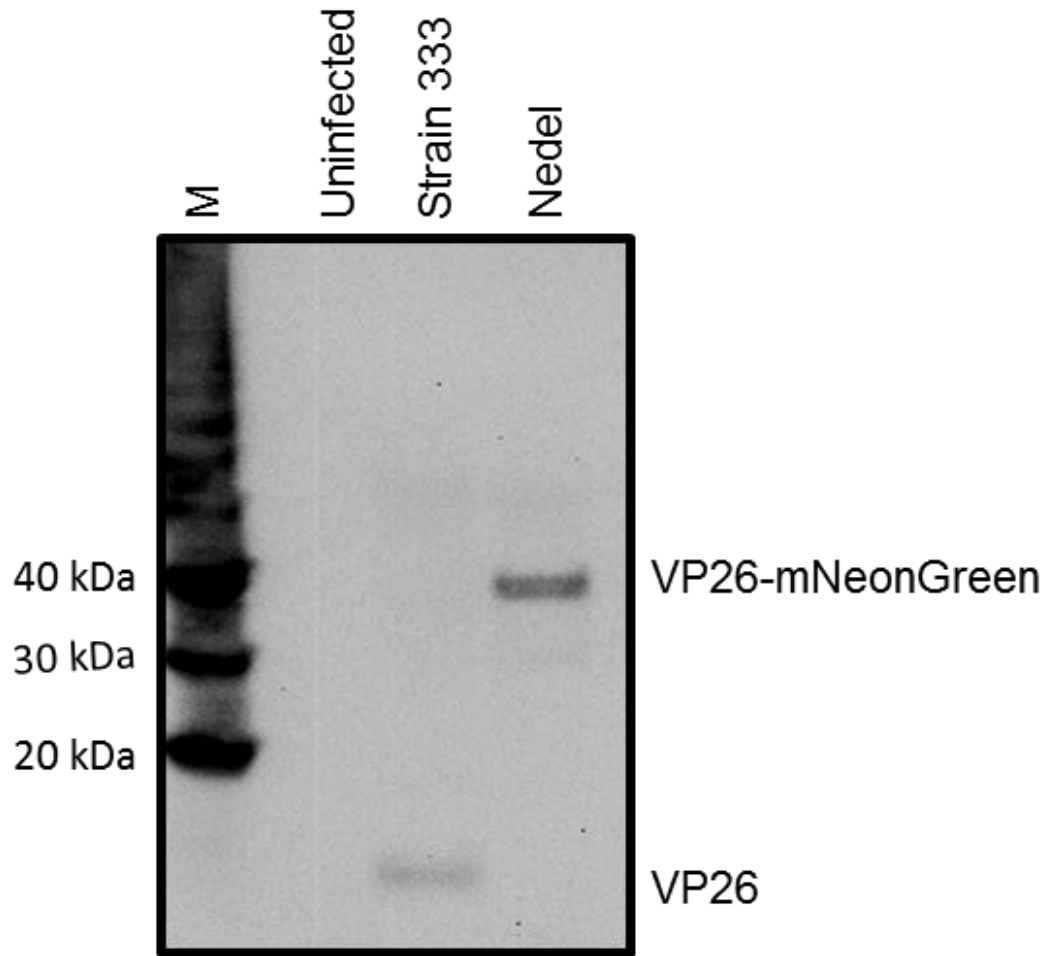


Figure 7. Western blot, stained with anti-VP26, indicating that in Nedel, VP26 is fused to mNeonGreen.  Vero cells were harvested 24 hours after infection at an MOI of 10 with either Strain 333 or Nedel. Magic Marker protein standards, uninfected Vero cells, HSV-2 Strain 333-infected Vero cells and Nedel-infected Vero cells are in the lanes left to right.

**E**
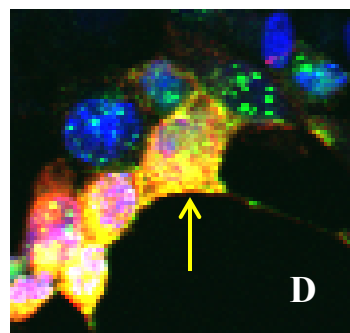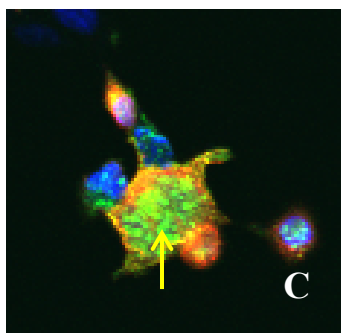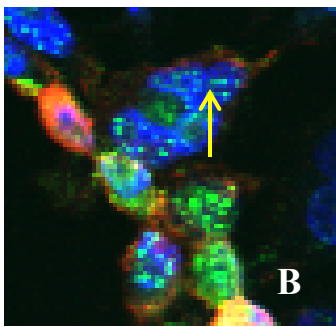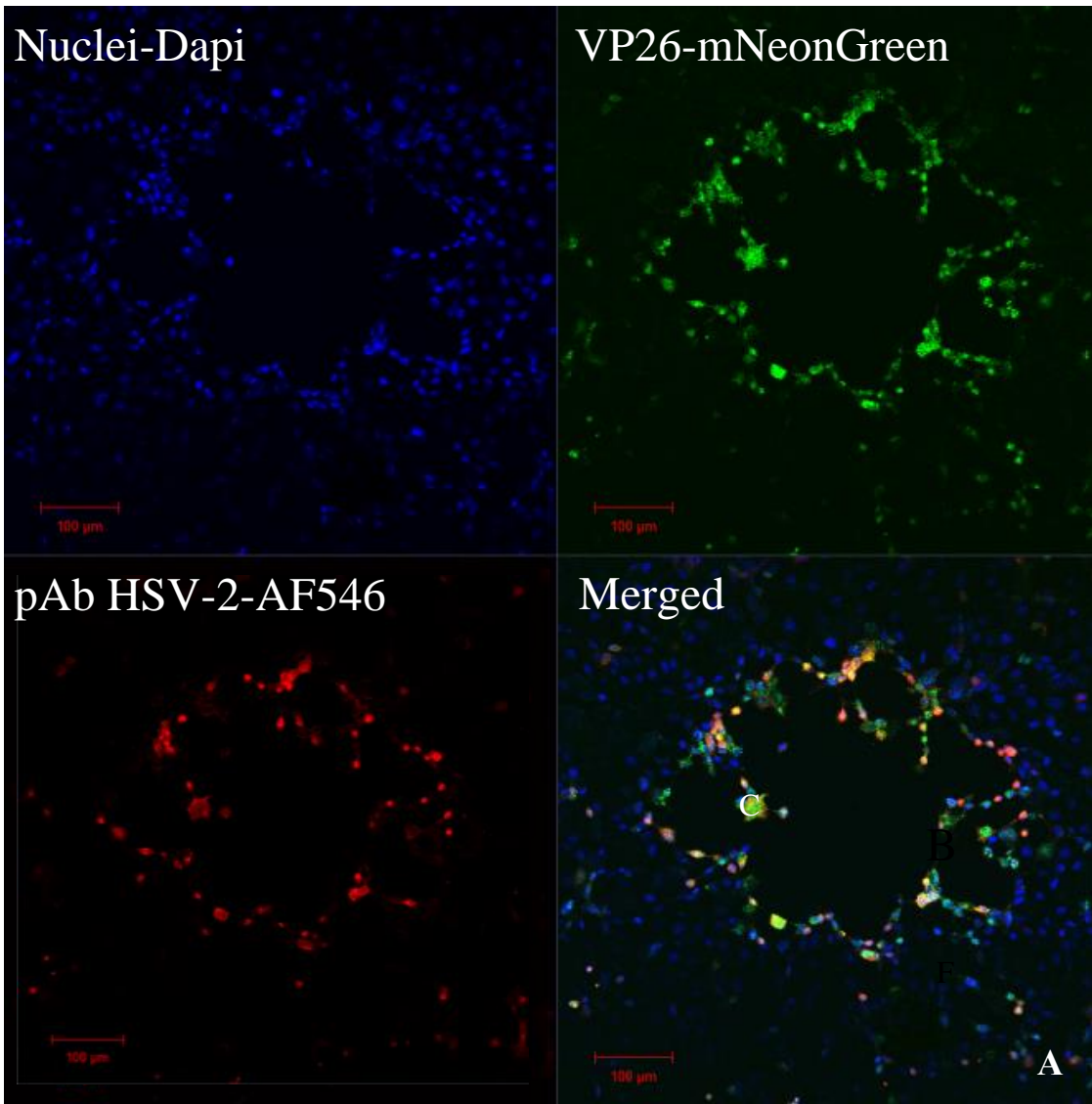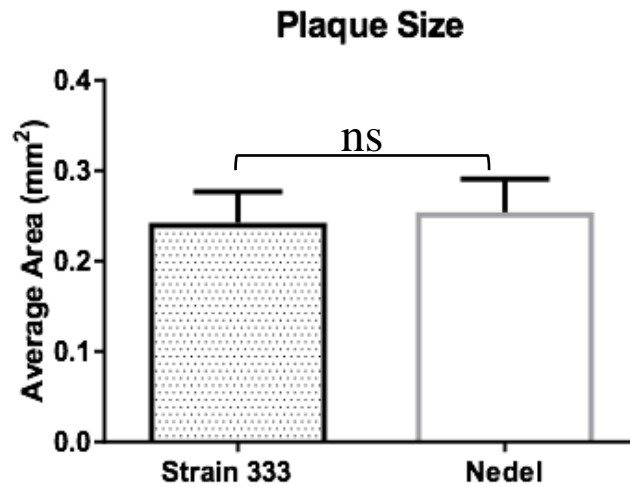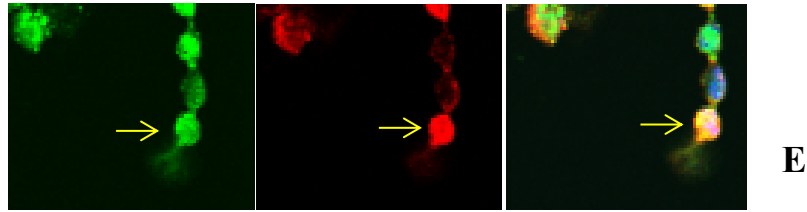


Figure 8. In Nedel-infected cells, mNeonGreen co-localizes with HSV antigen, and Nedel plaques are similar to wild-type. (A) Representative confocal image of a Nedel plaque. Nuclei (upper left) are stained with DAPI, mNeonGreen is detected (upper right) by fluorescence, and HSV-2 antigens are detected by immunofluorescent staining using a polyclonal HSV-2 antibody (lower left). Merged image is shown at lower right. Enlarged images taken from the plaque (B) Intranuclear ,(C) Cytoplasmic (D) and proximal outer-membrane (E) with intense co-localization obscuring fluorescent pattern.(F) Plaque size comparison, mean of 20 plaques, Error bars reflect SEM, Unpaired two-tailed t test p=0.8216.
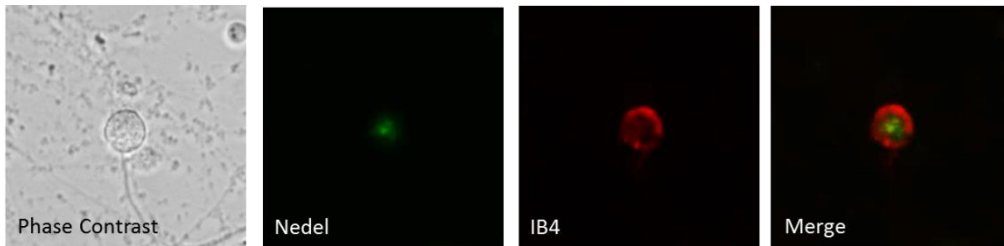
Figure 9. Nedel-infected primary murine neurons. mNeonGreen is detected within IB4-labeled neurons. Nedel replicates in IB4+ sensory dorsal root ganglia neurons, as described previously for wild type Strain 333(12).

**Growth Curve MOI .01**

Nedel
Strain 333
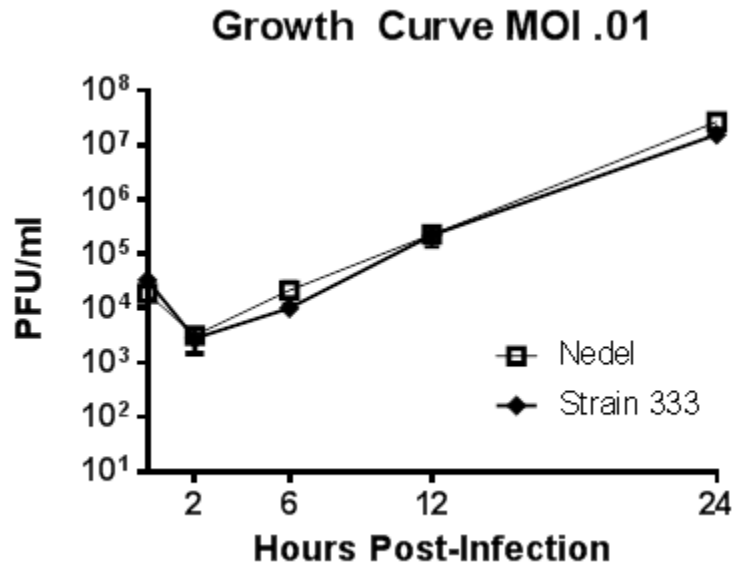
Strain 333

Nedel

A
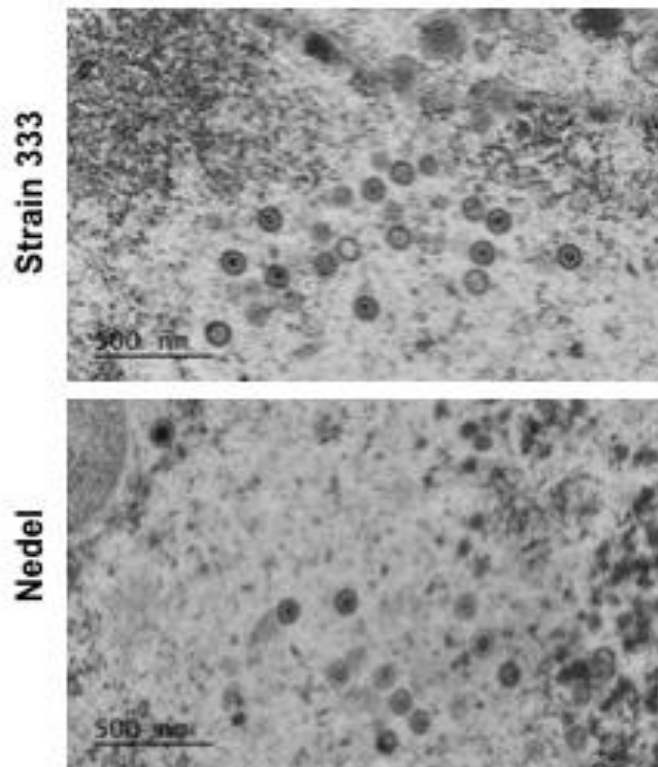
B

Figure 10. Replication of Nedel *in vitro*.( A) Growth Curves of Strain 333 and Nedel in Vero Cells. Data points are the mean of three separate titrations and error bars reflect 95% confidence intervals. Significance determined by Mann-Whitney, p=0.8983.  (B) Epoxy-Resin-Embedding Transmission Electron Microscopic images of Nedel and Strain 333 in Vero cells.

**Acute Infection**

Clinical Score (Mean) vs Reactivation
Strain 333 (n=7)
Nedel (n=13)

A

Cumulative Recurrences (Mean) vs Days Post Infection
Strain 333 (n=7)
Nedel (n=13)

B
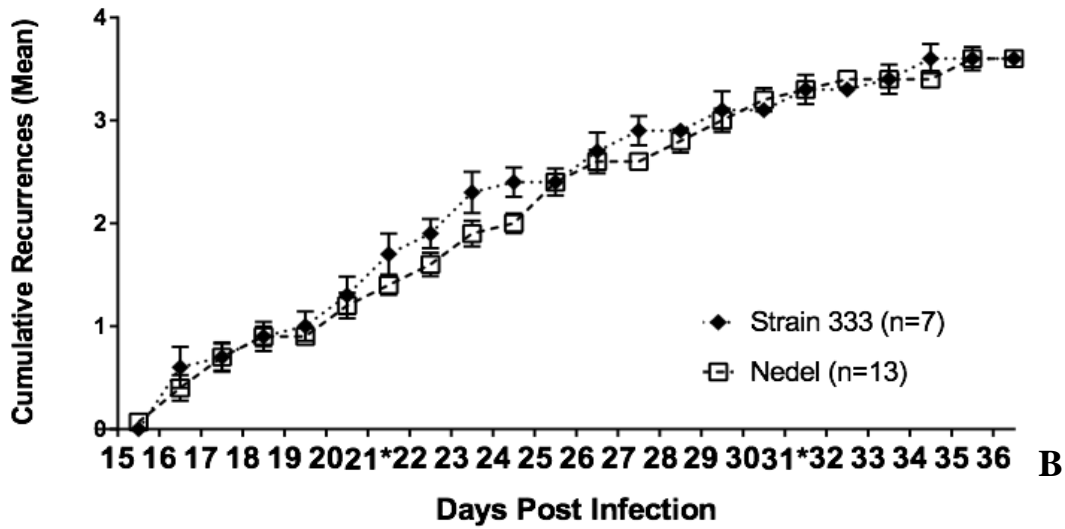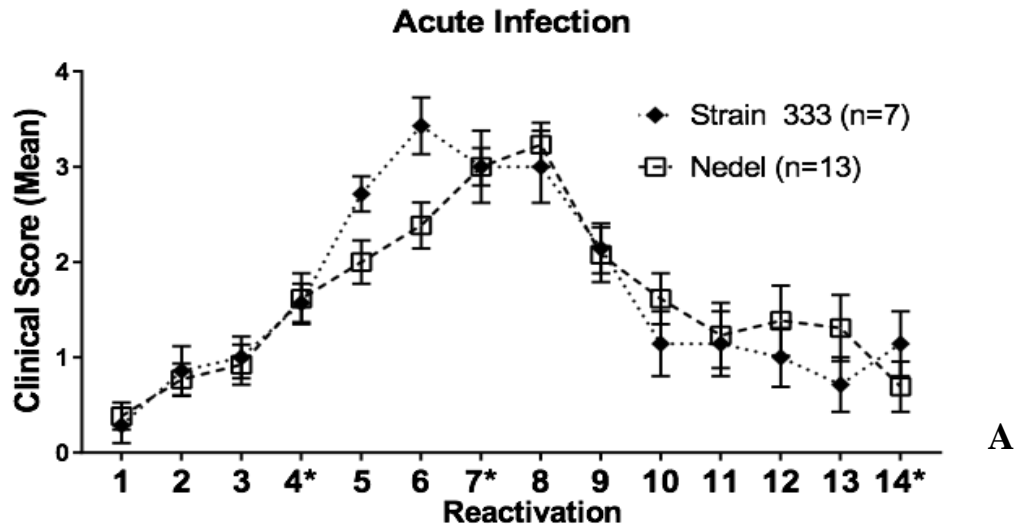
Figure 11. Characterization of Nedel in the guinea pig genital model of HSV infection (n=7 Strain 333, n=13 Nedel ) (A) Acute Severity determined by genital lesion scoring on a scale from 0-4. Error bars represent SEM. Significance determined by two-way ANOVA, p=0.868 (B) Mean cumulative number of recurrent genital skin lesions per guinea pig. Mean recurrence phenotype was determined by observing genital skin for new lesions. Error bars represent standard error of the mean. (Two-way ANOVA, p= 0.932 *Vaginal swabs with subsequent plaque assay on days 4 and 7: 13/13 Nedel-infected animals and 7/7 Strain 333-infected animals yielded 100% green and non-fluorescent plaques respectively. Day 14, 0% animals shedding detectable virus. Days 21 and 31, 2/13 of the Nedel-infected and 1/7 Strain 333-infected animals yielded 100% green plaques.

Strain 333



VP26 | pAb HSV-2-AF546

100 μm | 100 μm

Pan-Neuronal | Merged+Phase Contrast

100 μm | 100 μm

A

Nedel



VP26-mNeonGreen | pAb HSV-2-AF546

20 μm | 20 μm

Pan-Neuronal | Merged+Phase Contrast

20 μm | 20 μm

B

48

VP26-mNeonGreen

pAb HSV-2-AF546

Pan-Neuronal

Merged+Phase Contrast

C

VP26-mNeonGreen

pAb HSV-2-AF546

Pan-Neuronal

Merged

D
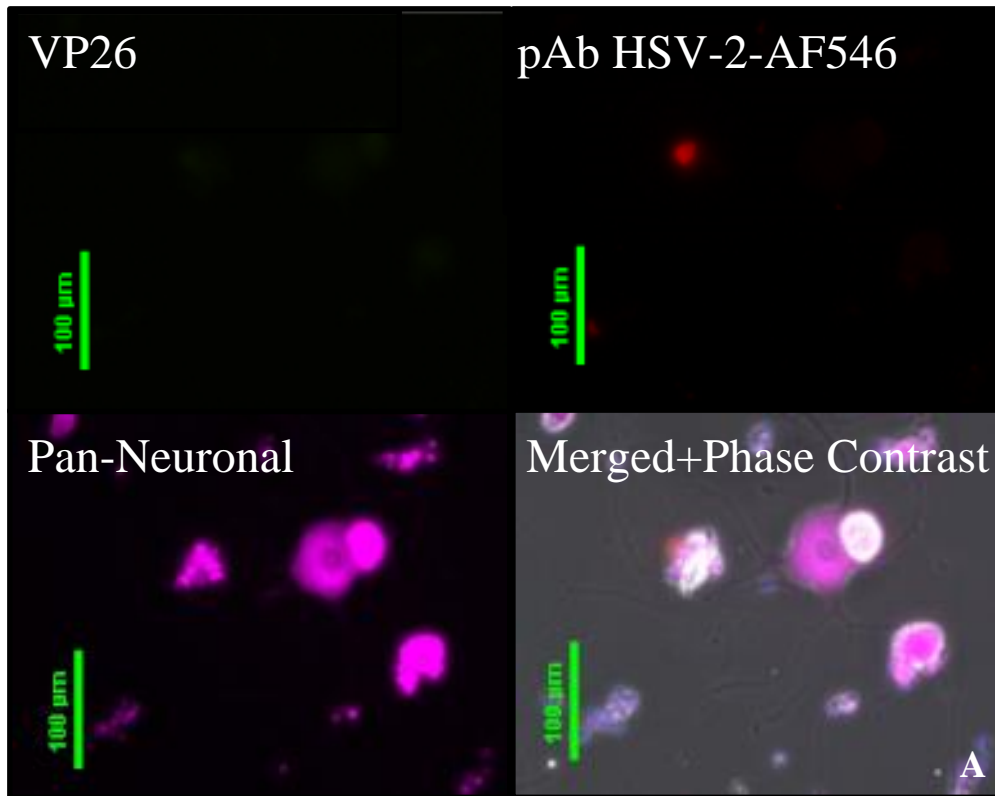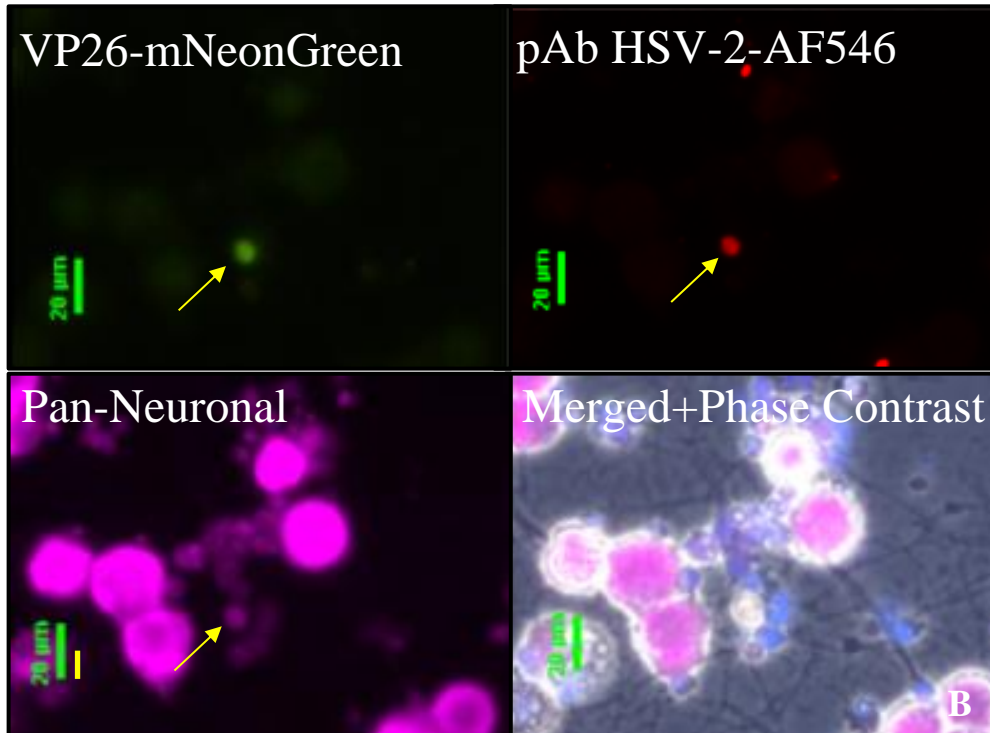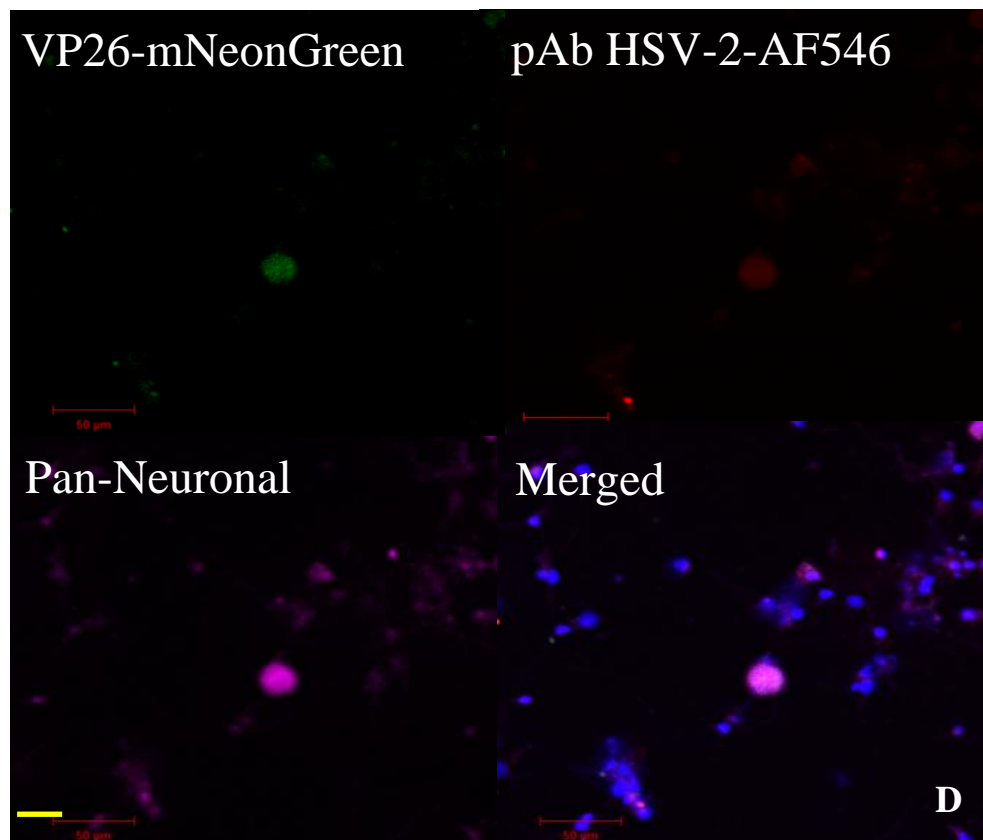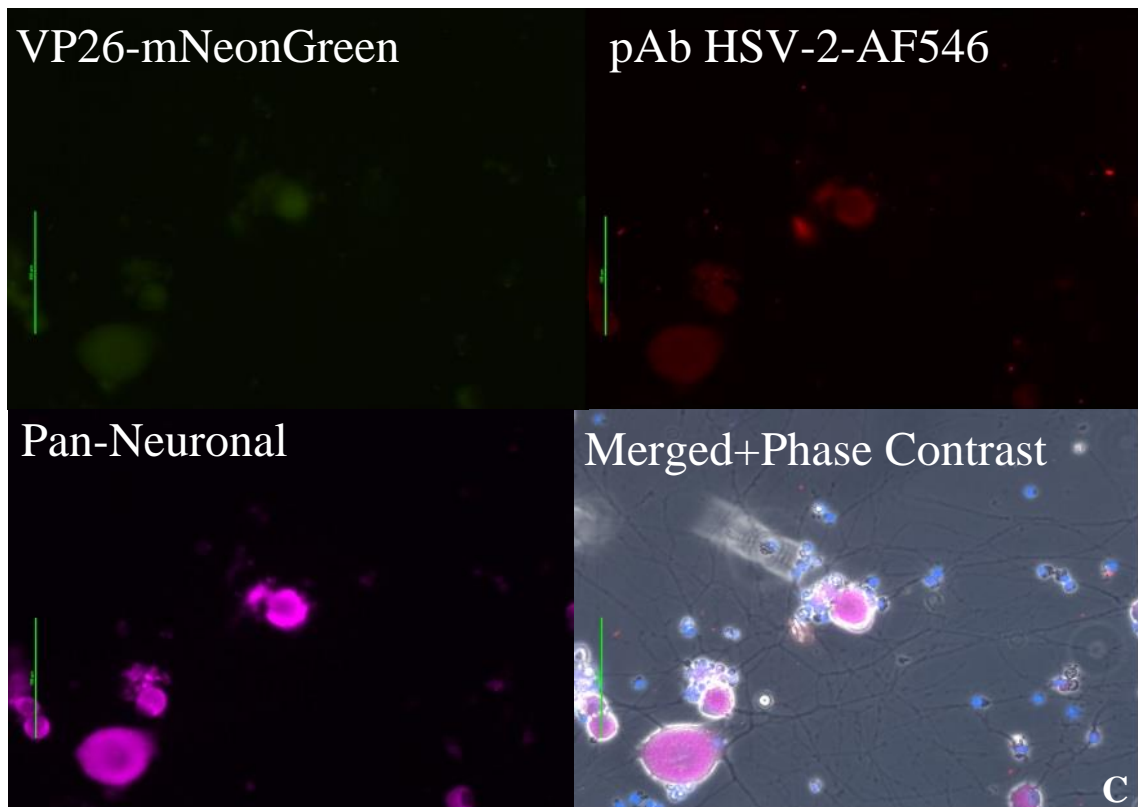
Figure 12. *Ex Vivo* Reactivation from explanted Sacral Dorsal Root Ganglia. Fluorescent images of enzymatically dissociated sensory neurons from guinea pigs 36 days post-infection and 72 hours post-plating with either (A) Strain 333 or (B) Nedel. Upper left: Detection of mNeonGreen fluorescence, Upper right: immunofluorescence using pAb HSV-2-AF546, Lower left: Pan-Neuronal stain, Lower right quadrant: Merged. Explant with (C) enlarged field of view with phase contrast, DAPI and a pan-neuronal stain. (D) Confocal image of explant with staining strategy used in A and B.
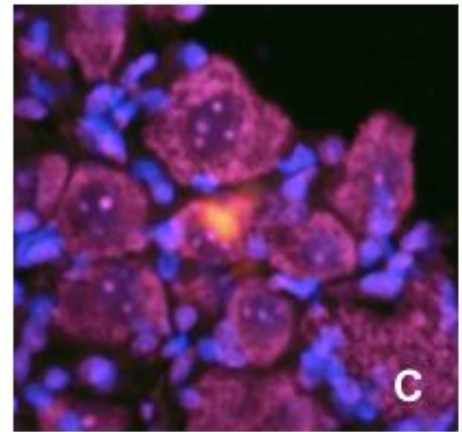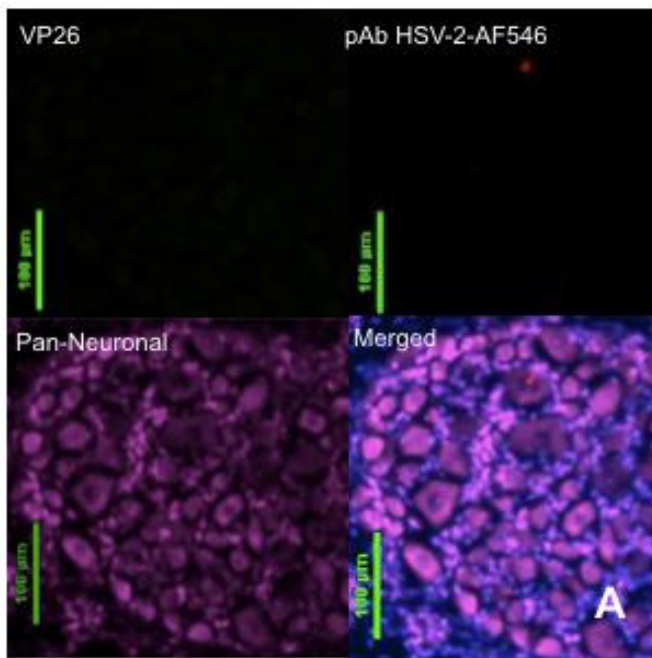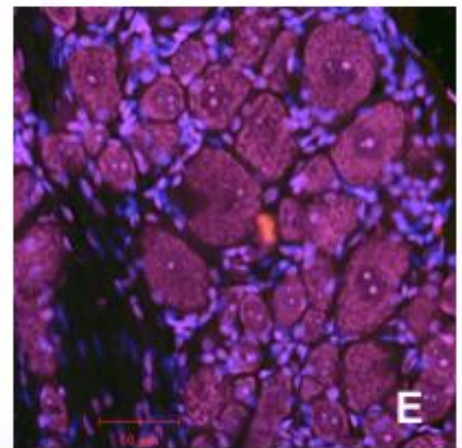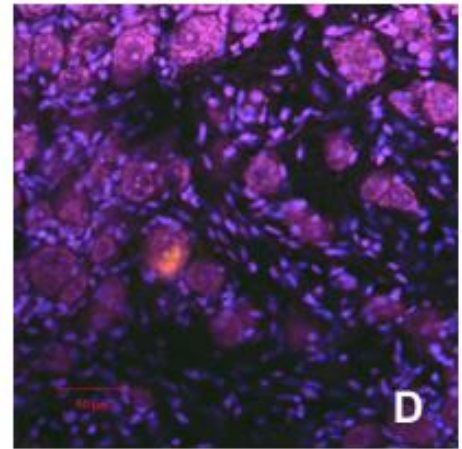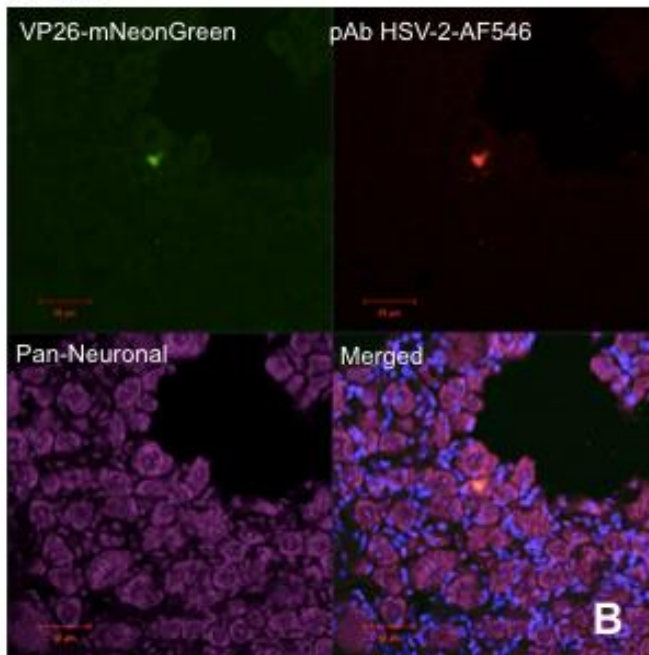
Figure 13. *In Vivo* Reactivation. Representative confocal microscopic images of immunolabelled cryosections of guinea pig sacral dorsal root ganglia (A) Strain 333 (B) Nedel. Upper left: Detection of mNeonGreen fluorescence, Upper right: immunofluorescence using pAb HSV-2-AF546, Lower left: Pan-Neuronal stain, Lower right: Merged. (C) Enlarged image of reactivation seen in B. (D,E) Additional neurons showing similar fluorescent spatial overlap, likely representing *in vivo* viral reactivation.

# Supplemental Figures



**Acute Infection**
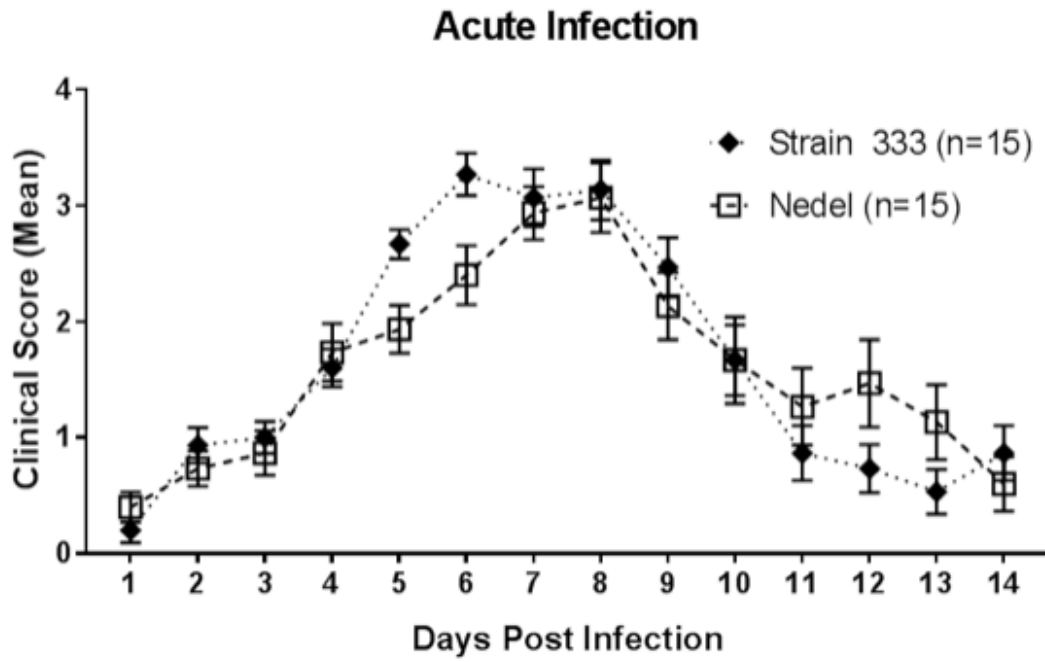
Figure 14. All Animals included in overall clinical score of genital skin.
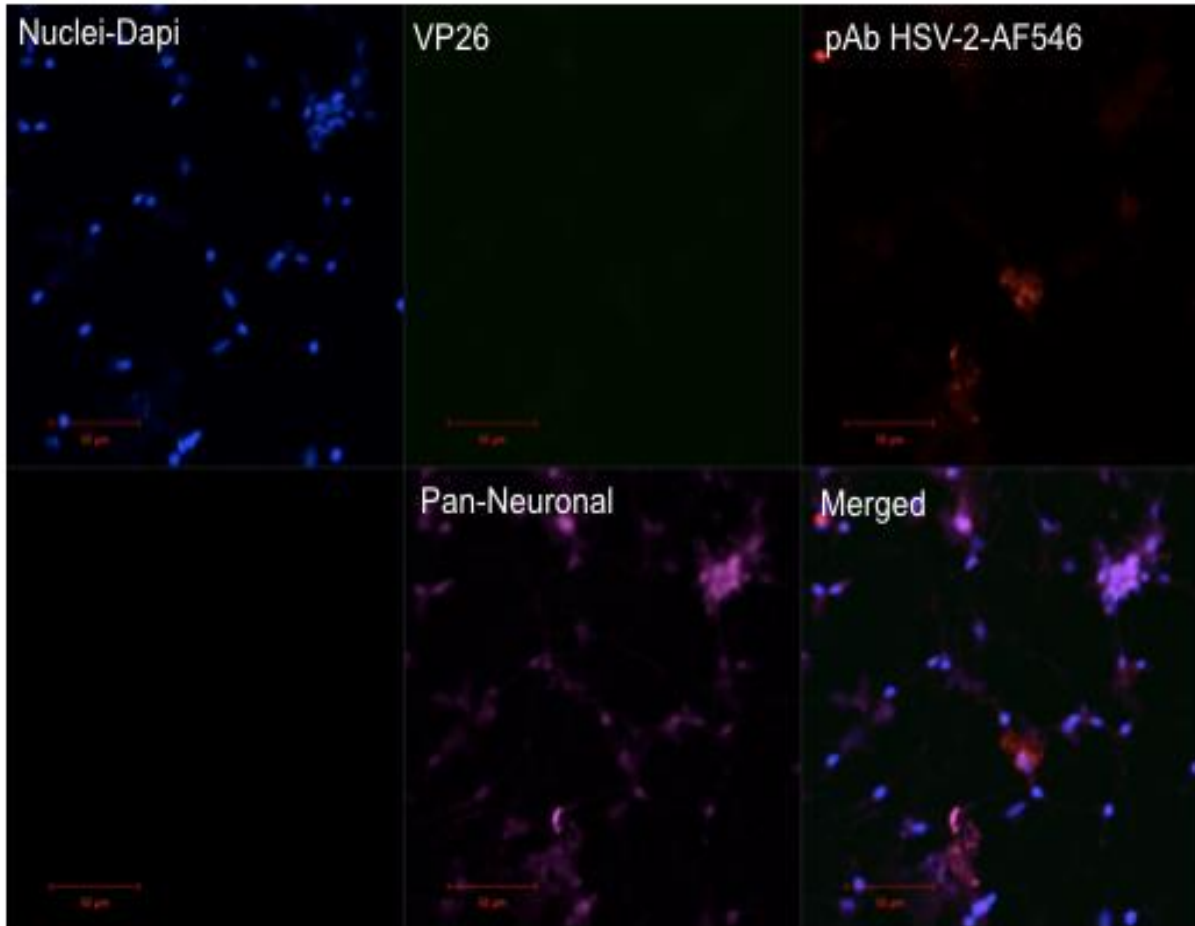
Figure 15. Confocal microscopic image of DRG explantation from Strain-333-infected animals. Control for pAb HSV-2-AF546, showing no bleed over into GFP channel.
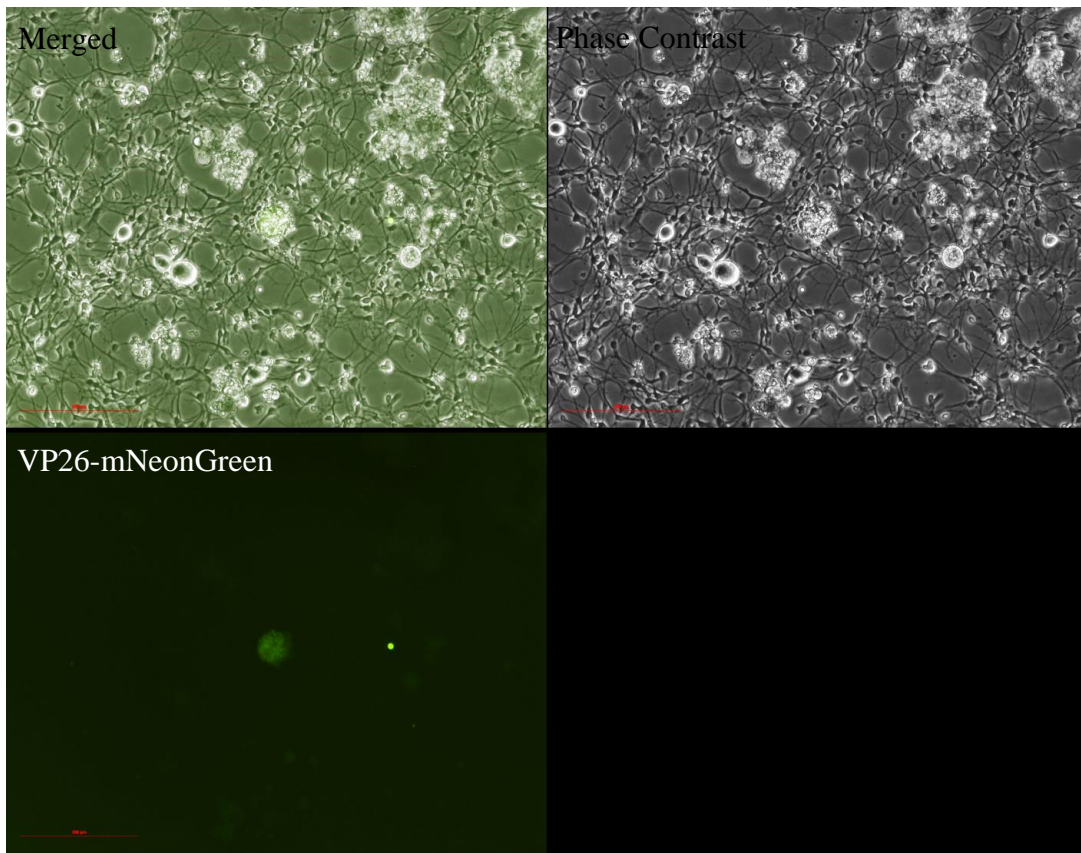
Figure 16. Low Magnification of fluorescence emerging 60 hours post-plating, pre-staining of explanted DRG.
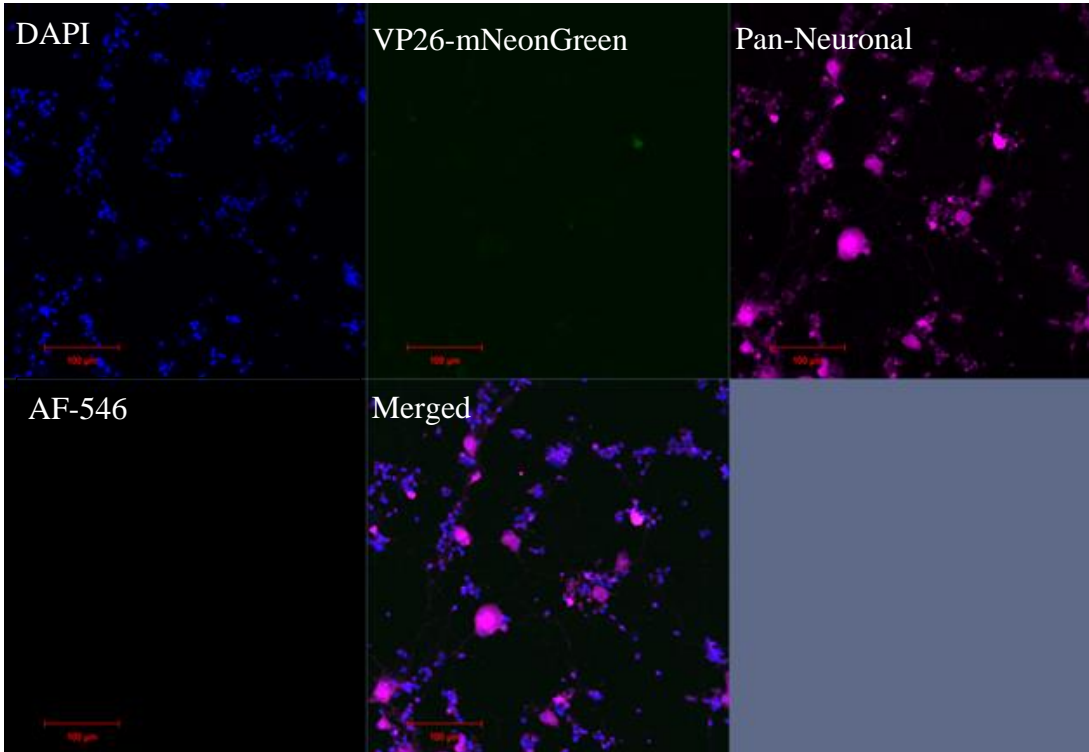
Figure 17. DAPI and Pan-Neuronal Stain only of Explanted, Nedel-Infected DRG. Parameters showing green fluorescence does not bleed into AF546 channel.
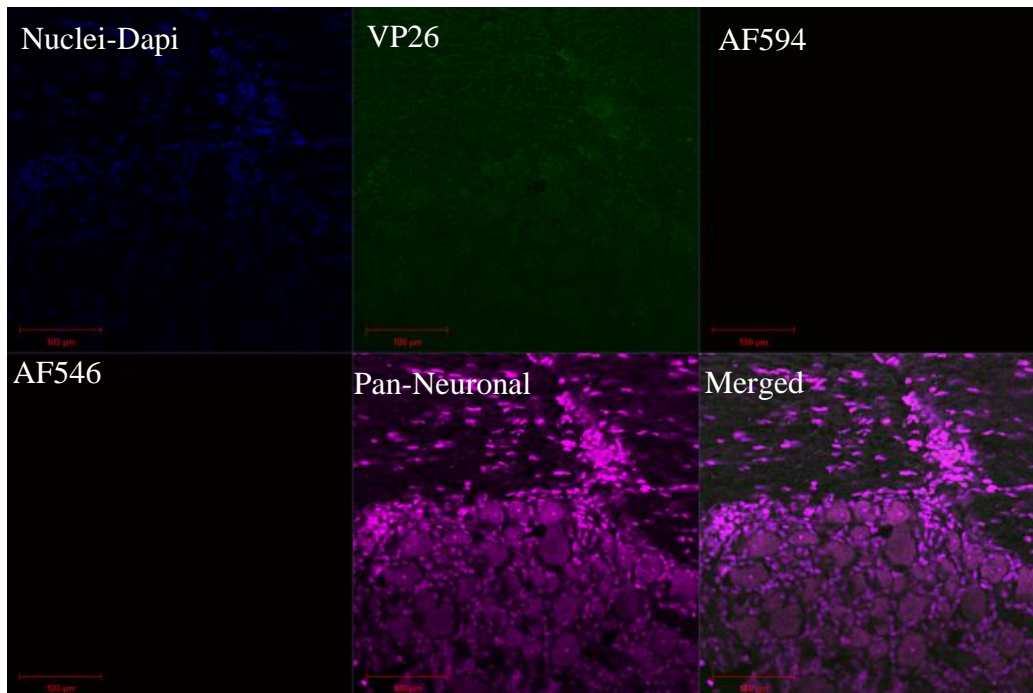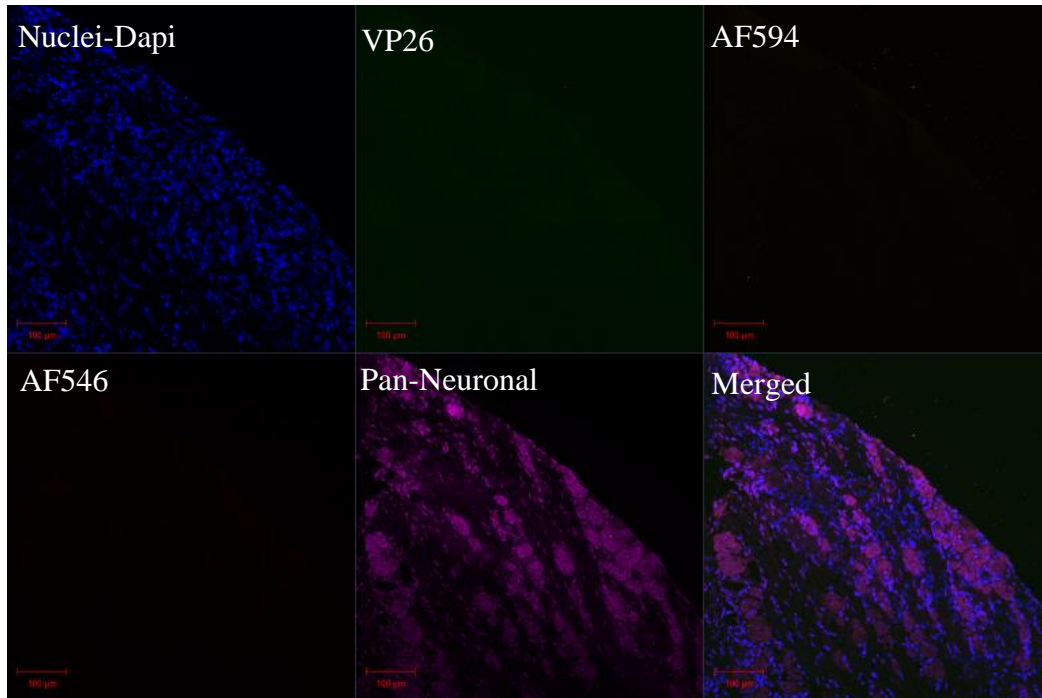
Figure 18. DAPI and Pan-Neuronal stain only, Strain 333-Infected. Parameters used to distinguish background levels or autofluorescence for confocal microscopy.

**Discussion**

We describe the construction and evaluation of a fluorescent HSV-2 variant. Unlike previously described fluorescent HSV, this virus is genetically stable, has normal morphology without aggregation, replicates *in vitro* and *in vivo* with normal kinetics, and has a wild-type spontaneous recurrence phenotype *in vivo*.

We attribute the successful construction of this virus to properties of the mNeonGreen fluorescent protein, which is much brighter than other fluorescent proteins and has no known tendency to aggregate. This likely allows for more normal VP26 interactions within the rest of the capsid, and prevents aggregation of capsid proteins before assembly and of the capsids themselves before envelopment. Monomeric NeonGreen emits a yellow-green fluorescence ($\lambda$em,max = 517 nm and $\lambda$ex,max = 506 nm), which may limit its use in highly autofluorescent tissues like the skin.

While Nedel exhibited Strain 333 kinetics of acute and recurrent infection of guinea pigs, we noted reduced neurovirulence during the acute infection when an inoculum of $10^6$ pfu was used. We did not construct a rescuant for Nedel since the recombinant virus otherwise behaved as wild type HSV-2 Strain 333, so it is not clear if this reduced neurovirulence is due to the VP26 mutation or to another unintentionally introduced mutation. Any reduced neurovirulence is in the range observed with other HSV-2 strains, and did not impact establishment of latency or viral reactivation.

We examined the capacity of Nedel to reactivate in three different ways. *In vivo* spontaneous reactivation evaluates the ability of reactivations to give rise to external recurrent lesions. *Ex vivo* reactivation after axotomy assesses the ability of the virus to

57

reactivate from within individual neurons after a strong stimulus, and typically led to altered morphology of neurons harboring reactivated virus. Identification of green fluorescence in cryosections indicated the capability of the virus to spontaneously reactivate from these neurons *in vivo*. The ability to scan unstained sections for green fluorescence greatly simplified the identification of these loci of viral reactivation. We did not identify morphological changes in the neurons harboring reactivating virus *in vivo*, which is consistent with a previous report (122).

Nedel is the first HSV-2 fluorescent strain with a normal reactivation phenotype. We intend to use this virus to study early reactivation events *in vivo* in more detail than has previously been possible. Inclusion of the mNeonGreen protein may also enhance the utility of fluorescent fusions of other herpesviruses and allow observation of infrequent or minimally produced proteins.

Nedel is the first HSV-2 fluorescent strain with normal reactivation phenotype. We intend to use this virus to study early reactivation events *in vivo* in more detail than has previously been possible. Inclusion of the mNeonGreen protein may also enhance the utility of fluorescent fusions of other herpesviruses and allow observation of infrequent or minimally produced proteins.

## Acknowledgements

Takeda for confocal microscopy guidance, Drs. Steve Rubin and Derek Ireland for instruction and use of the cryostats, and Preshant Desai for generous gift of the anti-VP26 pAb.

## Author Contributions

**Conflicts of Interest:** The authors declare no conflict of interest.

# CHAPTER 3: HSV-2 reactivates spontaneously from latency in autonomic ganglia

**Abstract**

Herpes Simplex Virus 2 (HSV-2) can be transmitted in the presence or absence of lesions, allowing efficient spread amongst the general population. Recurrent HSV genital lesions are thought to arise from reactivated latent virus in sensory cell bodies of the dorsal root ganglia (DRG). However, HSV-2 has also been found latent in autonomic ganglia. Spontaneous reactivation or a low level of chronic infection could theoretically also occur in these peripheral nervous tissues, contributing to the presence of infectious virus in the periphery and to viral transmission. Use of a recently described, optimized virus with a monomeric, mNeonGreen protein fused to viral capsid protein 26 (VP26) permitted detection of reactivating virus in explanted ganglia and cryosections of DRG and the sacral sympathetic ganglia (SSG) from latently infected guinea pigs. Immediate early, early, and late gene expression were quantified by Droplet Digital Reverse Transcriptase Polymerase Chain Reaction (ddRT-PCR), providing further evidence of viral reactivation not only in the expected DRG, but also the sympathetic SSG. These findings indicate that viral reactivation from autonomic ganglia is a feature of latent viral infection, and that these reactivations likely contribute to viral pathogenesis.

**Introduction**

Herpes Simplex Virus-2 (HSV-2) is globally pervasive, with approximately 417 million people aged 15–49 years infected, an estimated 11.3% global prevalence (90). Episode severity ranges from brief and asymptomatic, the most prevalent means of HSV-2 transmission, to extended periods with multitudes of painful genital lesions (96; 123). Regardless of severity, primary genital HSV-2 infections can cause acute sensory defects,

61

urinary retention, constipation, and erectile dysfunction (23; 53). Up to 15% of women report urinary retention following HSV-2 infection, but the mechanism remains unclear (146). In addition, HSV-2 infection during pregnancy can have devastating effects including spontaneous abortion, low birth weight, premature delivery, and, with neonates, localized infection, encephalitis, and disseminated infection. HSV-2 neonatal infections result in severe disability or death and 70% of their mothers were asymptomatic at the time of their birth (10; 72).

After the initial infection of epidermal and mucosal keratinocytes within the reproductive tract, the virus travels retrograde from the synaptic terminal, through the axon, to the soma of the sensory neuron. The virus forms an episome within the neuronal cell body's nucleus, persisting for the lifetime of the host in latency, evading detection and immunity, with episodic reactivation to cause lesions or asymptomatic shedding. Upon reactivation, the virus travels anterograde, exiting the dendrites to replicate in the periphery. It has long been suspected that virus also infects peripheral autonomic ganglia and innervated tissues, giving rise to autonomic symptoms during acute infection(113), but reactivation via autonomic pathways has not yet been demonstrated.

It is known that HSV-2 enters the termini of neurons whose sensory somas congregate in the coccygeal and sacral plexus of the dorsal root ganglion. These neurons innervate a specific dermatome of the genital skin and buttocks associated with sites of viral reactivation-induced lesions, but sensory neurons are not the only neurons that innervate the reproductive tract or this specific dermatome. Autonomic sympathetic and parasympathetic termini are also available escape routes for the virus. The parasympathetic preganglionic neurons that innervate the genitourinary tract arise from

62

the sacral region (S2-4), the same vicinity of HSV-2's primary site of latency in the

DRG. Similarly, the sympathetic ganglia, L4-L6 in humans and L6-S2 in small animal

models (79; 87), have highly branched axons that innervate the genitourinary tract, as

well as the dermis of the skin, therefore also serving as potential anterograde and

retrograde transport of virus to and from the peripheral tissues.

In the HSV-1 Rabbit eye model, HSV was detected not only in tears, but in saliva,

suggesting a wider dispersal of herpetic reactivation than could be explained by

reactivation within a single division of the sensory trigeminal ganglion (62). More

recently, clinical observations have led to a break from the paradigm that HSV

reactivation only occurs concurrently with repeated physiological locations of ulcerations

(70). Analyses of human biopsies have revealed multiple sites of reactivation, widely

distributed over the genital tract and deep within the dermis in the absence of obvious

lesions (70). The large number of concurrent non-contiguous reactivation sites suggests

that these recurrences also are not sourced from a reactivation that occurs in a single

sensory neuron, but might more likely represent recurrences in peripheral autonomic

ganglia which may disperse virus to multiple peripheral sites. This finding points to

potential sympathetic neuron involvement due to their termini's innervation of the deeper

dermis alongside those from the sensory neurons and could influence the strategy we take

to treat the infected (18).

While humans are the only natural host for HSV-2, mice, guinea pigs, and rabbits

can be infected and used for study of reactivation *in vivo*. In the murine vaginal infection

model, HSV-2 can spread not only to the dorsal root sensory ganglia (DRG), but to the

autonomic parasympathetic neurons of the major pelvic ganglia (MPG) and the sympathetic chain (109). In another murine vaginal infection model using HSV-1, the parasympathetic enteric neurons were involved in pathogenesis and lethality, though it did not appear that the sympathetic chain was involved by analysis of tissue homogenates (74). Because HSV does not spontaneously reactivate to cause lesions in latently infected mice, the role of these ganglia in recurrent disease could not be established in these experiments. In contrast, HSV-2 does reactivate and recur spontaneously from vaginally-infected female guinea pigs, more closely modeling human disease and allowing study both of acute infection and of viral reactivation. During acute infection of guinea pigs, typical human autonomic symptoms, such as urinary retention, may also be observed. Rapid but independent spread of acutely infecting virus both to DRG and spinal cord (SC) suggests that the virus may spread to SC via autonomic pathways (106). Using the guinea pig ocular infection model, investigators measured the presence of early gene expression in both the sympathetic and parasympathetic ganglia, but did not see obvious HSV-2 gene expression within parasympathetic ganglia (84). Thus, reactivation within peripheral autonomic ganglia could explain some important aspects of viral pathogenesis.

Using the guinea pig as a spontaneous reactivation model with a recently described and optimized fluorescing virus, we investigated the ability of HSV-2 to reactivate from autonomic ganglia. During latency, we used viral fluorescence in neurons to detect likely viral reactivation, which we confirmed by also detecting viral glycoproteins via antibody staining. We also quantified expression of viral genes in autonomic and dorsal root ganglia to assess potential viral reactivation from these locations.

**Methods**

**Viral strains and stock production.** HSV-2 strain 333 was originally obtained from Gary Hayward (Johns Hopkins University, Baltimore, MD). mNeonGreen was obtained from Allele Biotech (San Diego, CA) and the mutant virus Nedel has recently been described (paper under submission). The mutant and parental strain virus were propagated in Vero cells (ATCC® CCL-81™).

**Animals.** Female Hartley (5 for explant, 5 for cryosectioning, 20 for ddRT-PCR, 125-150g Charles River Breeding Laboratories, Wilmington, MA) were intravaginally inoculated with $1x10^6$ pfu HSV-2 (Strain 333 or mutant virus) as previously described(128). All animal experiments were performed under protocols approved by the Institutional Animal Care and Use Committee of the Food and Drug Administration (Protocol 1997-08).

*Ex vivo*

**Explant reactivation.** Dorsal root ganglia, major pelvic ganglia and sacral sympathetic ganglia were harvested and cultured as previously described(13). Ganglia were enzymatically dissociated in collagenase, papain and dispase (Worthington) before mechanically titurating and plating on Matrigel-coated 8-well Lab-Tek II chamber slides (ThermoScientific). Cultures were then fixed for 5min in 4% paraformaldehyde, gently rinsed in Phosphate Buffer Saline (PBS) and immunolabelled. Immunolabelled neuronal cultures were evaluated by Zeiss LSM 710 upright confocal laser scanning microscope.

*In vivo*

**Cryosectioning.** Animals were cardiac-perfused with PBS followed by cardiac-perfusion with 4% paraformaldehyde. Dorsal root ganglia, major pelvic ganglia and the sacral sympathetic chains were dissected, rinsed in PBS and sucrose-protected overnight. Tissues were embedded in OCT (TissueTek®) and 10μm sections were made with a cryostat (Leica). Sections were permeabilized, blocked and immunolabelled before viewing with a Zeiss LSM 710 upright confocal laser scanning microscope.

**Immunolabelling of explanted ganglia, and cryosections.** Antibodies used included: NeuroTrace™ 594 or 640/660 Deep-Red Fluorescent Nissl Stain (N21483, Thermofischer Scientific), Mouse anti-HSV-2 gH/gL (H2A269-100, Virusys, Taneytown, MD), Mouse anti-HSV gB (HA056-100, Virusys, Taneytown, MD), Mouse anti-HSV gD (HA025-100, Virusys, Taneytown, MD), Sheep anti-Rat Choline Acetyltransferase 1:500 (catalog# OSC00041W, Invitrogen), Goat anti-Mouse IgG (H+L) Highly Cross-Adsorbed Secondary Antibody, Alexa Fluor 546 (catalog# A-11030, Thermo Fisher Scientific), Donkey Anti-Sheep IgG H&L (Alexa Fluor® 594) (ab150180, Thermofischer Scientific). A primary pAb antibody was made in-house by combining equal amounts of the murine mAb to gB, gD, gH/L listed above. Post-permeabilization and blocking, samples were labelled with the primary antibody for 24 h at 4 °C, secondary antibody for 24 h at 4 °C, labelled with Nissl stain for 2 h at room temperature before DAPI staining. Cryosections also were treated with TrueBlack™ for 30 s.

**ddRT-PCR with Ganglia.** Tissue was harvested from $CO_2$-euthanized animals and homogenized using the Precellys 24 homogenizer and CKMix beads (ceramic zirconium

oxide mix beads of 1.4mm and 2.8mm in 2mL standard tubes). All animals were at least

21 days post-vaginal infection. Symptomatic animals were euthanized on the first day of

symptoms (after at least a 3-day symptom-free period), while asymptomatic animals were

lesion-free for at least 3-4 days prior to euthanasia. RNA was extracted per

manufacturer's instructions (TRISure[TM], Bioline, London, UK). Previously validated

primers and probes were used (Tang 2008, 2009). Bio-RAD's QX100 system was used to

generate and read droplets. Statistics were performed using GraphPad Prism version 7.0

for Windows (GraphPad Software, La Jolla, CA).


**Results**

To detect reactivation-competent latent virus in major pelvic ganglia and the

sacral sympathetic ganglion, we explanted ganglia from animals 36 days after vaginal

infection with our recently described fluorescing virus we've named "Nedel". This

mutant virus fluoresces due to a mNeonGreen minor capsid fusion (VP26), replicates

with wild-type kinetics and reactivates from latency *in vivo*. The infected ganglia were

gently enzymatically and mechanically dissociated for plating into chamber well slides.

In this model, the nutrient rich media allows for the regrowth of axons, while the

axotomy during dissection stimulates reactivation (122; 130). Fluorescence became

visible at 48 hours with maximum intensity materializing 72 hours post-plating.

Fluorescence emerged from the expected sensory DRG (Fig.19 A, B) and the SSG

(Fig.19 C, D, 25-27). The explanted ganglia at 72 hours were fragile and many did not

remain adherent to the slide following triple-labelling and intermittent washes, preventing

quantification of reactivation in these experiments. The major pelvic ganglia had too few

validated reactivations (both positive for VP26 and HSV-2-AF546), to conclusively

determine reactivation. It is likely that the virus does not efficiently reactivate from the

MPG in latency. The fluorescent green capsid protein co-localized with the red

fluorescent HSV-2 pAb within magenta labelled neurons from the DRG and SSG. Thus,

SSG that innervate the genital tract harbor reactivation-competent latent HSV, as do the

DRG.

To determine whether virus in autonomic ganglia is reactivation-competent *in vivo*, latently infected guinea pigs underwent cardiac perfusion with paraformaldehyde

euthanasia, followed by fluorescent immunolabelling of cryosections from the DRG,

MPG and SSG. The cardiac perfusion ensured that subsequent dissection would not

stimulate reactivation post-mortem, but instead accurately reflect what was occurring *in vivo*. Fluorescence was observed from within neurons in the DRG (Fig.20 A, B) and SSG

(Fig.21 A, B, 28-30), indicating the presence of fluorescent capsid protein. Again, after

using a stain to remove significant autofluorescence within the MPG, only 2 neurons

exhibited both green and red fluorescence within the same cell, which points to a lack of

reactivation-competent virus in these ganglia. In the DRG and SSG, again the capsid's

fluorescent signal co-localized with anti-HSV-2 glycoprotein pAb, further verifying the

presence of virus.

Twenty additional, latently infected guinea pigs were evaluated by digital droplet

Reverse Transcriptase Polymerase Chain Reaction (ddRT-PCR) for the presence of viral

RNA. In order to determine the quantity of genomes maintaining latency, we evaluated

the expression of the only transcript made during latency, aptly named the Latency

associated transcript (LAT). LAT was detected in 20/20 infected animals in both the

DRG and SSG, providing further evidence that latency can be established and maintained in the autonomic ganglia. There was significantly more LAT production in the DRG which suggest more latent genomes maintaining latency as opposed to reactivating or a larger pool of latent genomes (Fig.22A, B). LAT in the MPG was undetectable in most animals.

To detect reactivation, we measured early gene, thymidine kinase (TK) expression. There was a greater abundance of TK in the symptomatic animals (Fig. 23A) and more TK expression in the DRG (Fig. 23B). However the copy numbers were very low in both ganglia and expression of early gene production may represent early or abortive reactivation (44; 94), which may be expected to be present in proportion to the presence of latent virus, which likely is in turn proportional to LAT expression.  Levels of the early gene thymidine kinase (TK) in the SSG were not significantly different from that observed in the DRG when relative to LAT.

However, TK transcript levels do not reflect the relative abundance of fluorescent protein seen in the *in vivo* tissue sections. Expression of late genes is most likely to represent ongoing or recent reactivation.  The late gene gD relative transcript difference was not statistically significant between the DRG and SSG (Fig 22C, P= 0.1222), which did mirror our observations of labelled cryosections. While gD levels were not correlated with the presence of symptomatic recurrence (suggesting that gD expression in ganglia might sometimes either lead or trail peripheral observations), relatively high levels of gD were observed both in the DRG and SSG (Fig.24 A, B), with 20/20 and 16/20 animals showing detectable levels of gD in the DRG and SSG, respectively. There was more gD expression in the DRG versus the SSG in 12/20 animals. However 7/20 animals exhibited

69

more gD transcripts in the SSG than in the DRG. Identification of gD RNA in both of these locations is consistent with the qualitative findings in fluorescently-labeled cryosections, which also indicate that *in vivo* reactivations can occur in both of these ganglia (Fig. 24B). The animals with a greater abundance of LAT had fewer gD transcripts per LAT copy number (Fig 24 C). By framing the data in this light, we see a pattern of where there is more LAT expression, there are less reactivation events represented by gD expression, suggesting greater maintenance of latency as opposed to productive infection. We can also get a sense of the efficiency of reactivation by looking at late gene expression, gD, per latency associated transcripts, LAT (Fig. 24 C, D). In 10/20 animals, there was more relative gD expression in the SSG and 8/20 animals had higher relative expression in the DRG. In one animal, the relative amounts were similar and in another animal, there was too little gD in both the DRG and SSG in comparison to the abundance of LAT expression. When comparing the relative amounts of gD per LAT in the DRG and SSG, there is not a significant difference, indicating the same efficiency of reactivation from these two anatomical locations (Fig. 24 D).

**Figures**

VP26-mNeonGreen

50 μm

B
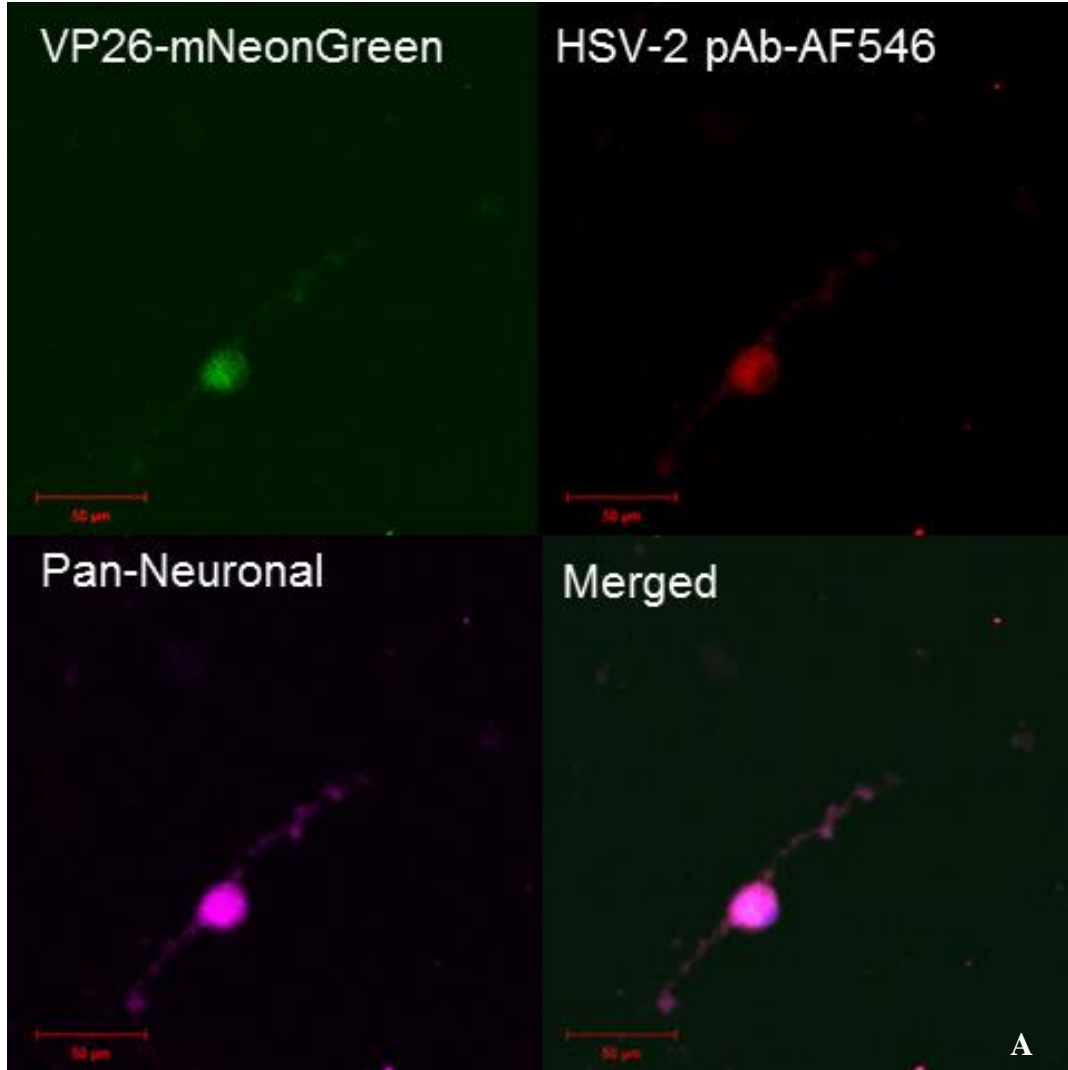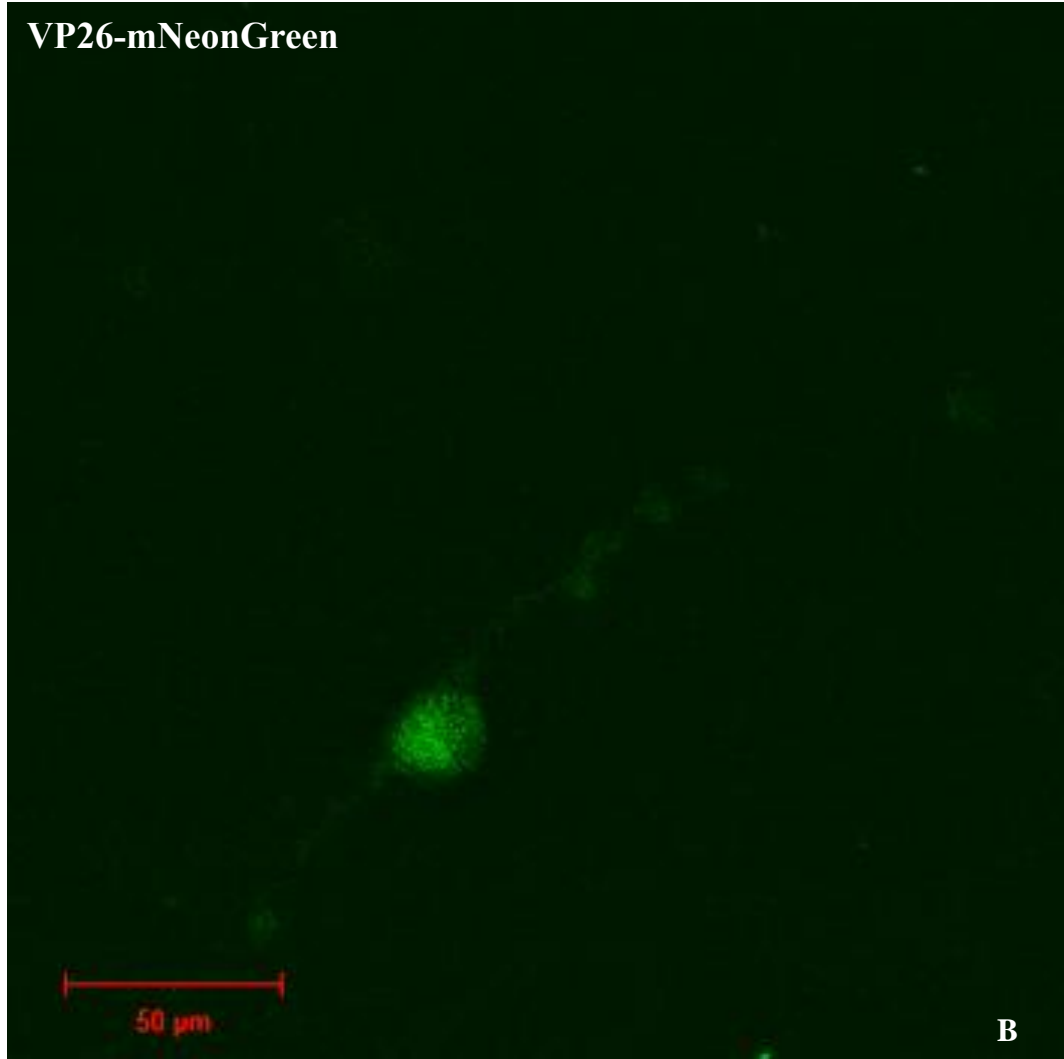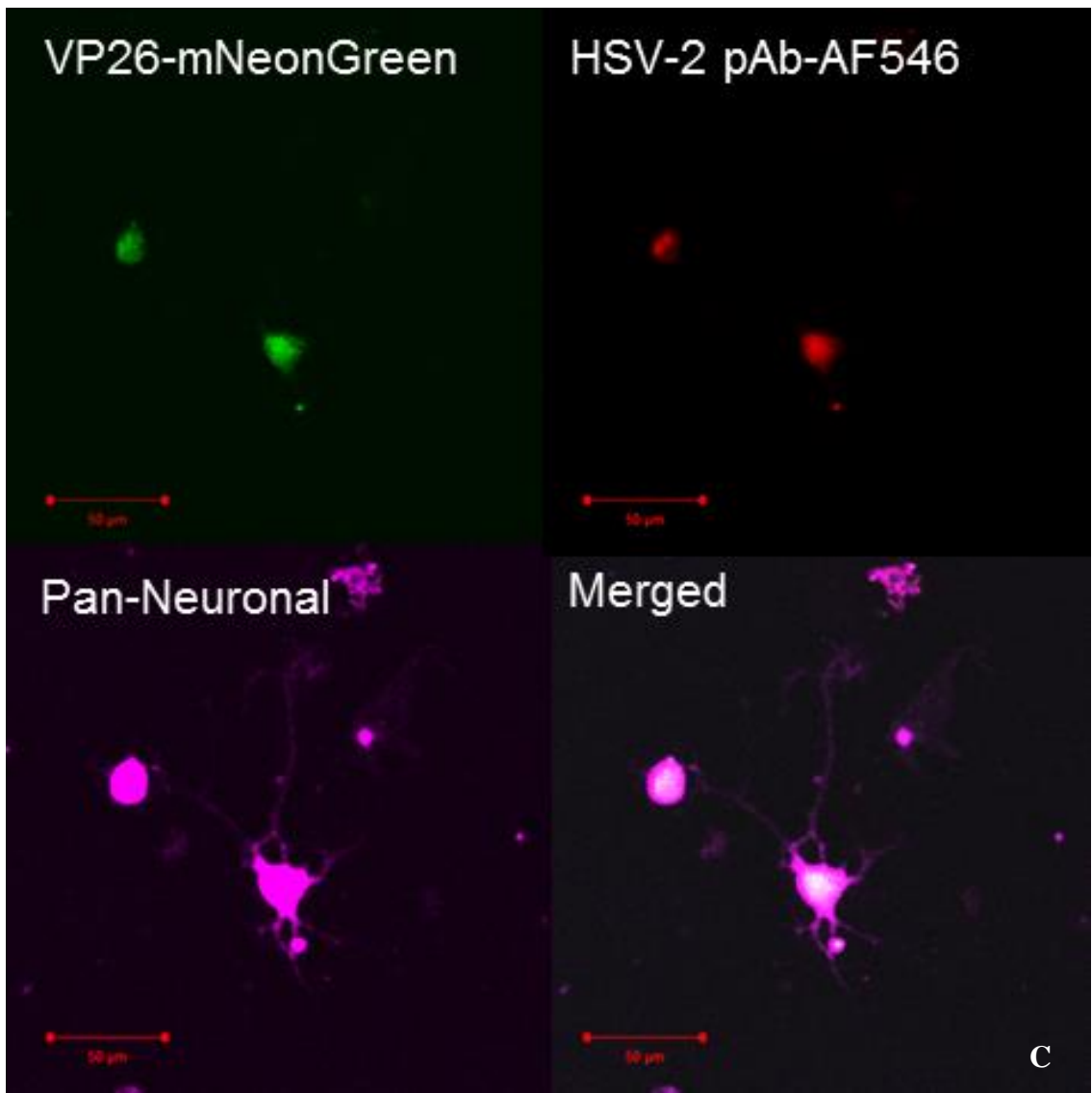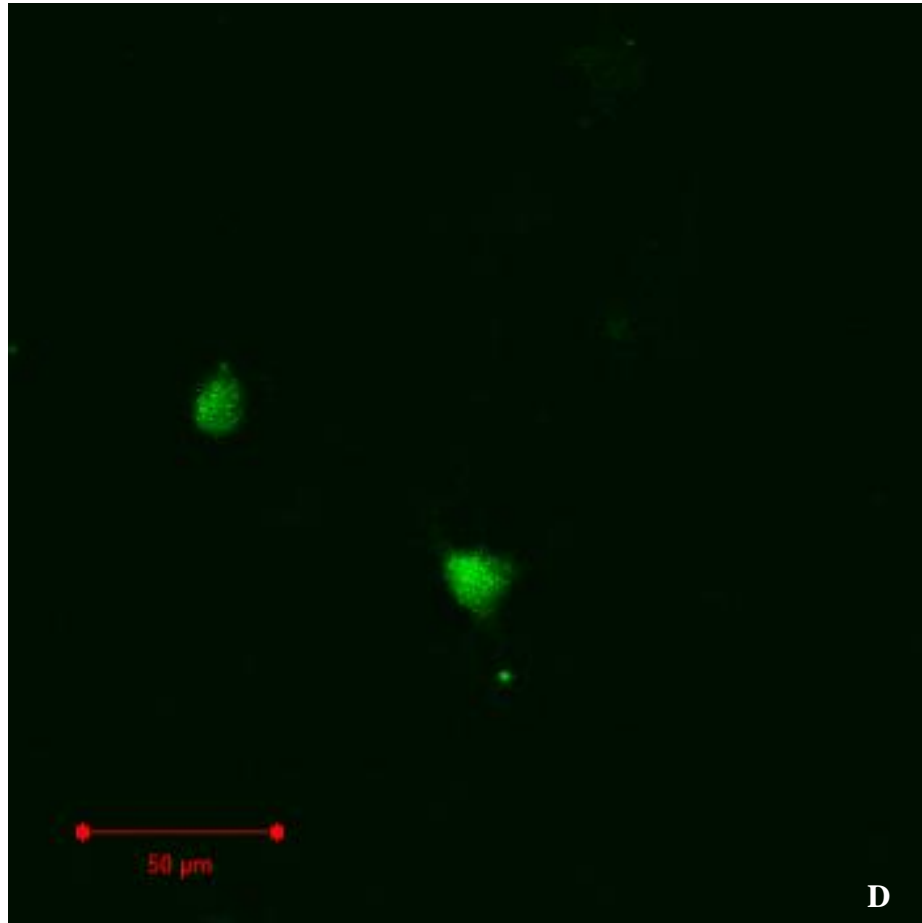
Figure 19. Ganglia Explantation: Representative images of *in vivo* Nedel-infected, dissociated and explanted (A) Sensory Dorsal Root Ganglia (B) Expanded image of VP26-mNeonGreen from A (DRG) (**C**) Sacral Sympathetic Ganglia (SSG) (D) Expanded image of VP26-mNeonGreen from C. Upper left: Detection of mNeonGreen fluorescence, Upper right: immunofluorescence using pAb HSV-2-AF546, Lower left: Pan-Neuronal stain, Lower right quadrant: Merged
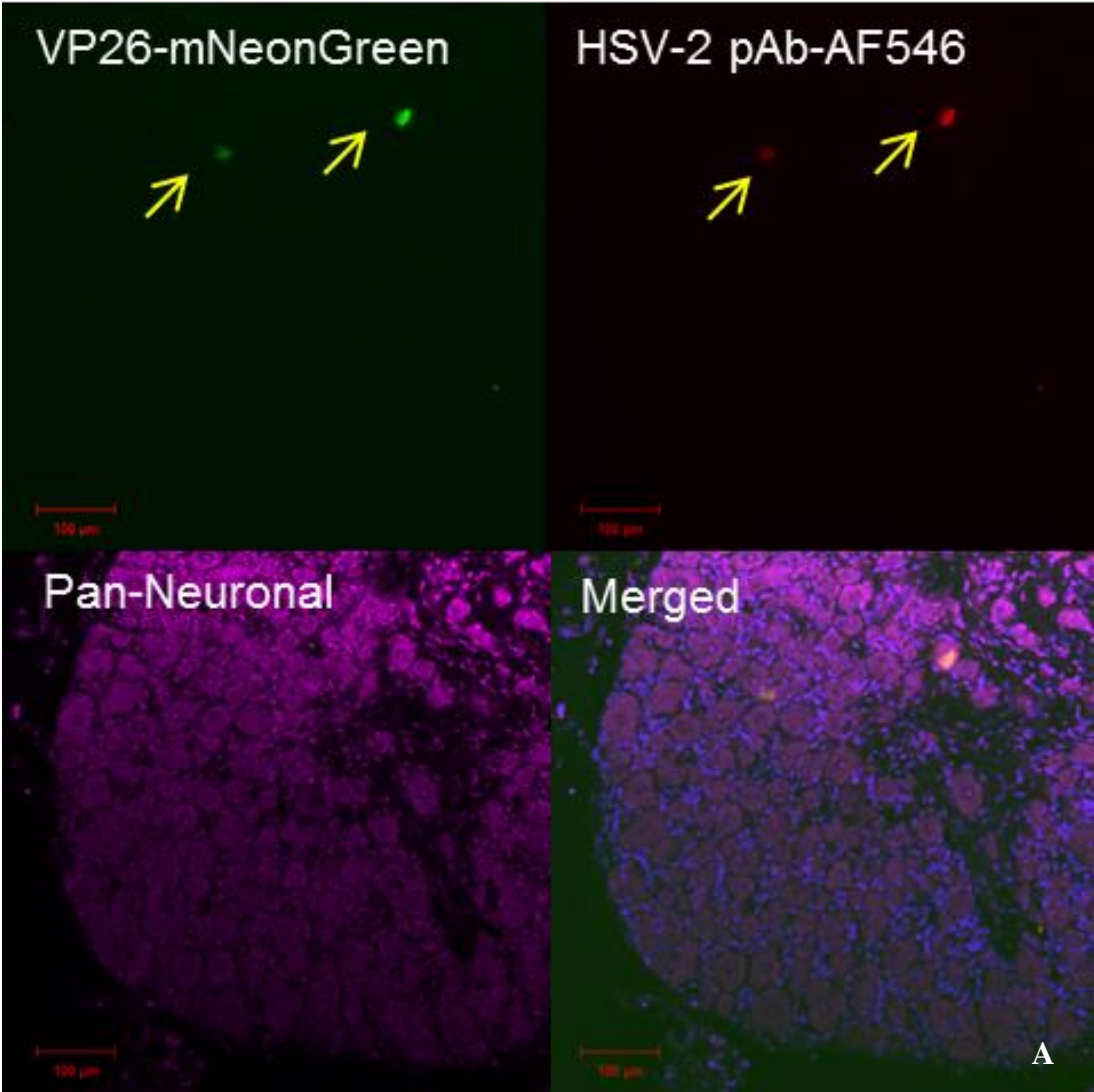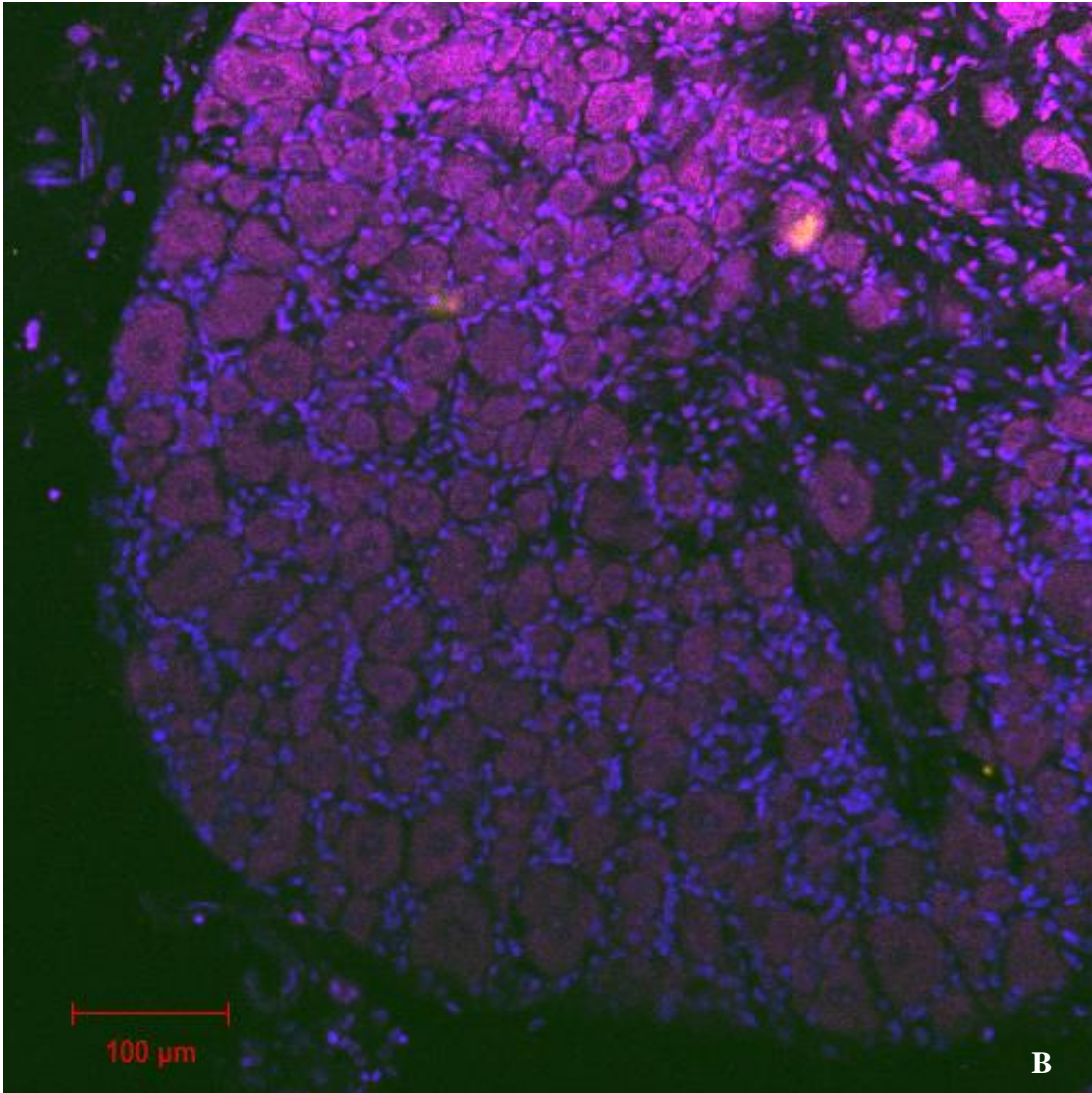
Figure 20. *In vivo* reactivation. Confocal images of immunolabelled, Nedel-infected frozen tissue section of the (A) DRG and (B) Expanded Merged A; Upper left: Detection of mNeonGreen fluorescence, Upper right: immunofluorescence using pAb HSV-2-AF546, Lower left: Pan-Neuronal stain Lower right quadrant: Merged. Arrows point to cells exhibiting fluorescent capsid and anti-HSV-2 pAb.
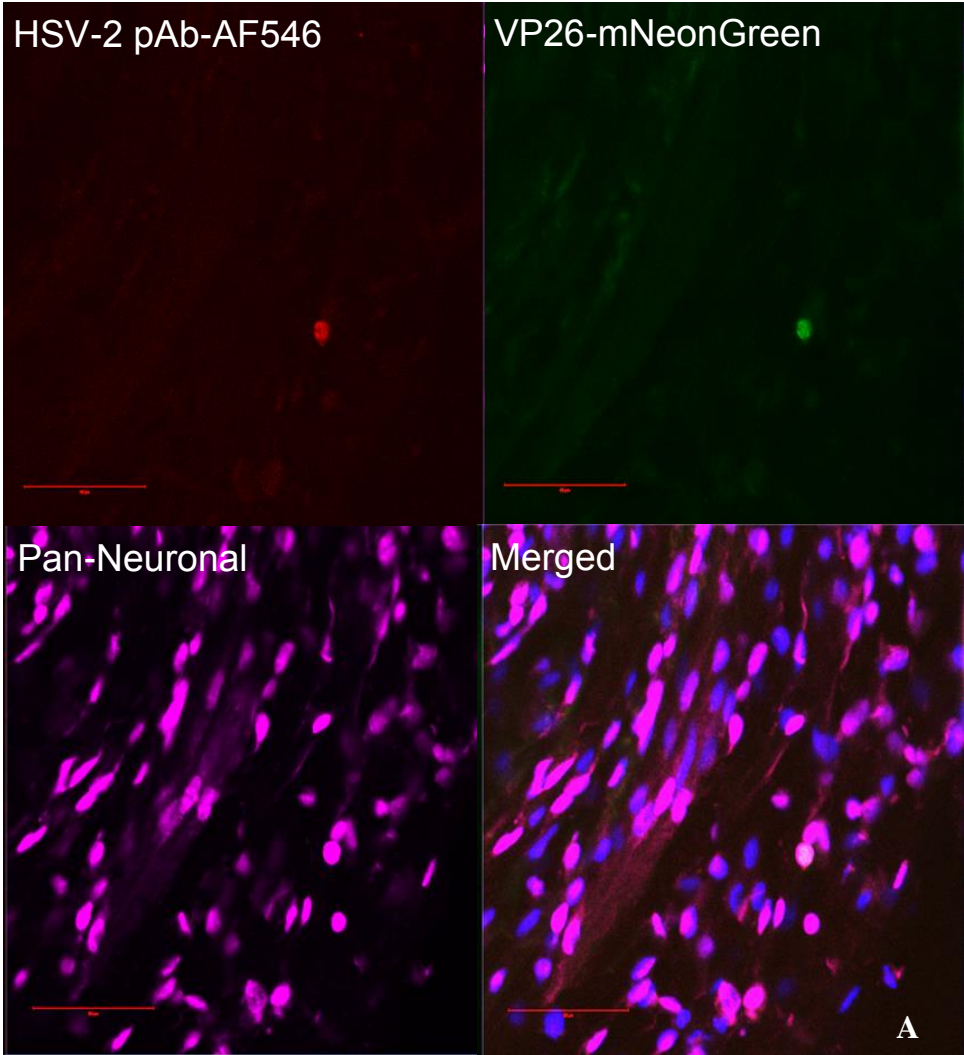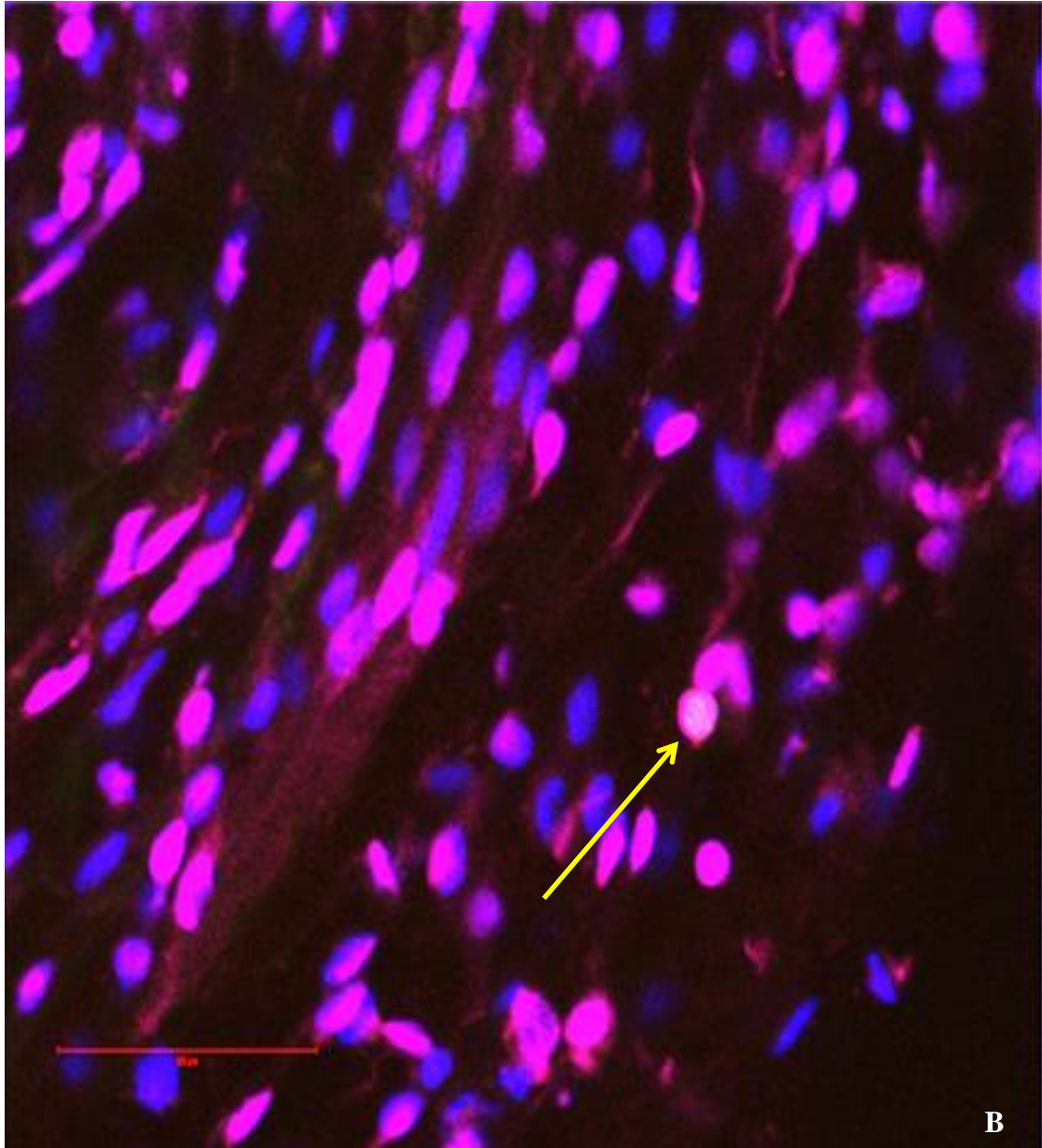
Figure 21. *In vivo* reactivation. Confocal images of immunolabelled, Nedel-infected frozen tissue section of the (A) SSG and (B) Expanded Merged A; Upper left: Detection of mNeonGreen fluorescence, Upper right: immunofluorescence using pAb HSV-2-AF546, Lower left: Pan-Neuronal stain Lower right quadrant: Merged. Arrows point to cells exhibiting fluorescent capsid and anti-HSV-2 pAb. Red bar = 50um.

**LAT**

(A) Bar graph showing Copies/200 ng Total RNA for DRG (red) and SSG (black) across individual animals grouped as Asymptomatic (Animal Numbers 1, 3, 5, 6, 10, 13, 14, 15, 17, 20) and Symptomatic (Animal Numbers 2, 4, 7, 8, 9, 11, 12, 16, 18, 19), with an uninfected control.

(B) Scatter plot comparing Copies/200ng Total RNA between DRG and SSG. *
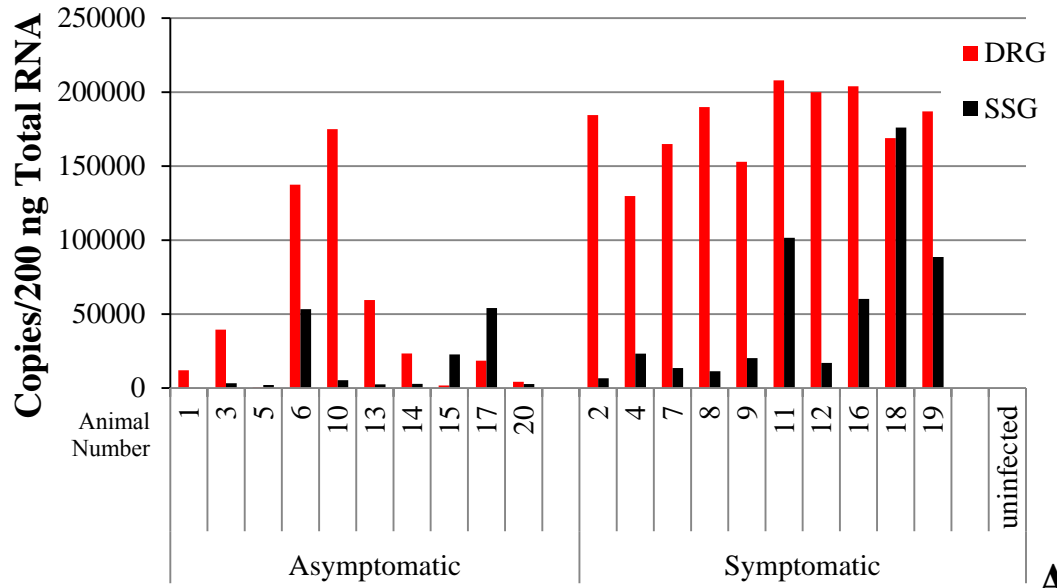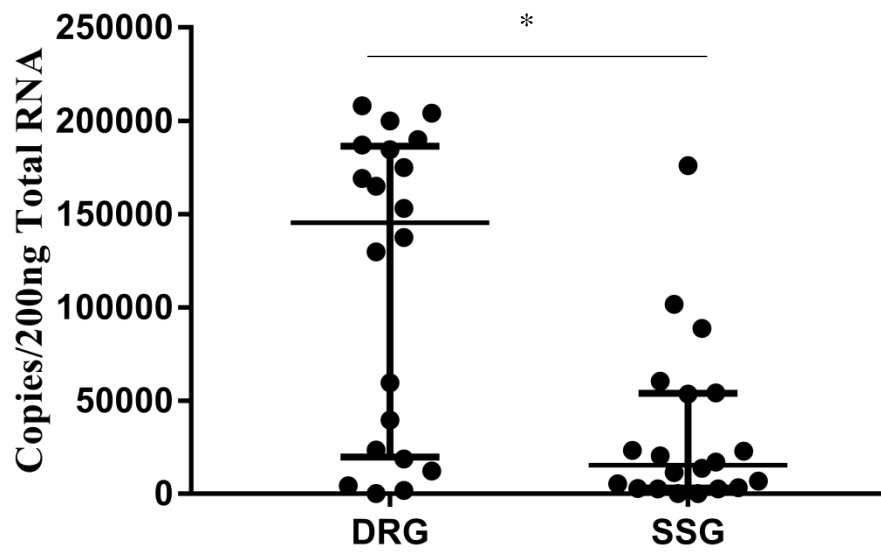
Figure 22. Latency Associated Transcript Gene Expression. (A) Raw copy number per individual Animal in the DRG and SSG, average of technical triplicates. (B) Summary of LAT expression (n=20) Mann-Whitney P value = 0.0032. Error bars represent median and inner quartile range.

**TK**

A

**TK**

B

**TK/LAT**

C

**TK/LAT**

D
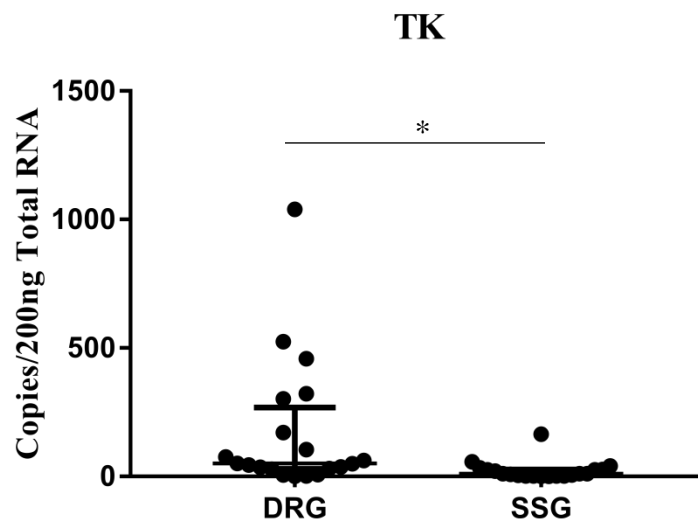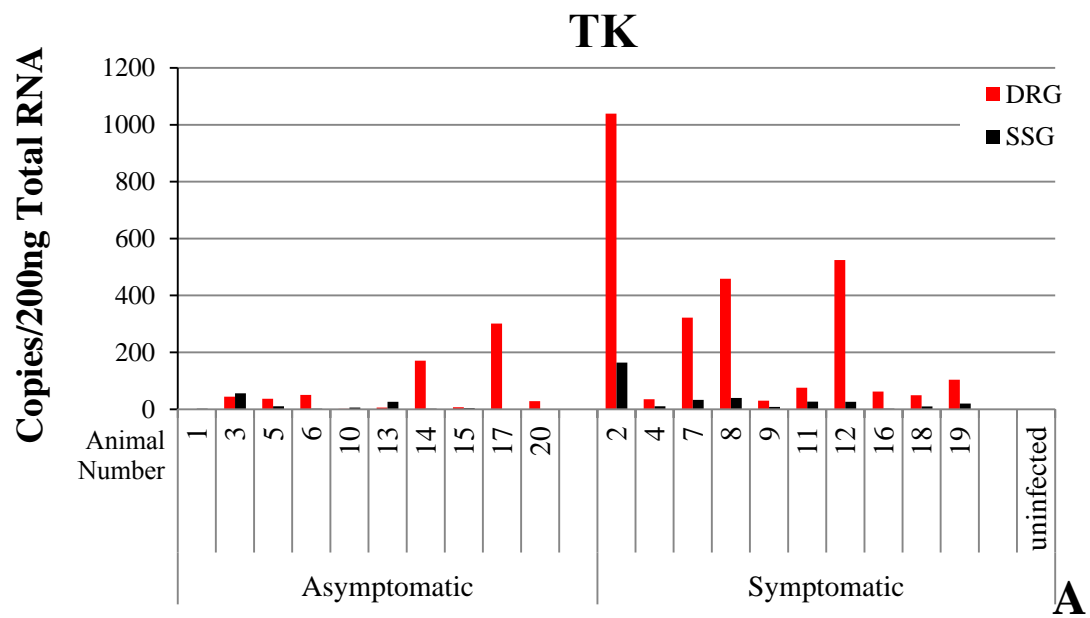
Figure 23. Early Gene Thymidine Kinase (TK) Expression (A) Raw copy numbers per individual animal, average of technical triplicates. (B) Summary TK expression (n=20), Mann-Whitney P value = 0.0011 (C) Relative expression, per copy of LAT (D) TK/LAT Relative Expression Summary, Mann-Whitney P value = 0.5966

gD

# gD/LAT



C

# gD/LAT



D

85
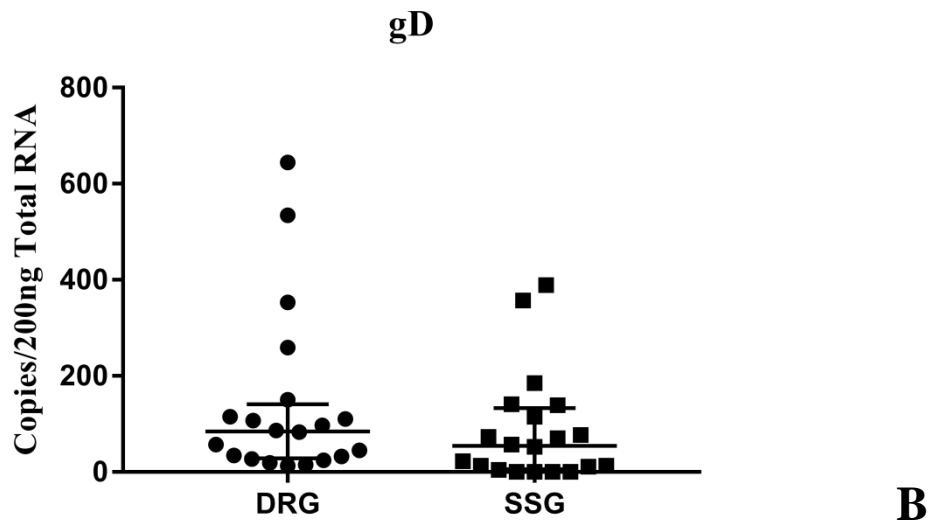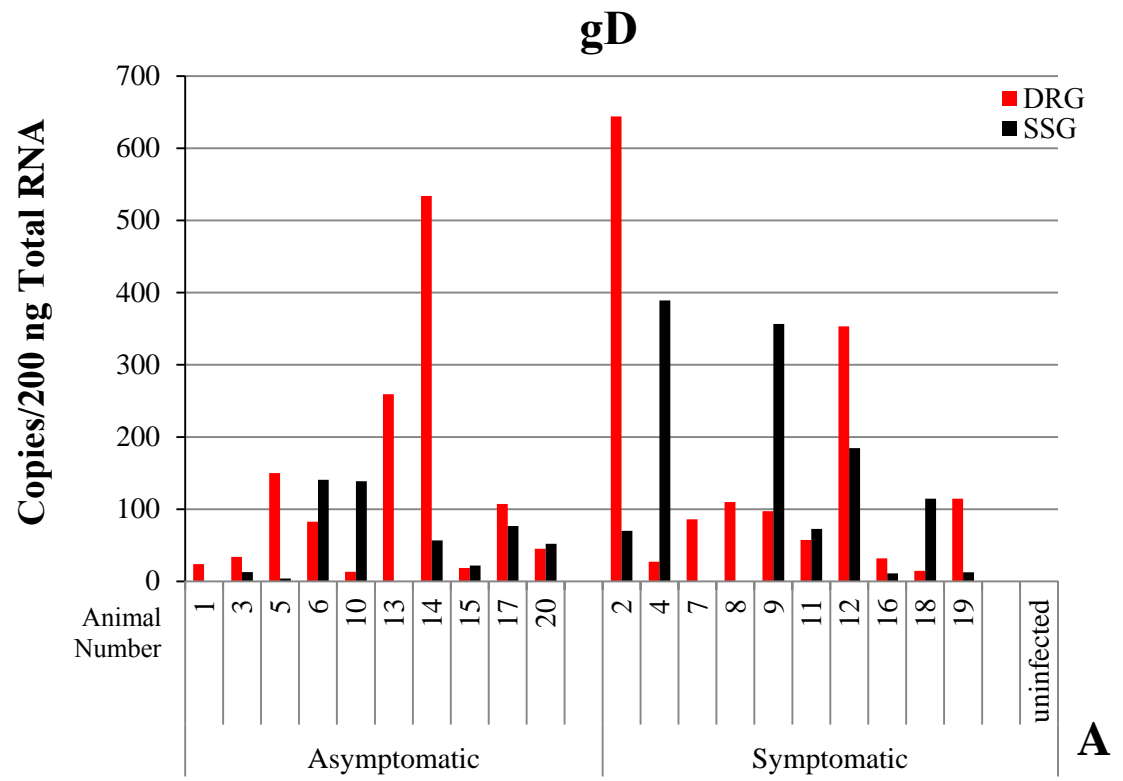
Figure 24. Late Gene gD Expression. (A) Individual Animals (B) Summary (n=20), Mann-Whitney P value = 0.1222  (C) Relative expression, per copy of LAT (D) Summary Relative Expression, Mann-Whitney P value = 0.7533

**Supplemental Figures**
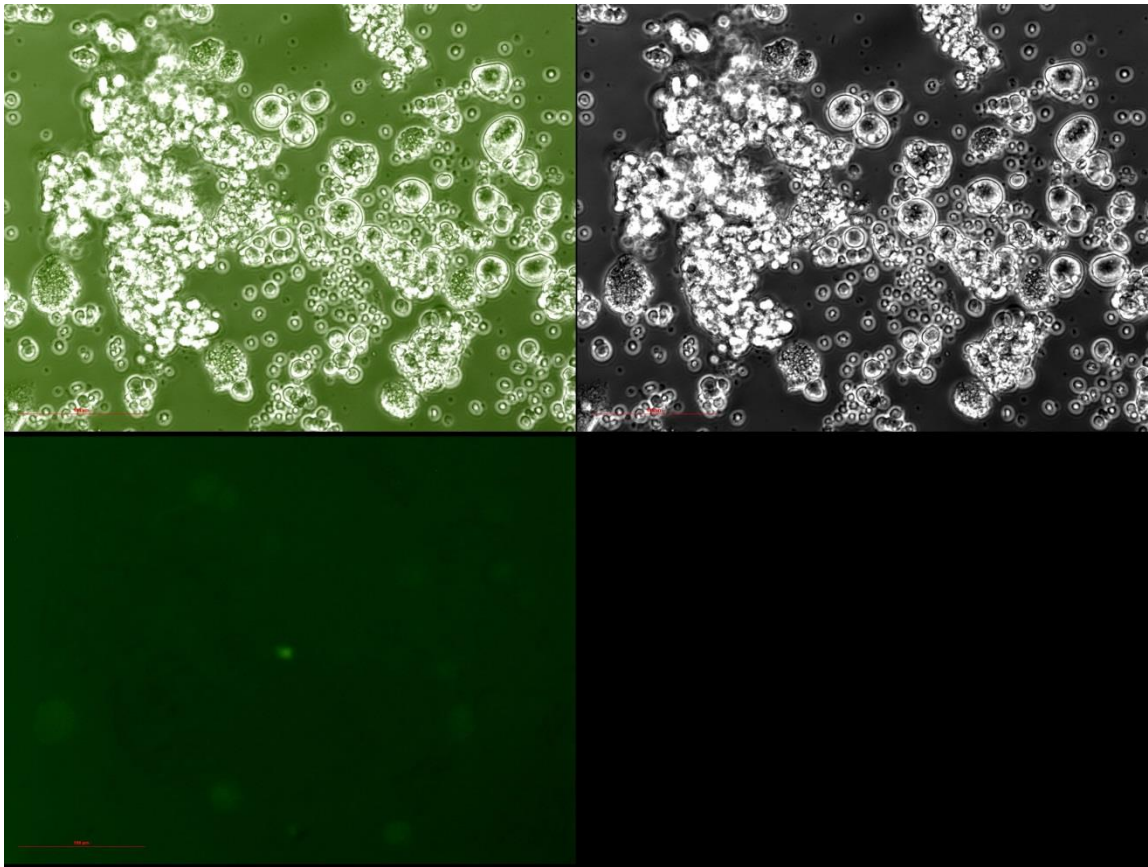


Figure 25. Unstained Sacral Sympathetic Ganglia Explantation at low magnification, 48 hours post-plating.
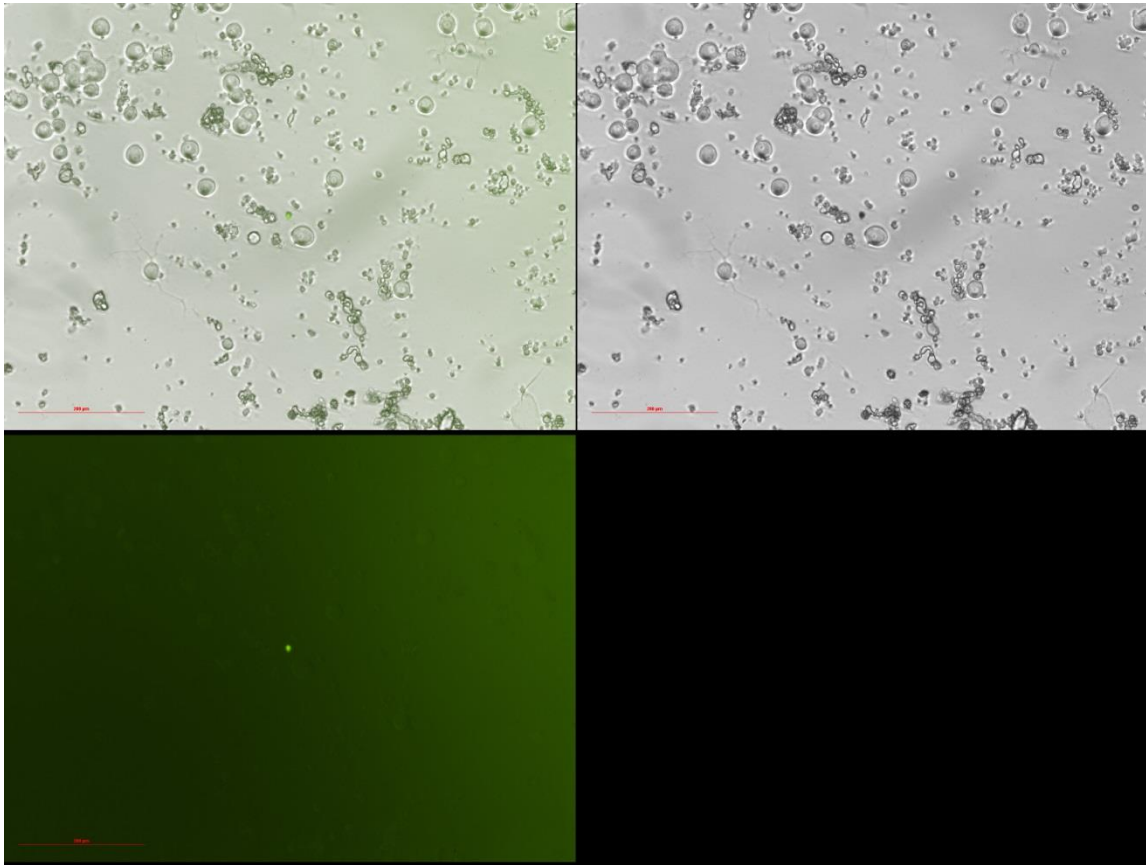
Figure 26. Unstained Sacral Sympathetic Ganglia Explantation at low magnification, 48 hours post-plating.
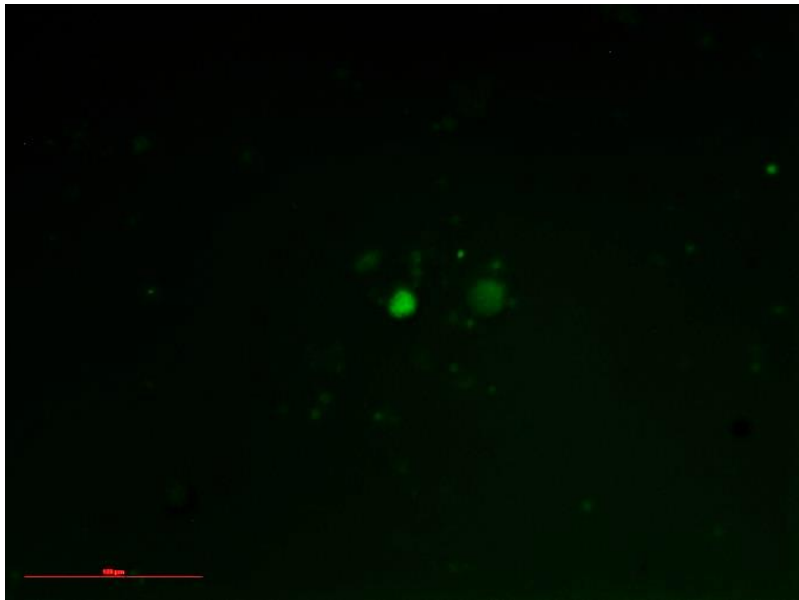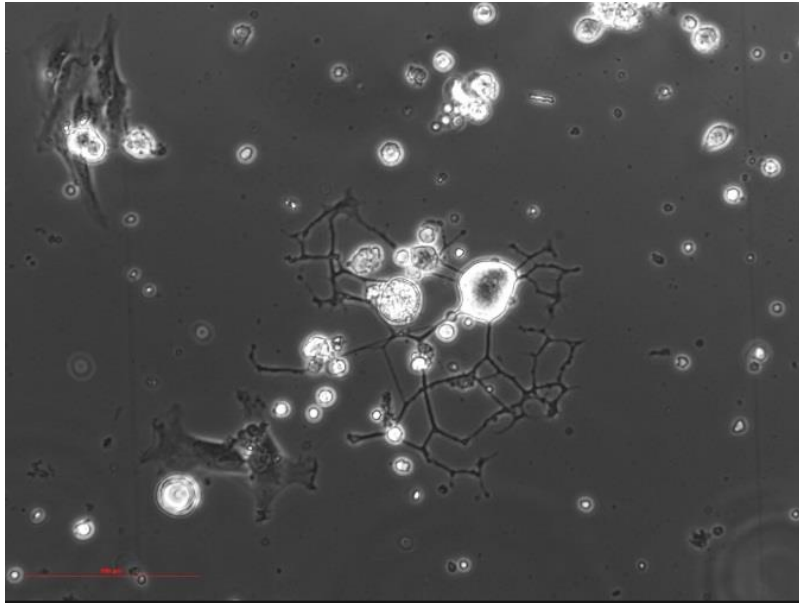
Figure 27. True Black stained Sacral Sympathetic Ganglia Explantation 72 hours post-plating, phase contrast above and VP-26-mNeonGreen below.
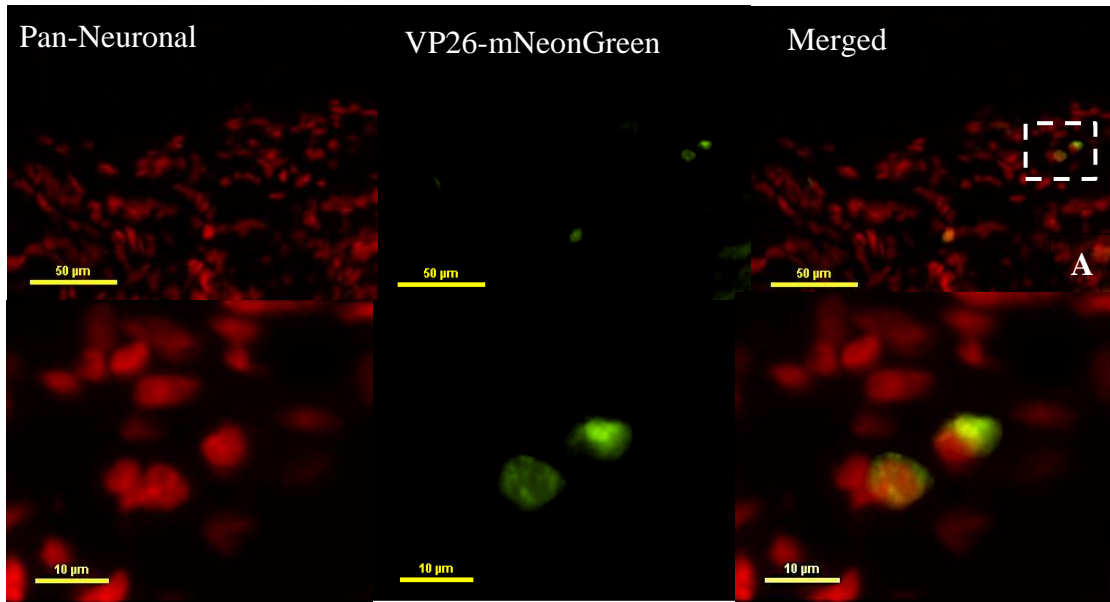
Figure 28. Cryosection of the SSG, single stain, pan-neuronal AF594.  A) Large field of view (B) Magnified selection from  A.
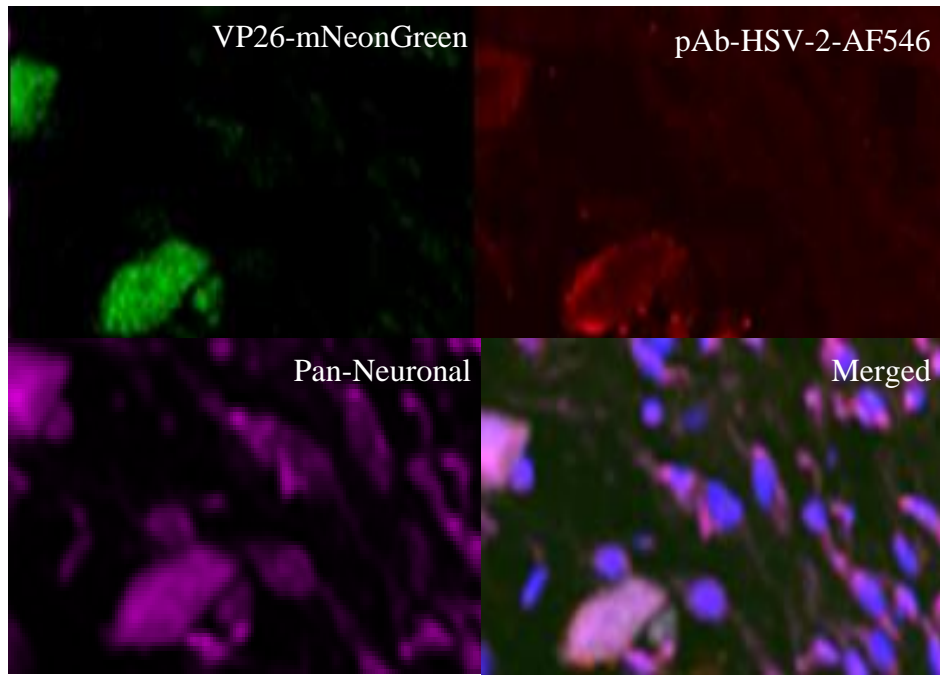
Figure 29. Confocal image of Cryosection of the SSG. Upper left: Detection of mNeonGreen fluorescence, Upper right: immunofluorescence using pAb HSV-2-AF546, Lower left: Pan-Neuronal stain Lower right quadrant: Merged. Arrows point to cells exhibiting fluorescent capsid and anti-HSV-2
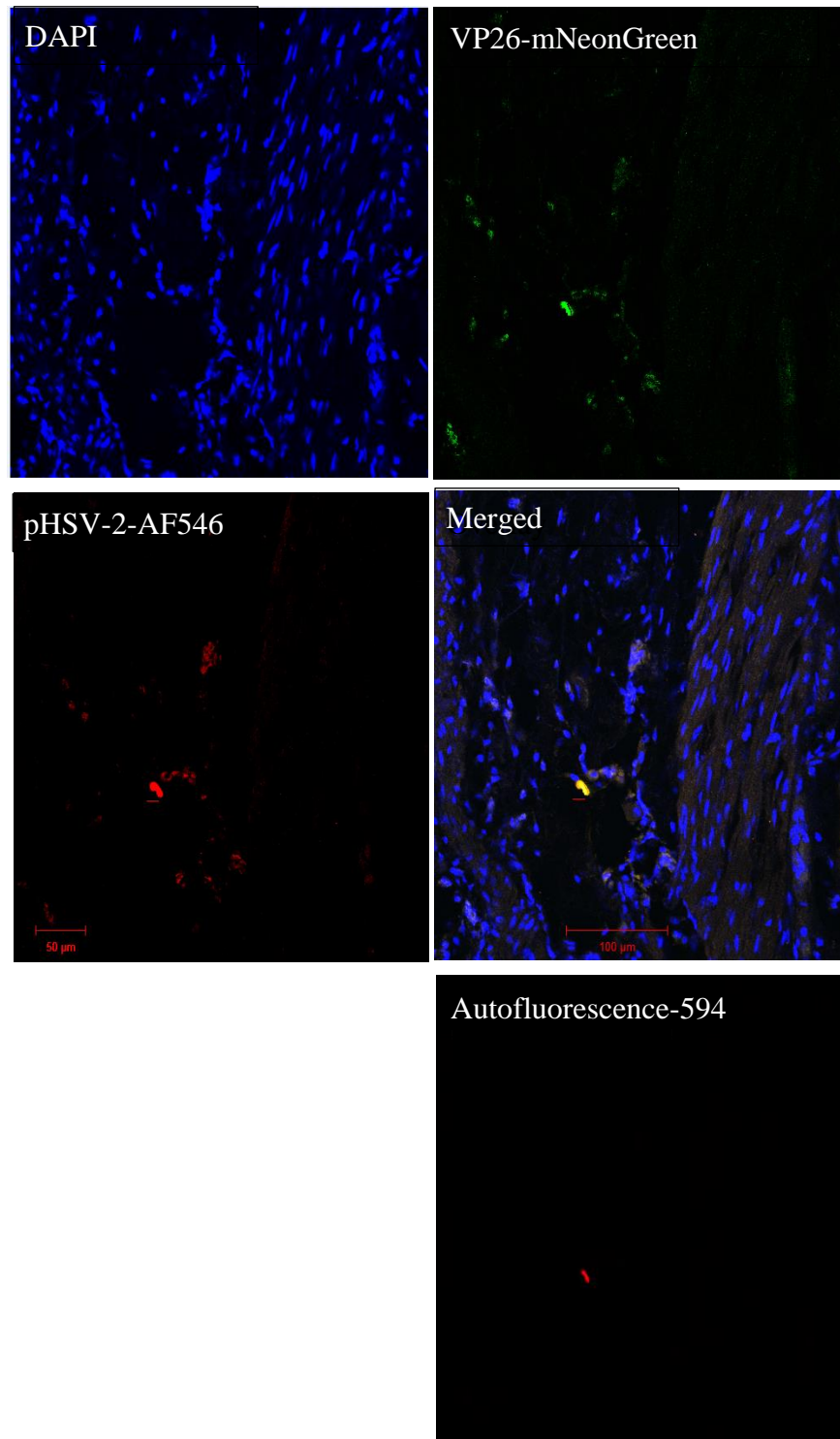
Figure 30. Confocal image of Nedel-infected sacral sympathetic ganglia with HSV-2 pAb and DAPI

**Discussion**

We found *ex vivo* evidence for the presence of reactivation competent virus in DRG and SSG, and also found *in vivo* evidence for reactivation of HSV-2 in DRG and SSG. Given previous experiments that revealed LAT and viral DNA in the autonomic ganglia, viral reactivation in ganglia following an axotomy-induced neural stress signal is not unexpected (4; 15; 22). However this is the first evidence showing HSV-2 reactivation from latently-infected autonomic ganglia in a clinically relevant vaginal model of infection.

The ability of HSV-2 to reactivate from autonomic ganglia has important implications for our understanding of viral latency. Autonomic reactivation may explain the relatively diffuse subclinical reactivations observed in otherwise asymptomatic humans. There may be value in evaluating interventions intended to influence viral latency and reactivation not only for their influence on latency in DRG, but also in autonomic neurons. The emergence of autonomic neurons as important sites of latency and reactivation also suggest that interventions specifically targeted to these neurons have the potential for benefit in affecting at least some viral reactivations.

One impediment to investigating the role of autonomic neurons in viral latency and reactivation is the difficulty in identifying and dissecting relevant ganglia in small animal models. Differences in tissue dissections and identification of neuronal tissue could account for some discrepancies in previous findings (73; 85; 109). For example, it is possible that some previous studies did not include the sacral sympathetic ganglia in their evaluation of viral reactivation from sympathetic murine neurons. Given that it is the sympathetic ganglia that are closest to the L6-S2 region of the spinal column that

93

innervate the skin and reproductive tract in small animal models, it is this region that is most likely impacted post-vaginal infection (79; 87). In a 200g guinea pig they are minute and are found behind a layer of adipose on the anterior surface of the sacrococcygeal junction. We could find no other investigations of the sympathetic chain that specified using the sacral sympathetic ganglia to assess HSV infection. Staining of neurons and careful description of dissections to identify neuronal types can help to reduce this type of confusion.

Detection of viral reactivation in explanted autonomic neurons required primary, secondary, and tertiary staining to confirm the presence of antigens other than capsid protein, to ascertain reactivation within a neuron, and to determine the location and state of the nucleus when reactivation occurs. When dissecting neuronal tissue, adipose, satellite glial, chromaffin, muscle, and epithelial cells can be dissected and explanted alongside. These non-neuronal cells can also be infected, which increases the difficulty of distinguishing neuronal reactivation from infection via a nearby cell. However, the explant cultures were evaluated hours after initial explant and greater fluorescence emerged over time within stained neurons (Fig.25-27).

While use of fluorescent virus simplified identification of reactivations *in vivo* in cryosections, the potential for autofluorescence is also present. We used tissue sections infected with non-fluorescing virus infected and uninfected sections to set the parameters for microscopy, increasing confidence that fluorescence observed over Nedel-infected neurons was truly above background. The co-localization of capsid fluorescence and HSV-2 antigen pattern was similar throughout the DRG. The green fluorescence and tagged pAb glycoprotein staining was typically observed emanating at the border

between the nucleus and cytoplasm of neurons. Glycoproteins gB, gD, gH, and gL that are detected by this antibody assist in egress through the plasma membrane, then re-associate again through the trans-Golgi network (69). Our observed fluorescence pattern is consistent with this previous observation.

The veracity of fluorescently-labelled neurons is strengthened with the examination and use of the proper controls. Microscopic imaging also benefits from molecular data support. By probing these anatomical locations for gene expression and using a sensitive and specific ddRT-PCR, we were able to further support our hypothesis that reactivation is occurring in autonomic neurons. We used raw copy numbers to evaluate gene expression. We found late gene expression occurring in the SSG in comparable quantities as the DRG.

Whether or not signals of reactivation events are reflective of the quantity of latent genomes producing LAT helps us parse out efficiency of reactivation. If there was a significant difference between the relative gD per LAT in the DRG versus SSG, we might expect that one ganglion was more efficient in its ability to reactivate. In this model and in this context, analysis leads us to surmise that it is reactivation from large pools of LAT-producing latent genomes and although there is a smaller pool of LAT in the SSG, reactivation is still efficiently occurring there.

Previous reports of autonomic neuron involvement following HSV infections drew varying conclusions. In the acute infection murine model, HSV-2 antigen was found in sympathetic neurons, while HSV-1 gene expression and infectious virus from homogenate was observed in only parasympathetic cells (73; 109). The findings from the

95

HSV-2 guinea pig ocular model revealed early gene expression in pooled ganglia of the sympathetics at a latent time point(85). Our findings from the clinically relevant guinea pig vaginal infection model support the hypothesis that HSV-2 is latent and reactivates from the sacral sympathetic ganglia as well as from the canonical sensory dorsal root ganglia.

The ability of HSV-2 to reactivate from autonomic ganglia has important implications for our understanding of viral latency. Autonomic reactivation may explain the relatively diffuse subclinical reactivations observed in otherwise asymptomatic humans. There may be value in evaluating interventions intended to influence viral latency and reactivation not only for their influence on latency in DRG, but also in autonomic neurons. The emergence of autonomic neurons as important sites of latency and reactivation also suggest that interventions specifically targeted to these neurons have the potential for benefit in affecting at least some viral reactivations.

**Author Contributions**

Philip Krause and Julianna Pieknik conceived and designed the experiments; Julianna

Pieknik and Andrea S Bertke performed the ganglia explantation jointly; and Julianna

Pieknik performed the dissections, cryosectioning, immunohistochemical staining, ddRT-

PCR, analyzed the data and wrote the paper.

# Chapter 4: Result Summary, Conclusions, Significance and Future Directions

**Result summary from chapter two**

Herpes Simplex Virus-2 has plagued mankind since before we were *Homo sapiens* yet our strategy thus far has only culminated in the diagnosis of symptomatic individuals and antiviral maintenance during an obvious outbreak. According to the World Health Organization, exponential spread throughout the population has resulted in over 400 million people infected worldwide. This most likely underestimated number is regarded as due to asymptomatic sexual transmission, though it can also be transmitted mother to child, of which, 70% of infected neonates are born to asymptomatic mothers. HSV-2 can cause painful lesions or neurological complications throughout the lifetime of the host. Due to its neurotropic nature, most studies rely on animal models and have focused on sensory neurons of the dorsal root ganglia (DRG). The goal of this dissertation was to elucidate if autonomic ganglia are also reservoirs of reactivating virus and whether symptomatic genital lesions are concurrent with viral gene expression in the DRG, MPG or SSG or multiple ganglia simultaneously.

Our first aim was to develop a tool that would allow exploration of where and when virus was reactivating. Unfortunately, a fluorescent HSV-2 had not yet been characterized to allow *in vivo* assessment. Existing fluorescent viruses had been characterized as causing virion aggregation in the nucleus, producing nuclear protein aggregates, diminished plaque sizes or a loss of fluorescence *in vivo*. Based on a

moderately successful HSV-1 construct, we engineered an N-terminal VP26 fusion, with a minor deletion to a novel monomeric fluorescent protein, mNeonGreen.

This substitution allowed the production of a successfully fused protein as indicated by western blot. The mutant virus, named Nedel, fluoresced brilliantly within the nuclei, cytoplasm and proximal outer membrane of cells, co-localizing with HSV-2 pAb-AF546.  This indicated incorporation into mature virions. The generated plaque sizes were not significantly different than those generated by the wild-type strain. An *in vitro* growth curve demonstrated its wild-type replication kinetics and electron microscopy revealed similar morphology. Nedel was then used to infect female guinea pigs intravaginally due to their ability to develop autonomic symptoms like urinary retention and constipation, genital skin lesions, and reactivate spontaneously. Over the acute phase, 0-14 days post-infection, animals developed the same quantity of lesions as wild-type infected. Vaginal swabs on days 4 and 7 revealed 100% green, fluorescent plaques, indicating the virus was replicating, maintaining infectivity and fluorescence *in vivo*. Over the next few weeks, intermittent reactivations resulting in recurrent lesions were observed at the same frequency and vaginal swabs on day 21 and 30 yielded 100% green plaques from 2 animals, providing further evidence that this mutant virus was capable of reactivation *in vivo* and maintaining its fluorescence. It is well-known that axotomy of the DRG alone can be a powerful impetus for reactivation. On day 35, the sacral DRGs were dissected from infected animals, enzymatically dissociated and plated. Fluorescence emerged and at 72 hours, neurons were stained with HSV-2 pAb, Pan-Neuronal and DAPI to reveal co-localization and confirm fluorescence was associated with non-capsid HSV-2 antigen. Other infected animals' sacral ganglia were processed

for similar staining of cryosections. This also revealed fluorescent co-localization within neurons which indicated that not only can the virus be induced to reactivate, but is also doing so spontaneously *in vivo.*

**Chapter two significance**

A tool that allows efficient localization of a spontaneous reactivation event is important and necessary. Trying to locate *in vivo* reactivation events, without a fluorescent marker, is incredibly costly and time consuming. Out of 20 wild-type-infected cryosections that were randomly labelled, only 1 revealed HSV-2 antigen. Even with a fluorescent marker, finding the fluorescent foci is an arduous task. However once they are found, the three-day immunolabelling is not in vain. Furthermore, tools for HSV-1 are in abundance as compared to HSV-2, and although related, key differences in DRG neuronal tropism have revealed that when evaluating the types of neurons impacted by herpes infection, they are not interchangeable (13). It was imperative that a fluorescent HSV-2 mutant be developed and characterized in order to study reactivation from latency, which brings us to our second aim.

**Result summary from chapter three**

Equipped with our newly characterized fluorescent virus, we finally had a tool that allows the efficient study of HSV-2 reactivation from latency. Using explanted *in vivo*-infected neurons from the sensory dorsal root ganglia, mixed population major pelvic ganglia and the sacral sympathetic ganglia, we observed induced reactivation from

mainly the DRG and the SSG with very little evidence of MPG involvement (Appendix A). We also addressed whether or not this reactivation was not only induced but spontaneously occurring. Fluorescently labelled cryosections revealed spontaneous reactivation, as evidenced by green fluorescent capsid protein production and co-localization with HSV-2 pAb within sensory neurons of the expected DRG, and for the first time, sympathetic neurons of the SSG. In order to put the reactivation from autonomic ganglia in perspective, we quantified gene expression from all three sites from 20 animals. They were either sacrificed on the first day of a reactivation (the emergence of a new lesion), or three days post-reactivation (lesion disappearance). By droplet digital RT-PCR we were able to detect immediate early, early and late viral gene expression from the DRG and the SSG. The major pelvic ganglia rarely yielded detectable transcripts. Interestingly, upon examination of immediate early and early genes, infected cell protein 0 and thymidine kinase, it would appear that although there was recognizable viral activity emanating from the SSG, it was still less than the DRG. The quantity of LAT was higher in the DRG, suggesting relatively higher quantities of latent virus in DRG vs. autonomic ganglia. However immediate and early gene expression and LAT are not truly indicative of complete reactivation. Late gene, gD is indicative of complete reactivation and we find relatively similar quantities between the DRG and SSG suggesting that there might be more abortive reactivations in the DRG than the SSG. Between gD per LAT in the DRG and SSG, there is not a significant difference, indicating the same efficiency of reactivation from these two anatomical locations and reactivation is occurring in the SSG in relative abundance as the DRG.

**Chapter 3 significance and future directions**

Although many have hypothesized that autonomic neurons could be infected, dysregulated and the cause of observed clinical symptoms such as urinary retention, constipation and erectile dysfunction, this is the first vaginal infection model to reveal induced and spontaneous HSV-2 reactivation from latency in the SSG. We have not only determined qualitatively that this occurs but quantitatively defined gene expression to further support our findings. Now that we understand these ganglia are relevant in the context of an *in vivo* guinea pig vaginal infection, we can further investigate the mechanism of dysregulation and potential reasons why there is less parasympathetic involvement during latency.

Primary cultured populations of adult guinea pig sensory, parasympathetic and sacral sympathetic ganglia could be uniformly infected to create homogenous, infected cell populations. Latency could be synthetically induced in these cells, followed by induced reactivation and total RNA isolation. RNA sequencing and subsequent Ingenuity Pathway Analysis could provide a global picture of what is happening in these different cell types and make the comparisons of how infection influences the neuronal transcriptome more apparent and easily distinguishable without the challenges of immune cell involvement. Alternatively, our fluorescent HSV-2 Nedel could be used to vaginally infect guinea pigs, followed by laser capture micro dissection of frozen tissue sections. Then, single cell analysis would take into account the extracellular environment at the time of spontaneous reactivation.

Next, we would want to verify that our observations in the vaginal infection model and those of our collaborator's using the ocular infection model are specific to

HSV-2. By repeating the experiments, substituting a fluorescent HSV-1 in the guinea pig vaginal infection model, we could make the involvement of parasympathetics versus sympathetic autonomic neurons clearer. We could also replicate this experiment with HSV-2 but instead switch to the murine vaginal infection model, to ensure this is a virus-specific phenomenon of a majority sympathetic but not parasympathetic neuronal reactivation as opposed to a finding only relevant to guinea pigs. The challenge with the murine model would be to limit mortality through the acute phase without disrupting the course of natural infection.

Another avenue to consider would be to probe HSV-2 positive human cadavers for sacral sympathetic chain involvement. Although DNA has been isolated in the sympathetic ganglia, timing would be imperative to collect RNA and the chance of catching HSV reactivation there. Along the same vein would be to explore current symptomatic and asymptomatic HSV-2 hosts for autonomic dysfunction and to see if viral shedding, or virus released into the reproductive tract regardless of the presence or absence of symptoms is correlated. Or, we could examine those that suffer from idiopathic autonomic dysfunction more closely for signs of asymptomatic or sub-clinical carriage of HSV-2.

Our aim to create and characterize a tool followed by its use in the guinea pig vaginal infection model has allowed us to observe for the first time, induced and spontaneous reactivation from the *in vivo*-infected autonomic ganglia. Our quantification of viral gene expression from all three anatomic locations has taught us that the sacral sympathetic ganglia are most likely an important reservoir of reactivating virus. The clinical prevalence and implications of HSV-2 infection in the sacral sympathetic ganglia

103

remain understudied. Understanding which neurons are infected in this guinea pig vaginal infection model might one day yield key insights into the entirety of HSV-2 reactivation-related pathogenesis and possibly human idiopathic autonomic disorders.

## Appendix A. Major Pelvic Ganglia Data

Originally it was our intention to also characterize viral reactivation from the major pelvic ganglia because it is a mixed population of parasympathetic and sympathetic neurons. The major pelvic ganglia's architecture complicates investigations. Isolating neurons from both the paracervical ganglia (where the vagina meets the branch of the uterine horns) and the pelvic plexus ganglia (nestled on either side, next to where the bladder meets ureter) is complex because the neurons are more dispersed, not as tightly bundled, and at times covered in adipose tissue. Often the paracervical ganglia, major pelvic plexus, and major pelvic ganglia labels are used interchangeably within the same journal article. By evaluating both the paracervical and para-ureter major pelvic ganglia, we found such little evidence of reactivation (figures30-32), that substantial conclusions could not be drawn. It is likely that the virus does not reactivate efficiently there. Also, there is some autofluorescence not quenched by the TrueBlack staining, therefore without further study, green fluorescence could not reliably be attributed to capsid protein production. The ddRT-PCR also confirms that if reactivation is occurring in the MPG, the signal is beneath the limit of detection.
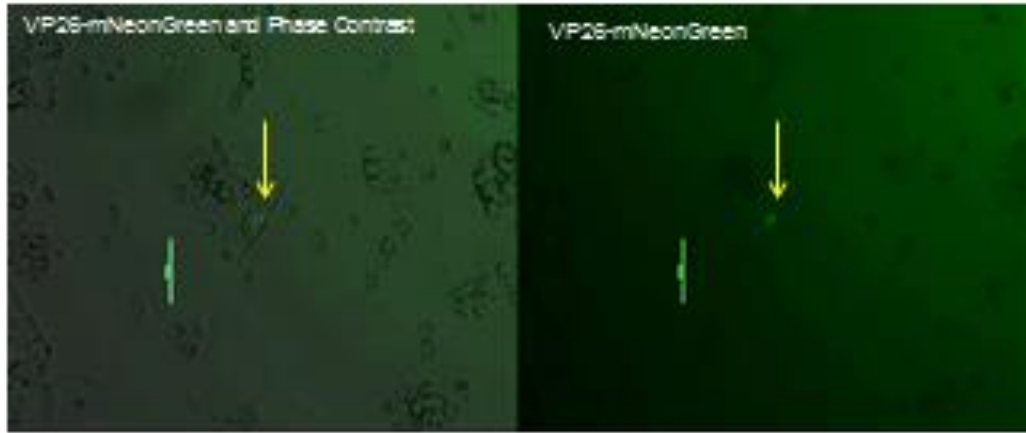
Figure 31. Fluorescence emergence, MPG explantation, unstained 48 hours post-plating. Phase contrast overlay and GFP filter settings.
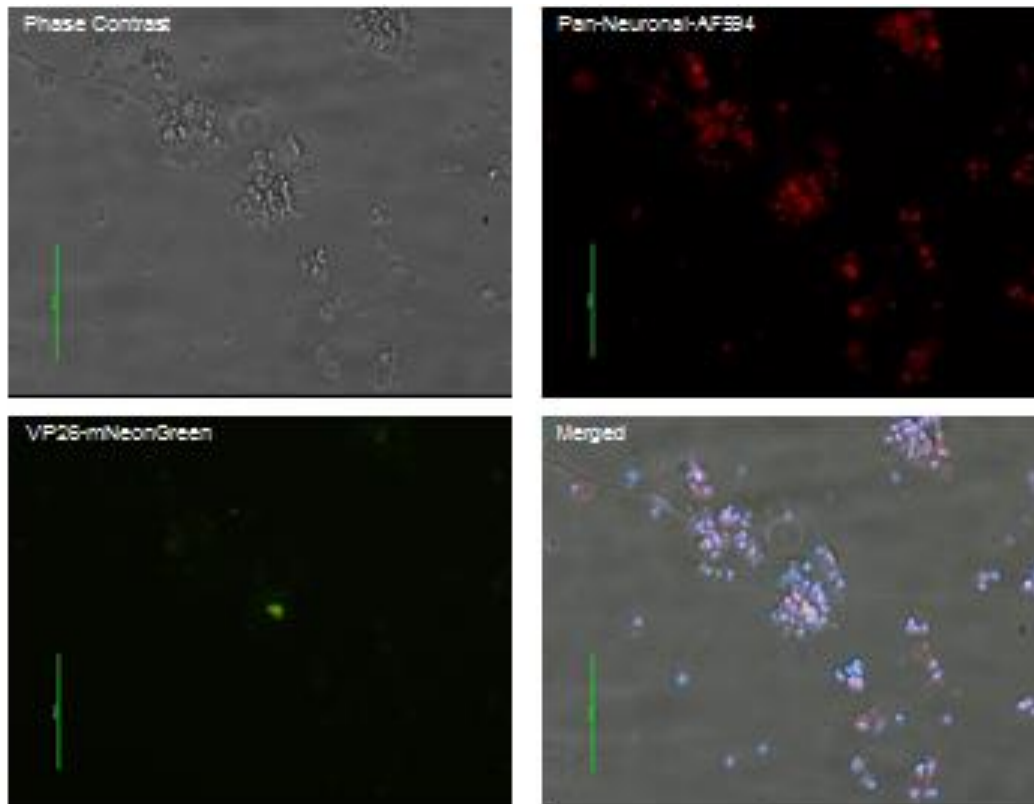
Figure 32. Fluorescence microscopic image of the MPG explantation with Pan-Neuronal Nissl 594 substitution, phase contrast and DAPI staining 60 hours post-plating.
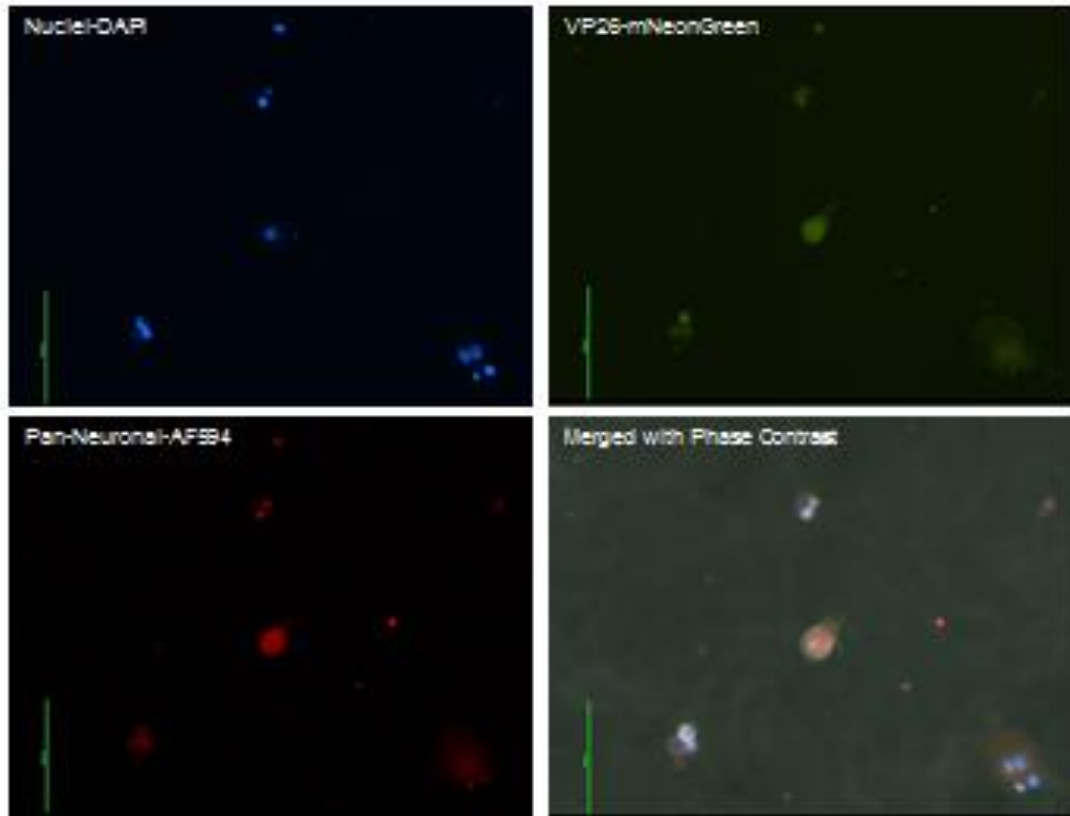
Figure 33. Fluorescence microscopic image of the MPG explantation with Pan-Neuronal Nissl 594 substitution, phase contrast, and DAPI staining 72 hours post-plating.

## Appendix B. Relative Expression

In order to address the possibility that the quality or quantity of RNA could skew the results and overall conclusion, we also normalized the data to GAPDH expression. Evaluating the data in this way did not impact the results nor alter the drawn conclusions.
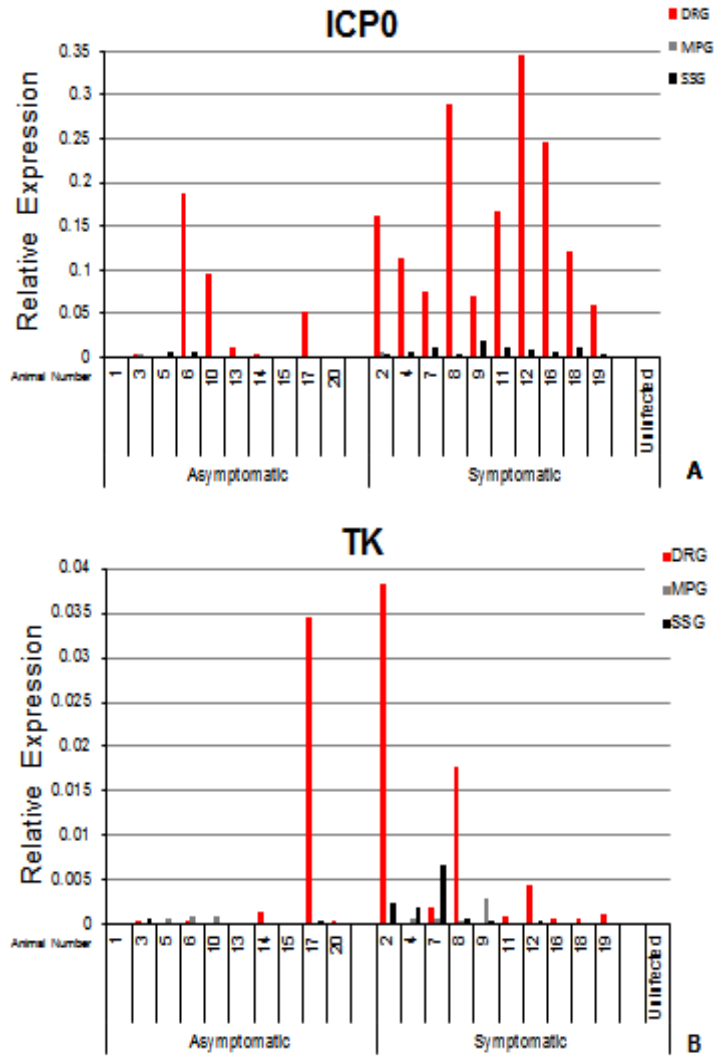


Figure 34. Quantification of relative gene expression in asymptomatic and symptomatic animals. Animals were euthanized at least 21 days post-infection based on the presence or absence of genital skin lesions. Droplet digital RT-PCR was performed on homogenized DRG, MPG and SSG. Data per individual animal shown, all normalized to GAPDH copies in 2 ng total RNA and the average of technical triplicates. (A) Immediate early gene ICP0 expression, (B) Early gene TK expression
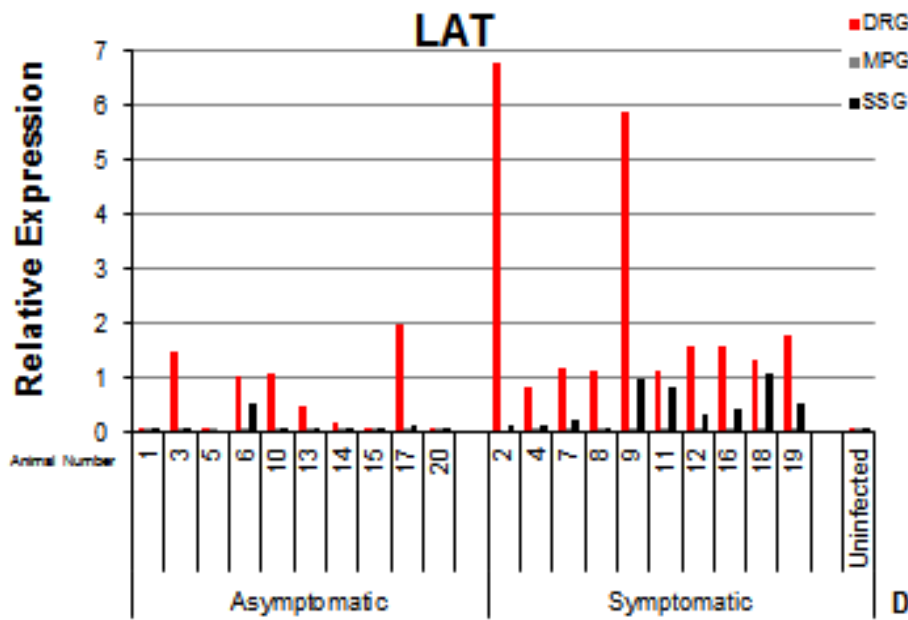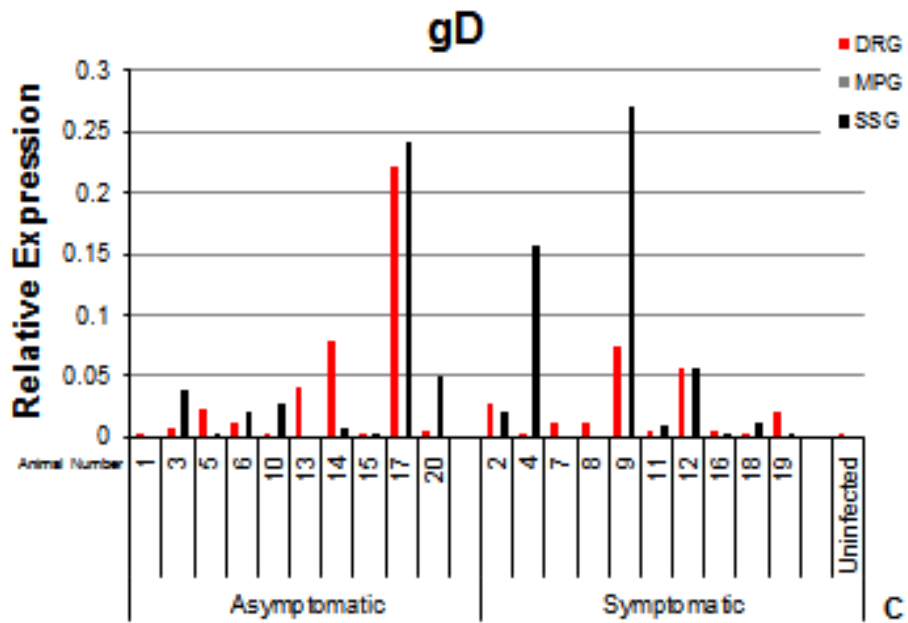
(C) Late gene gD expression (D) Latency associated transcript (LAT).
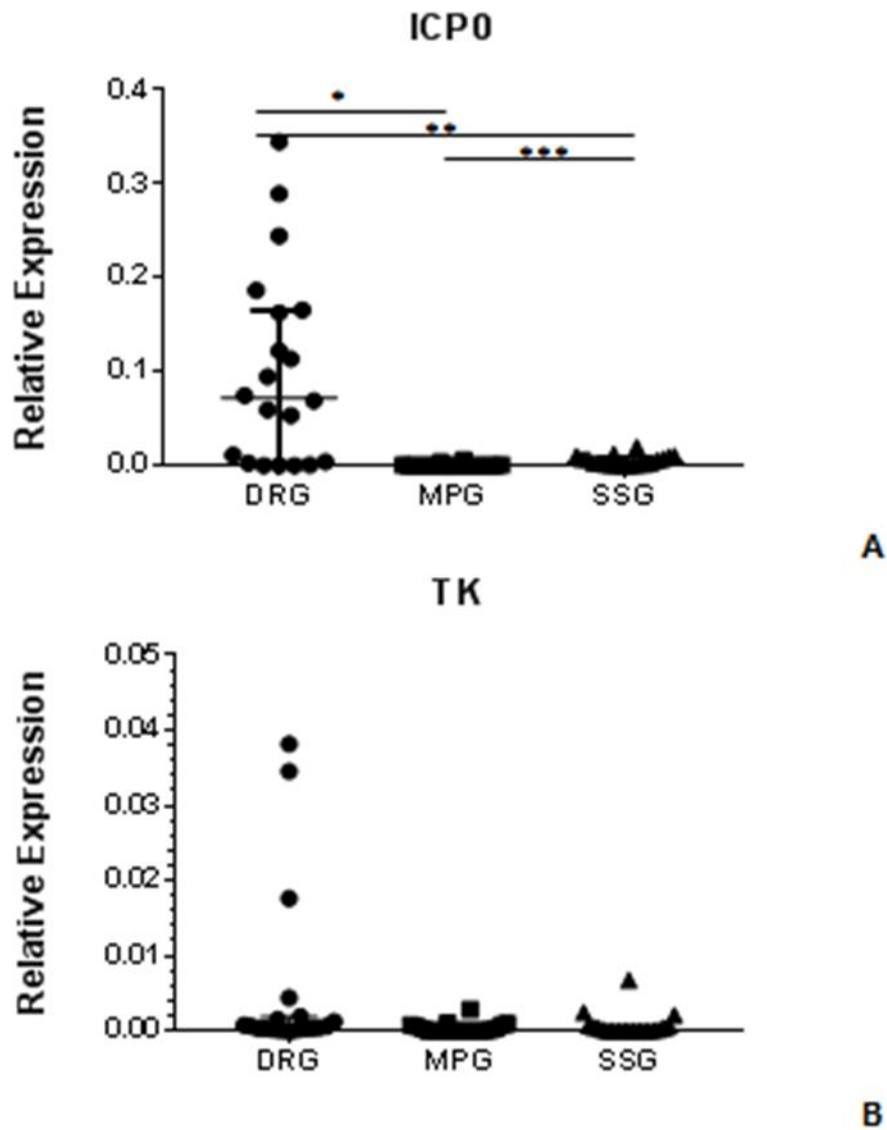
Figure 35. Summary of Asymptomatic and Symptomatic animal relative gene expression. (n=20). (A) Immediate early gene ICP0 expression, (DRG vs. MPG p=0.0011A-B, DRG vs. SSG p=0.0015; MPG vs. SSG p=0.0044) (B) Early gene TK expression (DRG vs. MPG p=0.1771, DRG vs. SSG p=0.2011; MPG vs. SSG p=0.6532)

**gD**

**LAT**
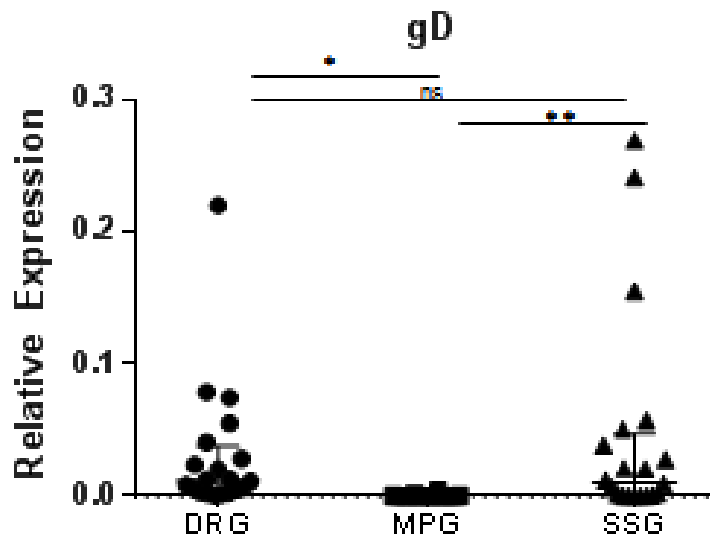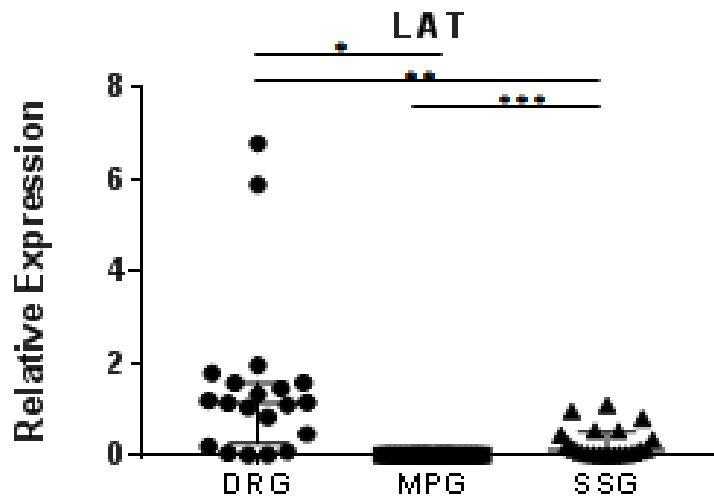
(C) Late gene gD expression (DRG vs. MPG p=0.0426, DRG vs. SSG p=0.2811A; MPG vs. SSG p=0.0426)(D) Latency associated transcript (LAT) (DRG vs. MPG p=0.0041, DRG vs. SSG p=0.0129; MPG vs. SSG p=0.0054). Error bars reflect median and inner quartile range. Significance determined by 1-way ANOVA Tukey's multiple comparison's test.

# References

1.      Abaitua F, Hollinshead M, Bolstad M, Crump CM, O'Hare P. 2012. A Nuclear
        localization signal in herpesvirus protein VP1-2 is essential for infection via
        capsid routing to the nuclear pore. *J Virol* 86:8998-9014
2.      Antinone SE, Shubeita GT, Coller KE, Lee JI, Haverlock-Moyns S, et al. 2006.
        The Herpesvirus capsid surface protein, VP26, and the majority of the tegument
        proteins are dispensable for capsid transport toward the nucleus. *J Virol* 80:5494-
        8
3.      Antinone SE, Shubeita GT, Coller KE, Lee JI, Haverlock-Moyns S, et al. 2006.
        The Herpesvirus Capsid Surface Protein, VP26, and the Majority of the Tegument
        Proteins Are Dispensable for Capsid Transport toward the Nucleus. *Journal of
        Virology* 80:5494-8
4.      Antinone SE, Zaichick SV, Smith GA. 2010. Resolving the Assembly State of
        Herpes Simplex Virus during Axon Transport by Live-Cell Imaging. *Journal of
        Virology* 84:13019-30
5.      Aravantinou M, Frank I, Arrode-Bruses G, Szpara M, Grasperge B, et al. 2017. A
        model of genital herpes simplex virus Type 1 infection in Rhesus Macaques. *J
        Med Primatol* 46:121-8
6.      Aurelius E, Johansson B, Skoldenberg B, Forsgren M. 1993. Encephalitis in
        immunocompetent patients due to herpes simplex virus type 1 or 2 as determined
        by type-specific polymerase chain reaction and antibody assays of cerebrospinal
        fluid. *J Med Virol* 39:179-86
7.      Balliet JW, Kushnir AS, Schaffer PA. 2007. Construction and characterization of
        a herpes simplex virus type I recombinant expressing green fluorescent protein:
        Acute phase replication and reactivation in mice. *Virology* 361:372-83
8.      Baringer JR. 1975. Herpes simplex virus infection of nervous tissue in animals
        and man. *Prog Med Virol* 20:1-26
9.      BenMohamed L, Osorio N, Srivastava R, Khan AA, Simpson JL, Wechsler SL.
        2015. Decreased reactivation of a herpes simplex virus type 1 (HSV-1) latency-
        associated transcript (LAT) mutant using the in vivo mouse UV-B model of
        induced reactivation. *J Neurovirol* 21:508-17
10.     Berger JR, Houff S. 2008. Neurological complications of herpes simplex virus
        type 2 infection. *Arch Neurol* 65:596-600
11.     Bertke AS, Apakupakul K, Ma A, Imai Y, Gussow AM, et al. 2012. LAT region
        factors mediating differential neuronal tropism of HSV-1 and HSV-2 do not act in
        trans. *PLoS One* 7:e53281
12.     Bertke AS, Ma A, Margolis MS, Margolis TP. 2013. Different mechanisms
        regulate productive herpes simplex virus 1 (HSV-1) and HSV-2 infections in
        adult trigeminal neurons. *J Virol* 87:6512-6
13.     Bertke AS, Swanson SM, Chen J, Imai Y, Kinchington PR, Margolis TP. 2011.
        A5-positive primary sensory neurons are nonpermissive for productive infection
        with herpes simplex virus 1 in vitro. *J Virol* 85:6669-77

14. Bertke AS, Swanson SM, Chen J, Imai Y, Kinchington PR, Margolis TP. 2011. A5-Positive Primary Sensory Neurons Are Nonpermissive for Productive Infection with Herpes Simplex Virus 1 In Vitro. *Journal of Virology* 85:6669-77

15. Booy FP, Trus BL, Newcomb WW, Brown JC, Conway JF, Steven AC. 1994. Finding a needle in a haystack: detection of a small protein (the 12-kDa VP26) in a large complex (the 200-MDa capsid of herpes simplex virus). *Proc Natl Acad Sci U S A* 91:5652-6

16. Booy FP, Trus BL, Newcomb WW, Brown JC, Conway JF, Steven AC. 1994. Finding a needle in a haystack: detection of a small protein (the 12-kDa VP26) in a large complex (the 200-MDa capsid of herpes simplex virus). *Proceedings of the National Academy of Sciences of the United States of America* 91:5652-6

17. Borst E-M, Mathys S, Wagner M, Muranyi W, Messerle M. 2001. Genetic Evidence of an Essential Role for Cytomegalovirus Small Capsid Protein in Viral Growth. *Journal of Virology* 75:1450-8

18. Boulais N, Misery L. 2008. The epidermis: a sensory tissue. *Eur J Dermatol* 18:119-27

19. Bourne N, Bravo FJ, Francotte M, Bernstein DI, Myers MG, et al. 2003. Herpes Simplex Virus (HSV) Type 2 Glycoprotein D Subunit Vaccines and Protection against Genital HSV-1 or HSV-2 Disease in Guinea Pigs. *The Journal of Infectious Diseases* 187:542-9

20. Brandt CR, Coakley LM, Grau DR. 1992. A murine model of herpes simplex virus-induced ocular disease for antiviral drug testing. *J Virol Methods* 36:209-22

21. Burkham J, Coen DM, Weller SK. 1998. ND10 protein PML is recruited to herpes simplex virus type 1 prereplicative sites and replication compartments in the presence of viral DNA polymerase. *J Virol* 72:10100-7

22. Cabrera JR, Viejo-Borbolla A, Martinez-Martin N, Blanco S, Wandosell F, Alcami A. 2015. Secreted herpes simplex virus-2 glycoprotein G modifies NGF-TrkA signaling to attract free nerve endings to the site of infection. *PLoS Pathog* 11:e1004571

23. Caplan LR, Kleeman FJ, Berg S. 1977. *Urinary retention probably secondary to herpes genitalis.*

24. Cherpes TL, Wiesenfeld HC, Melan MA, Kant JA, Cosentino LA, et al. 2006. The associations between pelvic inflammatory disease, Trichomonas vaginalis infection, and positive herpes simplex virus type 2 serology. *Sex Transm Dis* 33:747-52

25. Christensen J, Steain M, Slobedman B, Abendroth A. 2011. Differentiated neuroblastoma cells provide a highly efficient model for studies of productive varicella-zoster virus infection of neuronal cells. *J Virol* 85:8436-42

26. Clement C, Tiwari V, Scanlan PM, Valyi-Nagy T, Yue BY, Shukla D. 2006. A novel role for phagocytosis-like uptake in herpes simplex virus entry. *J Cell Biol* 174:1009-21

27. Cliffe AR, Arbuckle JH, Vogel JL, Geden MJ, Rothbart SB, et al. 2015. Neuronal Stress Pathway Mediating a Histone Methyl/Phospho Switch Is Required for Herpes Simplex Virus Reactivation. *Cell Host Microbe* 18:649-58

28. Cliffe AR, Garber DA, Knipe DM. 2009. Transcription of the herpes simplex virus latency-associated transcript promotes the formation of facultative heterochromatin on lytic promoters. *J Virol* 83:8182-90

29. Connolly SA, Jackson JO, Jardetzky TS, Longnecker R. 2011. Fusing structure and function: a structural view of the herpesvirus entry machinery. *Nat Rev Microbiol* 9:369-81

30. Davison AJ, Eberle R, Ehlers B, Hayward GS, McGeoch DJ, et al. 2009. The order Herpesvirales. *Arch Virol* 154:171-7

31. Davison MD, Rixon FJ, Davison AJ. 1992. Identification of Genes Encoding Two Capsid Proteins (VP24 and VP26) of Herpes Simplex Virus Type 1. *Journal of General Virology* 73:2709-13

32. de Abreu AL, Malaguti N, Souza RP, Uchimura NS, Ferreira EC, et al. 2016. Association of human papillomavirus, Neisseria gonorrhoeae and Chlamydia trachomatis co-infections on the risk of high-grade squamous intraepithelial cervical lesion. *Am J Cancer Res* 6:1371-83

33. de Oliveira AP, Glauser DL, Laimbacher AS, Strasser R, Schraner EM, et al. 2008. Live visualization of herpes simplex virus type 1 compartment dynamics. *J Virol* 82:4974-90

34. de Oliveira AP, Glauser DL, Laimbacher AS, Strasser R, Schraner EM, et al. 2008. Live Visualization of Herpes Simplex Virus Type 1 Compartment Dynamics. *Journal of Virology* 82:4974-90

35. Desai P, DeLuca NA, Person S. 1998. Herpes Simplex Virus Type 1 VP26 Is Not Essential for Replication in Cell Culture but Influences Production of Infectious Virus in the Nervous System of Infected Mice. *Virology* 247:115-24

36. Desai P, Person S. 1998. Incorporation of the Green Fluorescent Protein into the Herpes Simplex Virus Type 1 Capsid. *Journal of Virology* 72:7563-8

37. Deshmane SL, Fraser NW. 1989. During latency, herpes simplex virus type 1 DNA is associated with nucleosomes in a chromatin structure. *J Virol* 63:943-7

38. Döhner K, Ramos-Nascimento A, Bialy D, Anderson F, Hickford-Martinez A, et al. 2018. Importin α1 is required for nuclear import of herpes simplex virus proteins and capsid assembly in fibroblasts and neurons. *PLOS Pathogens* 14:e1006823

39. Dolan A, Jamieson FE, Cunningham C, Barnett BC, McGeoch DJ. 1998. The genome sequence of herpes simplex virus type 2. *J Virol* 72:2010-21

40. Douglas MW, Diefenbach RJ, Homa FL, Miranda-Saksena M, Rixon FJ, et al. 2004. Herpes Simplex Virus Type 1 Capsid Protein VP26 Interacts with Dynein Light Chains RP3 and Tctex1 and Plays a Role in Retrograde Cellular Transport. *Journal of Biological Chemistry* 279:28522-30

41. Elliott G, O'Hare P. 1997. Intercellular trafficking and protein delivery by a herpesvirus structural protein. *Cell* 88:223-33

42. Enders G, Risse B, Zauke M, Bolley I, Knotek F. 1998. Seroprevalence study of herpes simplex virus type 2 among pregnant women in Germany using a type-specific enzyme immunoassay. *Eur J Clin Microbiol Infect Dis* 17:870-2

43. Enquist LW. 2012. Five questions about viral trafficking in neurons. *PLoS Pathog* 8:e1002472

44.     Feldman LT, Ellison AR, Voytek CC, Yang L, Krause P, Margolis TP. 2002. Spontaneous molecular reactivation of herpes simplex virus type 1 latency in mice. *Proc Natl Acad Sci U S A* 99:978-83

45.     Fletcher GC, Xue L, Passingham SK, Tolkovsky AM. 2000. Death commitment point is advanced by axotomy in sympathetic neurons. *J Cell Biol* 150:741-54

46.     Freeman EE, Weiss HA, Glynn JR, Cross PL, Whitworth JA, Hayes RJ. 2006. Herpes simplex virus 2 infection increases HIV acquisition in men and women: systematic review and meta-analysis of longitudinal studies. *AIDS* 20:73-83

47.     Friedman HM. 2003. Immune evasion by herpes simplex virus type 1, strategies for virus survival. *Trans Am Clin Climatol Assoc* 114:103-12

48.     Fruh K, Ahn K, Djaballah H, Sempe P, van Endert PM, et al. 1995. A viral inhibitor of peptide transporters for antigen presentation. *Nature* 375:415-8

49.     Gibson W, Roizman B. 1971. Compartmentalization of spermine and spermidine in the herpes simplex virion. *Proc Natl Acad Sci U S A* 68:2818-21

50.     Goade DE, Nofchissey RA, Kusewitt DF, Hjelle B, Kreisel J, et al. 2001. Ultraviolet light induces reactivation in a murine model of cutaneous herpes simplex virus-1 infection. *Photochem Photobiol* 74:108-14

51.     Gobbi C, Tosi C, Stadler C, Merenda C, Bernasconi E. 2001. Recurrent myelitis associated with herpes simplex virus type 2. *Eur Neurol* 46:215-8

52.     Goel N, Docherty JJ, Fu MM, Zimmerman DH, Rosenthal KS. 2002. A modification of the epidermal scarification model of herpes simplex virus infection to achieve a reproducible and uniform progression of disease. *J Virol Methods* 106:153-8

53.     Goodell SE, Quinn TC, Mkrtichian E, Schuffler MD, Holmes KK, Corey L. 1983. Herpes Simplex Virus Proctitis in Homosexual Men. *New England Journal of Medicine* 308:868-71

54.     Greene LA, Tischler AS. 1976. Establishment of a noradrenergic clonal line of rat adrenal pheochromocytoma cells which respond to nerve growth factor. *Proc Natl Acad Sci U S A* 73:2424-8

55.     Gupta R, Warren T, Wald A. 2007. Genital herpes. *Lancet* 370:2127-37

56.     Hafezi W, Lorentzen EU, Eing BR, Muller M, King NJ, et al. 2012. Entry of herpes simplex virus type 1 (HSV-1) into the distal axons of trigeminal neurons favors the onset of nonproductive, silent infection. *PLoS Pathog* 8:e1002679

57.     Hagen C, Dent KC, Zeev-Ben-Mordehai T, Grange M, Bosse JB, et al. 2015. Structural Basis of Vesicle Formation at the Inner Nuclear Membrane. *Cell* 163:1692-701

58.     Handler CG, Eisenberg RJ, Cohen GH. 1996. Oligomeric structure of glycoproteins in herpes simplex virus type 1. *J Virol* 70:6067-70

59.     Handsfield HH. 2000. Public Health Strategies to Prevent Genital Herpes: Where Do We Stand? *Curr Infect Dis Rep* 2:25-30

60.     Harris RA, Preston CM. 1991. Establishment of latency in vitro by the herpes simplex virus type 1 mutant in1814. *J Gen Virol* 72 ( Pt 4):907-13

61.     Hill J, Patel A, Bhattacharjee P, Krause P. 2003. An HSV-1 chimeric containing HSV-2 latency associated transcript (LAT) sequences has significantly reduced adrenergic reactivation in the rabbit eye model. *Curr Eye Res* 26:219-24

62.   Hill JM, Nolan NM, McFerrin HE, Clement C, Foster TP, et al. 2012. HSV-1 latent rabbits shed viral DNA into their saliva. *Virology Journal* 9:221

63.   Hill JM, Quenelle DC, Cardin RD, Vogel JL, Clement C, et al. 2014. Inhibition of LSD1 reduces herpesvirus infection, shedding, and recurrence by promoting epigenetic suppression of viral genomes. *Sci Transl Med* 6:265ra169

64.   Ho HT, Woods KL, Bronson JJ, De Boeck H, Martin JC, Hitchcock MJ. 1992. Intracellular metabolism of the antiherpes agent (S)-1-[3-hydroxy-2-(phosphonylmethoxy)propyl]cytosine. *Mol Pharmacol* 41:197-202

65.   Hogue I, Bosse J, Engel E, Scherer J, Hu J-R, et al. 2015. Fluorescent Protein Approaches in Alpha Herpesvirus Research. *Viruses* 7:2915

66.   Honess RW, Roizman B. 1975. Regulation of herpesvirus macromolecular synthesis: sequential transition of polypeptide synthesis requires functional viral polypeptides. *Proc Natl Acad Sci U S A* 72:1276-80

67.   Hoshino Y, Qin J, Follmann D, Cohen JI, Straus SE. 2008. The number of herpes simplex virus-infected neurons and the number of viral genome copies per neuron correlate with the latent viral load in ganglia. *Virology* 372:56-63

68.   Ives AM, Bertke AS. 2017. Stress Hormones Epinephrine and Corticosterone Selectively Modulate Herpes Simplex Virus 1 (HSV-1) and HSV-2 Productive Infections in Adult Sympathetic, but Not Sensory, Neurons. *J Virol* 91

69.   Johnson DC, Baines JD. 2011. Herpesviruses remodel host membranes for virus egress. *Nat Rev Microbiol* 9:382-94

70.   Johnston C, Zhu J, Jing L, Laing KJ, McClurkan CM, et al. 2014. Virologic and immunologic evidence of multifocal genital herpes simplex virus 2 infection. *J Virol* 88:4921-31

71.   Kelly BJ, Fraefel C, Cunningham AL, Diefenbach RJ. 2009. Functional roles of the tegument proteins of herpes simplex virus type 1. *Virus Res* 145:173-86

72.   Kesson AM. 2001. Management of neonatal herpes simplex virus infection. *Paediatr Drugs* 3:81-90

73.   Khoury-Hanold W, Yordy B, Kong P, Kong Y, Ge W, et al. 2016. Viral Spread to Enteric Neurons Links Genital HSV-1 Infection to Toxic Megacolon and Lethality. *Cell Host Microbe* 19:788-99

74.   Khoury-Hanold W, Yordy B, Kong P, Kong Y, Ge W, et al. 2016. Viral Spread to Enteric Neurons Links Genital HSV-1 Infection to Toxic Megacolon and Lethality. *Cell Host & Microbe* 19:788-99

75.   Kim JY, Mandarino A, Chao MV, Mohr I, Wilson AC. 2012. Transient reversal of episome silencing precedes VP16-dependent transcription during reactivation of latent HSV-1 in neurons. *PLoS Pathog* 8:e1002540

76.   Kimberlin DM. 2007. Immunotherapy of HSV infections - antibody delivery. In *Human Herpesviruses: Biology, Therapy, and Immunoprophylaxis*, ed. A Arvin, G Campadelli-Fiume, E Mocarski, PS Moore, B Roizman, et al. Cambridge. Number of.

77.   Kimberlin DW, Whitley RJ. 2007. Antiviral therapy of HSV-1 and -2. In *Human Herpesviruses: Biology, Therapy, and Immunoprophylaxis*, ed. A Arvin, G Campadelli-Fiume, E Mocarski, PS Moore, B Roizman, et al. Cambridge. Number of.

78. Knipe DM, Cliffe A. 2008. Chromatin control of herpes simplex virus lytic and latent infection. *Nat Rev Microbiol* 6:211-21

79. Kozlowska A, Mikolajczyk A, Majewski M. 2017. Detailed Characterization of Sympathetic Chain Ganglia (SChG) Neurons Supplying the Skin of the Porcine Hindlimb. *Int J Mol Sci* 18

80. Krause PR, Stanberry LR, Bourne N, Connelly B, Kurawadwala JF, et al. 1995. Expression of the herpes simplex virus type 2 latency-associated transcript enhances spontaneous reactivation of genital herpes in latently infected guinea pigs. *J Exp Med* 181:297-306

81. Krautwald M, Maresch C, Klupp BG, Fuchs W, Mettenleiter TC. 2008. Deletion or green fluorescent protein tagging of the pUL35 capsid component of pseudorabies virus impairs virus replication in cell culture and neuroinvasion in mice. *Journal of General Virology* 89:1346-51

82. Laquerre S, Argnani R, Anderson DB, Zucchini S, Manservigi R, Glorioso JC. 1998. Heparan sulfate proteoglycan binding by herpes simplex virus type 1 glycoproteins B and C, which differ in their contributions to virus attachment, penetration, and cell-to-cell spread. *J Virol* 72:6119-30

83. Laycock KA, Lee SF, Brady RH, Pepose JS. 1991. Characterization of a murine model of recurrent herpes simplex viral keratitis induced by ultraviolet B radiation. *Invest Ophthalmol Vis Sci* 32:2741-6

84. Lee S Fau - Ives AM, Ives Am Fau - Bertke AS, Bertke AS. Herpes Simplex Virus 1 Reactivates from Autonomic Ciliary Ganglia Independently from Sensory Trigeminal Ganglia To Cause Recurrent Ocular Disease.

85. Lee S, Ives AM, Bertke AS. 2015. Herpes Simplex Virus 1 Reactivates from Autonomic Ciliary Ganglia Independently from Sensory Trigeminal Ganglia To Cause Recurrent Ocular Disease. *J Virol* 89:8383-91

86. Liang Y, Vogel JL, Narayanan A, Peng H, Kristie TM. 2009. Inhibition of the histone demethylase LSD1 blocks alpha-herpesvirus lytic replication and reactivation from latency. *Nat Med* 15:1312-7

87. Lindh B, Lundberg JM, Hokfelt T. 1989. NPY-, galanin-, VIP/PHI-, CGRP- and substance P-immunoreactive neuronal subpopulations in cat autonomic and sensory ganglia and their projections. *Cell Tissue Res* 256:259-73

88. Lo P, Yu X, Atanasov I, Chandran B, Zhou ZH. 2003. Three-Dimensional Localization of pORF65 in Kaposi's Sarcoma-Associated Herpesvirus Capsid. *Journal of Virology* 77:4291-7

89. Looker KJ, Elmes JAR, Gottlieb SL, Schiffer JT, Vickerman P, et al. 2017. Effect of HSV-2 infection on subsequent HIV acquisition: an updated systematic review and meta-analysis. *Lancet Infect Dis* 17:1303-16

90. Looker KJ, Magaret AS, Turner KM, Vickerman P, Gottlieb SL, Newman LM. 2015. Correction: Global estimates of prevalent and incident herpes simplex virus type 2 infections in 2012. *PLoS One* 10:e0128615

91. Looker KJ, Magaret AS, Turner KM, Vickerman P, Gottlieb SL, Newman LM. 2015. Global estimates of prevalent and incident herpes simplex virus type 2 infections in 2012. *PLoS One* 10:e114989

92. Lubinski JM, Lazear HM, Awasthi S, Wang F, Friedman HM. 2011. The herpes simplex virus 1 IgG fc receptor blocks antibody-mediated complement activation and antibody-dependent cellular cytotoxicity in vivo. *J Virol* 85:3239-49

93. Malkin JE, Morand P, Malvy D, Ly TD, Chanzy B, et al. 2002. Seroprevalence of HSV-1 and HSV-2 infection in the general French population. *Sex Transm Infect* 78:201-3

94. Margolis TP, Elfman FL, Leib D, Pakpour N, Apakupakul K, et al. 2007. Spontaneous reactivation of herpes simplex virus type 1 in latently infected murine sensory ganglia. *J Virol* 81:11069-74

95. Margolis TP, Imai Y, Yang L, Vallas V, Krause PR. 2007. Herpes simplex virus type 2 (HSV-2) establishes latent infection in a different population of ganglionic neurons than HSV-1: role of latency-associated transcripts. *J Virol* 81:1872-8

96. Mark KE, Wald A, Magaret AS, Selke S, Olin L, et al. 2008. Rapidly Cleared Episodes of Herpes Simplex Virus Reactivation in Immunocompetent Adults. *The Journal of infectious diseases* 198:1141-9

97. McCorry LK. 2007. Physiology of the autonomic nervous system. *Am J Pharm Educ* 71:78

98. Mertz GJ, Benedetti J, Ashley R, Selke SA, Corey L. 1992. Risk factors for the sexual transmission of genital herpes. *Ann Intern Med* 116:197-202

99. Mettenleiter TC, Muller F, Granzow H, Klupp BG. 2013. The way out: what we know and do not know about herpesvirus nuclear egress. *Cell Microbiol* 15:170-8

100. Morimoto T, Arii J, Akashi H, Kawaguchi Y. 2009. Identification of multiple sites suitable for insertion of foreign genes in herpes simplex virus genomes. *Microbiol Immunol* 53:155-61

101. Nagel C-H, Döhner K, Binz A, Bauerfeind R, Sodeik B. 2012. Improper Tagging of the Non-Essential Small Capsid Protein VP26 Impairs Nuclear Capsid Egress of Herpes Simplex Virus. *PLOS ONE* 7:e44177

102. Nagel C-H, Döhner K, Fathollahy M, Strive T, Borst EM, et al. 2008. Nuclear Egress and Envelopment of Herpes Simplex Virus Capsids Analyzed with Dual-Color Fluorescence HSV1(17+). *Journal of Virology* 82:3109-24

103. Nagel CH, Dohner K, Fathollahy M, Strive T, Borst EM, et al. 2008. Nuclear egress and envelopment of herpes simplex virus capsids analyzed with dual-color fluorescence HSV1(17+). *J Virol* 82:3109-24

104. Ndjamen B, Farley AH, Lee T, Fraser SE, Bjorkman PJ. 2014. The herpes virus Fc receptor gE-gI mediates antibody bipolar bridging to clear viral antigens from the cell surface. *PLoS Pathog* 10:e1003961

105. Neumann DM, Bhattacharjee PS, Giordani NV, Bloom DC, Hill JM. 2007. In vivo changes in the patterns of chromatin structure associated with the latent herpes simplex virus type 1 genome in mouse trigeminal ganglia can be detected at early times after butyrate treatment. *J Virol* 81:13248-53

106. Ohashi M, Bertke As Fau - Patel A, Patel A Fau - Krause PR, Krause PR. Spread of herpes simplex virus to the spinal cord is independent of spread to dorsal root ganglia.

107. Ohashi M, Bertke AS, Patel A, Krause PR. 2011. Spread of herpes simplex virus to the spinal cord is independent of spread to dorsal root ganglia. *J Virol* 85:3030-2

108. Padgett DA, Sheridan JF, Dorne J, Berntson GG, Candelora J, Glaser R. 1998. Social stress and the reactivation of latent herpes simplex virus type 1. *Proc Natl Acad Sci U S A* 95:7231-5

109. Parr MB, Parr EL. 2003. Intravaginal administration of herpes simplex virus type 2 to mice leads to infection of several neural and extraneural sites. *J Neurovirol* 9:594-602

110. Perng GC, Jones C, Ciacci-Zanella J, Stone M, Henderson G, et al. 2000. Virus-induced neuronal apoptosis blocked by the herpes simplex virus latency-associated transcript. *Science* 287:1500-3

111. Pertel PE, Fridberg A, Parish ML, Spear PG. 2001. Cell fusion induced by herpes simplex virus glycoproteins gB, gD, and gH-gL requires a gD receptor but not necessarily heparan sulfate. *Virology* 279:313-24

112. Preston CM, Efstathiou S. 2007. Molecular basis of HSV latency and reactivation. In *Human Herpesviruses: Biology, Therapy, and Immunoprophylaxis*, ed. A Arvin, G Campadelli-Fiume, E Mocarski, PS Moore, B Roizman, et al. Cambridge. Number of.

113. Price RW. 1977. Viral infections of the autonomic nervous system and its target organs: pathogenetic mechanisms. *Med Hypotheses* 3:33-6

114. Radtke K, Kieneke D, Wolfstein A, Michael K, Steffen W, et al. 2010. Plus- and Minus-End Directed Microtubule Motors Bind Simultaneously to Herpes Simplex Virus Capsids Using Different Inner Tegument Structures. *PLOS Pathogens* 6:e1000991

115. Resources MHaVML. 2018. *Peripheral Nervous System*. http://histology.medicine.umich.edu/resources/peripheral-nervous-system#iii-ganglia

116. Rodahl E, Stevens JG. 1992. Differential accumulation of herpes simplex virus type 1 latency-associated transcripts in sensory and autonomic ganglia. *Virology* 189:385-8

117. Rode K, Dohner K, Binz A, Glass M, Strive T, et al. 2011. Uncoupling uncoating of herpes simplex virus genomes from their nuclear import and gene expression. *J Virol* 85:4271-83

118. Roizman B. 1979. The structure and isomerization of herpes simplex virus genomes. *Cell* 16:481-94

119. Roth S, Kummer W. 1994. A quantitative ultrastructural investigation of tyrosine hydroxylase-immunoreactive axons in the hairy skin of the guinea pig. *Anat Embryol (Berl)* 190:155-62

120. Sanjuan NA, Lascano EF. 1986. Autonomic nervous system involvement in experimental genital infection by herpes simplex virus type 2. *Arch Virol* 91:329-39

121. Sawtell NM, Thompson RL. 1992. Rapid in vivo reactivation of herpes simplex virus in latently infected murine ganglionic neurons after transient hyperthermia. *J Virol* 66:2150-6

122. Sawtell NM, Thompson RL. 2004. Comparison of Herpes Simplex Virus Reactivation in Ganglia In Vivo and in Explants Demonstrates Quantitative and Qualitative Differences. *Journal of Virology* 78:7784-94

123. Schiffer JT, Corey L. 2013. Rapid host immune response and viral dynamics in herpes simplex virus-2 infection. *Nature medicine* 19:280-90

124. Shaner NC, Lambert GG, Chammas A, Ni Y, Cranfill PJ, et al. 2013. A bright monomeric green fluorescent protein derived from Branchiostoma lanceolatum. *Nature Methods* 10:nmeth.2413

125. Smith JS, Herrero R, Munoz N, Eluf-Neto J, Ngelangel C, et al. 2001. Prevalence and risk factors for herpes simplex virus type 2 infection among middle-age women in Brazil and the Philippines. *Sex Transm Dis* 28:187-94

126. Smith TJ, Morrison LA, Leib DA. 2002. Pathogenesis of herpes simplex virus type 2 virion host shutoff (vhs) mutants. *J Virol* 76:2054-61

127. Snyder A, Wisner TW, Johnson DC. 2006. Herpes Simplex Virus Capsids Are Transported in Neuronal Axons without an Envelope Containing the Viral Glycoproteins. *Journal of Virology* 80:11165-77

128. Stanberry LR, Kern ER, Richards JT, Overall JC, Jr. 1985. Recurrent genital herpes simplex virus infection in guinea pigs. *Intervirology* 24:226-31

129. Stanberry LR, Kit S, Myers MG. 1985. Thymidine kinase-deficient herpes simplex virus type 2 genital infection in guinea pigs. *J Virol* 55:322-8

130. Steiner I, Spivack JG, Deshmane SL, Ace CI, Preston CM, Fraser NW. 1990. A herpes simplex virus type 1 mutant containing a nontransinducing Vmw65 protein establishes latent infection in vivo in the absence of viral replication and reactivates efficiently from explanted trigeminal ganglia. *Journal of Virology* 64:1630-8

131. Stephen AS, William AS, Martin WW. 1999. Reduction of Lipofuscin-like Autofluorescence in Fluorescently Labeled Tissue. *Journal of Histochemistry & Cytochemistry* 47:719-30

132. Sugimoto K, Uema M, Sagara H, Tanaka M, Sata T, et al. 2008. Simultaneous Tracking of Capsid, Tegument, and Envelope Protein Localization in Living Cells Infected with Triply Fluorescent Herpes Simplex Virus 1. *Journal of Virology* 82:5198-211

133. Sugimoto K, Uema M, Sagara H, Tanaka M, Sata T, et al. 2008. Simultaneous tracking of capsid, tegument, and envelope protein localization in living cells infected with triply fluorescent herpes simplex virus 1. *J Virol* 82:5198-211

134. Tandrup T. 2004. Unbiased estimates of number and size of rat dorsal root ganglion cells in studies of structure and cell survival. *J Neurocytol* 33:173-92

135. Tang S, Bertke AS, Patel A, Wang K, Cohen JI, Krause PR. 2008. An acutely and latently expressed herpes simplex virus 2 viral microRNA inhibits expression of ICP34.5, a viral neurovirulence factor. *Proceedings of the National Academy of Sciences* 105:10931

136. Tang S, Bosch-Marce M, Patel A, Margolis TP, Krause PR. 2015. Characterization of herpes simplex virus 2 primary microRNA Transcript regulation. *J Virol* 89:4837-48

137. Thellman NM, Triezenberg SJ. 2017. Herpes Simplex Virus Establishment, Maintenance, and Reactivation: In Vitro Modeling of Latency. *Pathogens* 6

138. Tongtako W, Lehmbecker A, Wang Y, Hahn K, Baumgartner W, Gerhauser I. 2017. Canine dorsal root ganglia satellite glial cells represent an exceptional cell population with astrocytic and oligodendrocytic properties. *Sci Rep* 7:13915

139. Vanover J, Sun J, Deka S, Kintner J, Duffourc MM, Schoborg RV. 2008. Herpes simplex virus co-infection-induced Chlamydia trachomatis persistence is not mediated by any known persistence inducer or anti-chlamydial pathway. *Microbiology* 154:971-8

140. Varela JA, Garcia-Corbeira P, Aguanell MV, Boceta R, Ballesteros J, et al. 2001. Herpes simplex virus type 2 seroepidemiology in Spain: prevalence and seroconversion rate among sexually transmitted disease clinic attendees. *Sex Transm Dis* 28:47-50

141. Wagstaff AJ, Faulds D, Goa KL. 1994. Aciclovir. A reappraisal of its antiviral activity, pharmacokinetic properties and therapeutic efficacy. *Drugs* 47:153-205

142. Warren KG, Marusyk RG, Lewis ME, Jeffrey VM. 1982. Recovery of latent herpes simplex virus from human trigeminal nerve roots. *Arch Virol* 73:84-9

143. Watson-Jones D, Weiss HA, Rusizoka M, Baisley K, Mugeye K, et al. 2007. Risk factors for herpes simplex virus type 2 and HIV among women at high risk in northwestern Tanzania: preparing for an HSV-2 intervention trial. *J Acquir Immune Defic Syndr* 46:631-42

144. Weller SK, Coen DM. 2012. Herpes simplex viruses: mechanisms of DNA replication. *Cold Spring Harb Perspect Biol* 4:a013011

145. Wertheim JO, Smith MD, Smith DM, Scheffler K, Kosakovsky Pond SL. 2014. Evolutionary origins of human herpes simplex viruses 1 and 2. *Mol Biol Evol* 31:2356-64

146. Whitley RJ, Kimberlin DW, Roizman B. 1998. Herpes Simplex Viruses. *Clinical Infectious Diseases* 26:541-55

147. Wilcox CL, Johnson EM, Jr. 1988. Characterization of nerve growth factor-dependent herpes simplex virus latency in neurons in vitro. *J Virol* 62:393-9

148. Wingfield PT, Stahl SJ, Thomsen DR, Homa FL, Booy FP, et al. 1997. Hexon-only binding of VP26 reflects differences between the hexon and penton conformations of VP5, the major capsid protein of herpes simplex virus. *Journal of Virology* 71:8955-61

149. Wisner TW, Johnson DC. 2004. Redistribution of cellular and herpes simplex virus proteins from the trans-golgi network to cell junctions without enveloped capsids. *J Virol* 78:11519-35

150. Wolfstein A, Nagel C-H, Radtke K, Döhner K, Allan VJ, Sodeik B. 2006. The Inner Tegument Promotes Herpes Simplex Virus Capsid Motility Along Microtubules in vitro. *Traffic* 7:227-37

151. Yang J, Yang F, Campos L, Mansfield W, Skelton H, et al. 2017. *Quenching autofluorescence in tissue immunofluorescence [version 1; referees: 2 approved with reservations, 1 not approved].*

152. Yu X, Shah S, Atanasov I, Lo P, Liu F, et al. 2005. Three-Dimensional Localization of the Smallest Capsid Protein in the Human Cytomegalovirus Capsid. *Journal of Virology* 79:1327-32

153. Zhou ZH, He J, Jakana J, Tatman JD, Rixon FJ, Chiu W. 1995. Assembly of VP26 in herpes simplex virus-1 inferred from structures of wild-type and recombinant capsids. *Nat Struct Biol* 2:1026-30